FAILURE MODES OF AN ALUMINA-BASED MACHINING CERAMIC

by

John Raymond Telfer, C.Eng. M.I.Prod.E.

Thesis submitted to the Council for National Academic Awards

in Partial Fulfilment of the requirements for

The Master of Philosophy Degree.

Middlesex Polytechnic
Resource Centre for Engineering
Science and Mathematics.

September 1979.

DECLARATION

The author hereby declares that while he has been a registered candidate for the degree of Master of Philosophy he has not been a registered candidate for another award of the CNAA or of another University during the research programme.

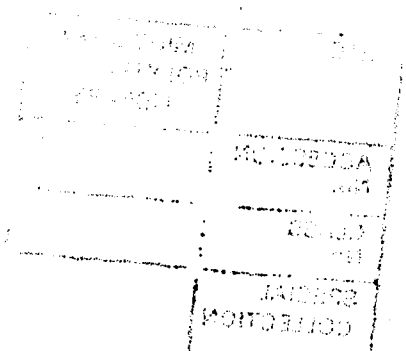

ACKNOWLEDGEMENTS

I wish to extend my sincere thanks to Dr.R.D.Johnston for his encouragement and help throughout this work.

I am indebted to the late Mr.Robin Sinclair, my internal supervisor until his tragic death in a road accident. His generous help during the early stages of this research was invaluable.

My sincere thanks are also extended to Dr.C.J.Spears who willingly assumed the responsibilities of director of studies during the closing stages of the work.

I am most grateful to the Governors of Middlesex Polytechnic for the opportunity and facilities which have enabled me to undertake this research. In particular, I would like to thank those concerned in the Resource Centre of Engineering for their assistance and co-operation.

ABSTRACT

Failure Modes of an Alumina-Based Machining Ceramic

by John Raymond Telfer

Attempts have been made to reproduce "comb" cracks in disposable cuboid alumina tool tips as a preliminary to an investigation into catastrophic failure during machining.

During lathe tests the tips withstood rates of machining several times greater than the normally accepted "comb" crack thresholds.

Chemical analysis revealed the anomalous presence of calcia in the current tips which was thought to be responsible for the presence of a liquid phase during sintering.

Examination by electron microscopy of the broken tool tips revealed a predominance of intergranular fracture and two distinct modes of transgranular cleavage, one of which was influenced by pore concentrations in geometric patterns.

Moduli values were some 40% lower than previously used batches of tips, which permitted the absorption of greater strain induced by either mechanical or thermal sources.

No damage was evident in the tool tips after the first cut up to a feed rate of 0.03125 in/rev but catastrophic failure always occurred at the instance of re-engagement at feed rates of 0.028 in/rev or greater.

The difference in chemical analysis, porosity and modulus would appear to be responsible for the absence of "comb" cracking and for the phenomenon of catastrophic failure.

A test rig was designed for operation on an induction heater to simulate the condition of abrupt disengagement during machining. Failure thresholds were established for a variety of induction coils under closely controlled conditions of heating and loading.

INDEX

INTRODUCTION

Aluminium oxide (Al_2O_3) is the second most abundant constituent of the earth's crust, silica being the most common. It exists in many different kinds of clays, kaolins, rocks and other minerals, bauxite, (named after les Beaux in Southern France where the ore was first discovered), being perhaps the most well-known of these. However, bauxite ores are comparatively rare, but the yield of alumina from them reaches about 90% in high grade ores and up to 85% in lower grades. Le Chatelier discovered the first commercial method of converting bauxite into pure aluminium oxide by the pyrogenic treatment. Since then, other methods of extracting alumina from bauxite ores have been discovered, such as the Bayer wet method, the combination method and the Pedersen process.

Pure aluminium oxide is a rare mineral called corundum which, in its purest known form, is represented by the valuable "Padparaja" gem-stone - white sapphire. In most cases corundum is associated with other oxides such as Cr_2O_3, TiO_2, SiO_2 and Fe_2O_3. Ruby, the most valuable corundum, is a solid solution of chromium oxide in alumina. Yellow sapphire contains traces of nickel oxide and magnesia, whilst the traditional blue sapphire contains titanium oxide. Corundum containing small amounts of silica and ferric oxide is known commercially as emery and is widely used as an abrasive.

Alumina is extremely hard, although it is softer than diamond, which is the hardest known substance. For a quantitative comparison of hardness some Zeiss microhardness values are included:-

mild steel	750 kg/mm^2
hardened steel	1350 kg/mm^2
tungsten carbide	1700 kg/mm^2
aluminium oxide	3000 kg/mm^2
silicon carbide	4500 kg/mm^2
boron carbide	7000 kg/mm^2

Alumina has high abrasion and wear-resistant properties, although, according to King and Wheildon[1], the rate of wear increases severalfold when used wet. They did not, however, specify the type of wear mechanism. It is sensitive to thermal shock and manufacturers recommend that alumina tool tips are used dry during machining, except for light finishing cuts, to avoid the probability of cracking at the heated zone of the chip/tool interface. Alumina is also sensitive to mechanical shock, particularly in the vicinity of edges, where it may frequently fail by flaking. In addition, it is sensitive to vibration typical of that encountered in the machining processes and this invariably results in catastrophic failure of the tool tip. Its use in the manufacture of grinding wheels for machining hard metals is commonplace. In this form, particles of alumina are embedded in a matrix of softer material such as vitrified clay. However, its use as a single-point cutting tool has not been widely adopted by industry in the same way as high-speed steel or tungsten carbide. One of the major obstacles to the economic use of alumina tool tips is the need for high-power rated and rigid equipment which precludes its use on old or worn machine tools. Problems arose in the 1930's when tungsten carbide (Widia) was introduced and compared with high speed steel. Reports from users complained

of its unpredictability due to chipping, cracking or disintegration as a result of brittleness characteristics[1].

Tool tips are manufactured by a sintering process. The base material Al_2O_3 is dosed with controlled quantities of sintering auxiliaries and a grain growth inhibitor, usually another oxide such as MgO. This mixture is then ground in water to a fine powder of between 2 and 3 μm particle size, during which time a uniform distribution of the components is achieved. Water is removed from the slurry by spray drying and the free-flowing powder is cold pressed into cutting tip blanks using automatic presses. The tips are then sintered in specially designed furnaces and shrinkage commences at about 1200°C. Required densification[2], of about 98.5%, is achieved at between 1700°C and 1750°C. The tip blanks are then accurately ground to shape by means of diamond impregnated wheels and finally chamfered on all edges to reduce the incidence of fracture.

Solid state sintering by diffusion is a complex phenomenon. Transformation from a porous compact to a strong dense ceramic can be explained in terms of simultaneous changes in grain shape and grain size, together with changes in pore shape and a reduction in pore size. The rate of sintering decreases with time and the continued heating of the tips leads to a deterioration in their mechanical properties. Rapid grain growth occurs by secondary recrystallisation without any perceptible increase in densification since the residual porosity at this stage is trapped within the grains.

Alumina was first used at the turn of the century for machining steel. Patents were issued in England in 1912 and in Germany in 1913[1], which was, perhaps, an indication that early researchers met with some

degree of success, although there are no records to confirm any industrial applications at that time.

In 1936, Ryshkewitch[3] conducted research on pure alpha-aluminium oxide at Degussa in Germany. He continued his work at a later date in the United States, which culminated in the first commercially available ceramic tool material (Degusset), for which a U.S. patent was issued in 1942. Interest in alumina cutting tools was revived during World War II as a result of a shortage of conventional tool materials. In 1943 similar work began at the Institute of Chemical Technology in Moscow and a paper was published, ten years later, by Pavlushkin[4] on Micro-lite, a new strong Al_2O_3 cutting tool material. Following Ryshkewitch's work on Degusset, research was started in 1945 at Watertown Arsenal in the United States. The investigation compared silicon carbide, boron carbide and aluminium oxide with tungsten carbide. It was concluded in the report[5] that alumina was the most suitable of the ceramics tried for single point cutting tools, but also that its performance was inferior to tungsten carbide. In the light of such reports, alumina was regarded, until recently, as being suitable for finishing cuts only. It is known that a high cutting velocity with a shallow depth of cut and a low feed rate results in an extremely fine surface finish with good dimensional accuracy.

Contemporary researchers have shown that alumina tool tips easily out-perform tungsten carbide on all but a few work-piece materials for both roughing and finishing cuts. Manufacturers do not recommend the use of alumina for machining aluminium or aluminium alloys because of a chemical reaction between it and the tool material, causing built-up cutting edges on the tool with a resultant deterioration of the

machining process. Problems are also encountered when machining titanium which is tough and ductile and has a marked rubbing effect on the tool tip with the net result that wear is rapid and the surface finish and dimensional accuracy poor. King and Wheildon[1] reported that when machining nickel the cutting edge of the Al_2O_3 tip was broken down in a progressive minute chipping action. On the other hand, alumina may be particularly recommended for machining stellites and all other chromium base alloys.

For optimum cutting conditions on different materials, modifications to the tool geometry and changes in the cutting angles may be necessary.

In 1966, Pekelharing and Orelio[6] demonstrated the superiority of alumina over tungsten carbide in an industrial environment at the Rotterdam Dry-Dock Company's Workshop. Their machine shop was equipped with a 147 h.p. (110 kW) lathe capable of handling a marine propellor shaft 670 mm (26 in) diameter, 6000 mm (20 ft) long, which they rough-turned, uninterrupted over its entire length in 51 minutes. Observers were impressed by the metal removal rate of 655 cm^3/min (40 in^3/min) from a cutting speed of 250 m/min (818 ft/min) at 2.5 mm (0.1 in) depth of cut and 1 mm/rev (0.040 in/rev) feed rate. Pekelharing and Orelio selected modest cutting conditions to safeguard the success of the demonstration. The cutting time saved amounted to as much as 60% when compared with the normal procedure of machining with cemented carbide at 80 m/min (260 ft/min) and requiring at least one tool change over the twenty foot length.

Further care was taken to avoid the possibility of tool tip failure at engagement and dis-engagement by the introduction of a programmed feed rate so that mechanical and thermal shock, which are more severe at the beginning and end of the cut, were reduced. By controlling the saddle independently of the lead screw, it was possible to commence cutting with the low feed rate of 0.4 mm/rev (0.016 in/rev) and thus avoid the initial impact of the alumina tool tip into the work-piece. Once engaged, the feed was increased steplessly to a value of 1.0 mm/rev (0.040 in/rev) and then reduced to the low value again just prior to the end of the cut.

According to Pekelharing and Orelio[6], metal removal rates on steel of 3000 cm^3/min (183 in^3/min) were achieved in the Laboratory at Delft University using an SPK tool tip. The tip had been modified geometrically and used in a redesigned tool holder, much more robust than that supplied by SPK. No data is available for the cutting forces involved but the cutting speed was 500 m/min (1640 ft/min) with an undeformed chip cross-section of 4 x 1.5 mm^2 (0.16 x 060 in^2) at 140 hp rating.

During machining, even under light load conditions, some alumina tool tips exhibited a series of small equally-spaced cracks on the rake face and around the corner radius, which were roughly perpendicular to the cutting edge where the tip had been in contact with the work-piece. King[7] observed the formation of a "reticulated" crack pattern in alumina cutting tools whilst machining steels. Similar crack patterns in other refractory materials were reported by Sibley and Allen[8] during experiments on friction and wear at high temperatures

and high velocities. Thijssen[9] also noted the frequent occurrence of the same type of cracking during his work on ceramic tool tip failure. He did not, however, classify such tips as failures.

Pekelharing[10] made a comprehensive survey of cracking in alumina tool tips used for machining steel. He identified no less than five types although, initially, he concentrated on the "reticulated" type which he called "comb" cracks because of their resemblance to the real article. He concluded that the cracks initiated during the first cut but that they were invisible until after the second cut when steel was forced into them and they could then be seen with the naked eye. Pekelharing described them as having the appearance of thin pencil lines and 1 mm (0.04 in) long, between 0.1 and 0.2 mm (0.004 to 0.008 in) apart and of the same magnitude in depth. Later, he deduced that the incidence of "comb" cracking was not time-dependent when similar results were obtained with the cutting times reduced to 5 seconds on both the first and second cuts.

He then concentrated on the effects of tip heating on engagement and cooling at disengagement as probable causes of cracking. In an attempt to retard the cooling rate after disengagement a "tea-cosy" of insulating material, (externally heated by a gas torch), was placed over the tool as quickly as possible after cutting; but cracking still occurred. Pekelharing estimated the rate of heating of the tool tip on engagement as being in the order of 10^6°C/sec or 1000°C in a millisecond, and concluded that this was the cause of cracking.

More recently, Miles[11] investigated the incidence of "comb" cracking in SPK SN37 alumina tool tips. He derived a mathematical relationship determining crack thresholds in terms of cutting

velocities, feed rates and depths of cut. "The criterion implies that cracking occurred when the power input to the tool tip per unit depth of cut exceeded a certain definite level".

King, Thijssen and Pekelharing subscribed to the view that "comb" cracking was not necessarily a precursor to catastrophic failure since a "comb" cracked corner could be used repeatedly without disintegration. Thijssen suggested that the cracks were initiated by surface irregularities on the rake face of the tips, resulting in local stress concentrations. He polished some tips in order to reduce the surface roughness and in so doing succeeded in reducing the incidence of catastrophic failure, but the "comb" cracking still occurred at the same level as before.

According to Griffith's classical crack theory[12], crack nuclei existed as flaws in the surface of a material. He suggested that the significant factor in brittle materials was the concentrated stress σ_c at the tip of the flaw and not the normal stress σ_n. Griffith's (Inglis) formula relates the normal stress σ_n and the concentrated stress σ_c to the physical dimensions of the flaws in the following manner:-

$$\frac{\sigma_c}{\sigma_n} = 2\sqrt{\frac{c}{r}}$$

where c is the depth of the crack and r is the radius of curvature at the tip of the crack. The ratio $\frac{c}{r}$ may be of the order of 10^2 or 10^3 so that the concentrated stress may well approach the theoretical strength of the material.

King and Wheildon[1] stated that the transverse fracture strength of alumina was increased by about one third when chemically polished. This increase in strength was obtained by the removal of a surface

layer of about 5 μm (0.002 in), which took with it deleterious surface flaws by immersion in a borax fusion at 250°C for five minutes.

The foregoing results are in accord with the Griffith crack theory, although "comb" cracking appears to be related to some other phenomenon. Regardless of how fracture occurs, it is generally agreed that maximum strength of alumina tips is obtained with materials of high density and small grain size, together with "perfect" surface condition.

It is probable that grain boundaries and pores constitute internal flaws, although it must be said that the tips used in the present research programme always exhibited a proportion of transgranular fracture, as typified in fig.1.1. Brittle ceramics are usually of low crystal symmetry but always highly anisotropic so that, when cooled during fabrication, they develop differential internal residual stresses.

Knudsen[13] introduced the following empirical equation in 1959 relating the grain size and porosity to the normal fracture strength:-

$$\sigma_f = \frac{K_x}{d^a e^{bP}}$$

where d is the grain diameter

P is the porosity

K_x is an experimental factor

a is grain size coefficient

b is porosity coefficient

Later, in 1969, Carniglia[14,15], re-examined the data for well-documented single-phase oxide ceramics and formulated the relationship for normal fracture strength, where:-

$$\sigma_f = \sigma_y + \frac{K_y}{d^{\frac{1}{2}}} \quad \text{(for small grain sizes)}$$

$$\sigma_f = \frac{K_x}{d^{\frac{1}{2}}} \quad \text{(for large grain sizes)}$$

The values of σ_y, K_y and K_x depend on the material and the grain size. The above relationships have similar forms to the Griffith equation when the flaw dimension c is likened to the $d^{\frac{1}{2}}$ term. However, according to Stokes[16], the significance of the $d^{\frac{1}{2}}$ term has been the subject of much discussion on brittle ceramic materials where dislocation motion does not take place. It has been suggested by Coble[17] that the growth of surface flaws under stress limits brittle fracture to the dimensions equivalent to the grain diameters, and any extension beyond this microstructural barrier results in catastrophic failure at the critical fracture stress. This theory was questioned by Clarke[18] on the grounds that most cracks propagated intergranularly in brittle ceramics and that there was no possibility for a dislocation mechanism by which incipient cracks could grow. Instead, he proposed that the driving force for brittle fracture in a brittle ceramic was the relaxation of residual stresses caused by anisotropic thermal contraction. He showed that a relationship to the derived $d^{\frac{1}{2}}$ term in the previous equations could be obtained by considering a balance of energies, namely, surface energy supplied during the propagation of an intergranular crack and strain energy lost by relaxation of internal stress caused by anisotropic thermal contractions across a grain boundary interface. King[19] et al have shown that dense fine grained alumina has been stressed to more than 15×10^4 lbf/in^2 but this figure cannot be extrapolated to the maximum fracture strengths of single crystal alumina, so that it would

appear that the introduction of pores and grain boundaries must adversely affect the mechanical properties of brittle ceramics.

Similarly, the introduction of pores and grain boundaries also affects the plastic deformation characteristics of alumina. Kronberg[20] has reported evidence of plastic deformation at temperatures in excess of 1000°C, above which plastic deformation is strongly temperature and strain rate dependent. Slip is achieved by the synchronous movement of aluminium and oxygen ions through a complex partial dislocation machanism. It is therefore possible that the nucleation of surface cracks, which may subsequently lead to catastrophic failure, is related to such deformation processes.

The main objective of this work was to examine the conditions under which catastrophic failure occurred in one particular grade of alumina tool tip. All machine tool tests were to be carried out using test piece material of the same specification, and a fixed tool geometry, so that the only apparent variables were the cutting speed, the depth of cut and feed rate. The programme of work outlined included re-examination of the incidence of "comb" cracking and its possible correlation to catastrophic failure. The programme also included the measurement of cutting forces and temperature at the tool tip, and other miscellaneous thermal shock tests.

A second objective was to design and construct a test rig to be used in conjunction with a 12kW Radyne induction heater so that the effects of various applied loads at closely controlled temperatures could be observed. The test rig offered the additional advantages that trials could be more safely monitored in the absence of hot swarf.

CHAPTER 2

APPARATUS AND EQUIPMENT

2:1 VDF Lathe

2.1.1 Turning tests were carried out on a VDF (Vereinigte Drehbank-Fabriken) S.500 lathe of high rigidity, fig.2.1.1. It was fitted with a Ward-Leonard drive, facilitating continuous speed control of the nose spindle up to 4500 rev/min with gear drive and up to 5600 rev/min with belt drive. The VDF had a high speed headstock with a balanced chuck and air-cooled bearings. The tailstock was hydraulically controlled to provide axial thrusts of up to 500 kg (1125 lbf) through a "live" centre. The cross-slide and saddle movements were controlled by conventional nut and feed-screw mechanisms, providing a choice of 50 automatic feed rates longitudinally or axially. Manual control, for precise location of the tool tip relative to the workpiece, was achieved by means of graduated collars attached to the control wheels. The power available at the nose spindle was 30 kW (40 hp).

2:2 Tool-Holder

2.2.1 Tool-holders were available in a variety of sizes and clamping head designs for different tool orientations to suit the type of workpiece material to be machined. They were manufactured by SPK to suit their ceramic tool tips, fig.2.2.1, and were of robust design in order to minimise the deleterious effects of vibration during machining. The clamp was designed to accommodate a detachable dual-purpose tungsten carbide chip breaker with serrations on the top rear surface to provide a means of adjustment in relationship to the cutting edge,

fig.2.2.2. The bottom surface which was flat, located on the rake face of the tip so that when the clamping screw was tightened the clamping pressure retained the alumina tool in position in the tool holder. When the tool holder was located in the tool post on the cross-slide, perpendicular to the work-piece axis, the cutting geometry of the tip was -6° rake angle, -4° angle of inclination with a 20° approach angle on the front face, fig.2.2.3.

2.3 Alumina Tool Tips (Type SN37)

2.3.1 Fig.2.3.1 shows a reversible prismoidal tool tip of the type SN37 used in the experimental programme. The dimensions were 12.7 x 12.7 x 10 mm thick with a nose radius of 0.8 mm and a chamfer of 0.25 mm x 20° on each edge and corner. Each tip had eight potential cutting edges although, when catastrophic failure occurred, it invariably resulted in the loss of the cutting edge and corner below the one in contact with the work. Tips that sustained less severe damage were used on other corners, with the exception of the corner below the damaged one.

2.3.2 A qualitative, and subsequent quantitative, chemical analysis of the various tips was carried out by an industrial laboratory using a Q80 direct reading spectrograph. Some variation of composition was indicated. (Reference 3.2.1).

2.3.3 Bend tests on alumina prisms cut from tool tips, fig.2.3.3(a) were carried out on a Hounsfield tensometer for which special adaptors were made, fig.2.3.3(b), to accommodate the 12.7 mm (0.5 in) long alumina prisms.

2.3.4 For this purpose, a jig, fig.2.3.4, was designed and a number of tool tips were sliced into small rectangular prisms of approximately 1.5 mm x 2.0 mm (0.060 in x 0.080 in) cross-sectional area

by means of a diamond impregnated copper slitting wheel.

2.3.5 Hardness tests on the tool tips were carried out using a Leitz micro-hardness tester and a Vickers Pyramid hardness testing machine.

2:4 Materials

2.4.1 The material chosen for the machining tests was EN30(B), a low alloy steel noted for its toughness. It was supplied in lengths of 1.5m (5 ft) of 108 mm (4.25 ins) diameter in the hot rolled condition and machined into test pieces to the dimensions shown in fig.2.4.1. Journal A was located in the three-jaw self-centering chuck, whilst Journal B provided an abutment against the chuck jaw faces to prevent axial slip from the thrust of the hydraulic tail-stock. It also provided clearance for the tool to "run-out" after machining Journal C at the end of each cut. Journal D provided clearance between the saddle and the tail-stock so that the tool could be positioned for any required depth of cut before engagement of the saddle-free mechanism. Test pieces were abandoned when Journal C was reduced to 50 mm (2 in) diameter to avoid induced vibration from deflection under the influence of heavy cutting forces. To ensure that there was uniformity in the material supplied, a chemical analysis of each consignment was carried out. The analysis of a batch of test material and the EN30(B) chemical specification are included for comparison, (see section 3.1.1).

2.4.2 Accurate cutting velocities were maintained on all lathe tests by use of a Hasler surface speed meter applied to the test piece, fig.2.4.2.

2.4.3 Tangential and axial cutting forces were measured using a type AA Mecalex pneumatic dynamometer, fig.2.4.3. This instrument was

designed specifically for use with Solex air gauging units which operate on a back pressure principle. The measuring orifice was incorporated in a transducer which, when distorted under load, restricted the escape of air to atmosphere. The transducers were in the form of eccentric split rings made from heat-treated silicon steel.

2.5 Test Rig

2.5.1 A test rig, fig.2.5.1(a), was designed and built to simulate conditions of heating and loading on a small section of the tool tip approximating in area to that encountered during machining on a lathe. This was accomplished by retaining a tool tip in a split spherical housing, figs.2.5.1(b) and (c), which, when located in its hemispherical seating in the water-cooled horizontal beam, had three rotational degrees of freedom for ease of adjustment. The horizontal beam was mounted on two large compression springs placed over the pillars. A setting piece, fig.2.5.1(d), was used with its top face compound-angled to -6° and -4° to achieve the correct tool tip orientation. This setting was maintained throughout each test by securing the spherical tool tip housing in the water-cooled horizontal beam by means of a hemispherical retaining clamp.

2.5.2 Loads were gently applied direct to the horizontal beam which compressed the supporting springs until the tool tip contacted a heated anvil made of Stellite 80, fig.2.5.2, for the required period. Removal of the load separated the tip from the anvil rapidly, thus simulating the sudden removal of load to which the tip was subjected at the end of a cut on the lathe.

2.5.3 Heat was supplied to the anvil, mounted on a susceptor, (see fig.2.5.1), from a 12 kW Radyne inductance heater equipped with

automatic timing and manual control. The temperature of the anvil was monitored by a NiCr/NiAl thermo-couple and a Comark electronic thermometer, type 1609, fig.2.5.3.

2.5.4 Tests were carried out using inductance coils of different diameters and number of turns to vary the rate of heating. Each coil was calibrated for heat output to the susceptor from given power inputs over the entire working range.

2.5.5 To minimise the effects of scaling due to oxidation of the heated components on the test rig, a perspex cover was made so that the enclosed atmosphere could be purged prior to and during each test run, fig.2.5.5.

2:6 Modified Test Rig

2.6.1 Following the completion of the initial experiments on the test rig, it was modified, fig.2.6.1(a), in an endeavour to change the static mode of testing to a dynamic one whereby small sections of a heated test piece could be cut by a tool tip under load. To accomplish this, a new susceptor, fig.2.6.1(b), was designed with a dovetail machined in the top surface to accommodate a small test piece. Provision was made to index the test piece forward by precise amounts equal to the required depths of cut by means of a micrometer spindle with the barrel attached to the rigid perspex cover. The spindle could thus be withdrawn from the heated zone during tests to avoid oxidation and the possible loss of accuracy when indexing. The test piece locking screws were also accessible through the perspex cover. This allowed remote control of the test piece without the time-consuming procedure of disconnecting the purging gas and water supplies and removal of the perspex cover between tests on repeated runs.

2:7 Shaping Machine

2.7.1 Tests with the modified rig were disappointing. The tool tip did not cut through the heated test piece as expected and it became apparent, after several attempts with different loads and depths of cut, that the "dead" weight method of simulated cutting would not be successful with the existing test rig. However, during cutting on a shaping machine, fig.2.7.1, the work-piece was static. The tool was mounted at the front of a horizontal ram which had a reciprocating motion and cutting took place during the forward stroke only. At the end of the backward stroke the work was in-fed automatically by means of a feed screw and nut mechanism. Depths of cut were controlled by adjustment to the tool holder by means of a screw with a graduated collar. It was thus possible to control the cross-sectioned area of the chip removed during each cutting stroke. Movement of the ram resembled simple harmonic motion in that acceleration was at a maximum at the beginning and at the end of the stroke. In order to minimise impact, the work-piece was positioned as near as possible to the back of the stroke so that the tool tip was accelerating and the velocity still low at commencement of cutting. A discarded lathe test piece of EN30(B) with the end spigots removed and machined flat was used as the work-piece material. Cutting geometry was maintained by using the standard SPK tool holder previously modified to suit the Mecalex dynamometer.

2:8 Electron Microscopy

2.8.1 An AEI EM6G high resolution general purpose transmission electron microscope, giving magnitudes up to 120,000X was used to examine replicas of fracture surfaces of the tool tips. Some of the replicas were shadowed with aluminium to increase the relief effects.

2:9 Crack Detection

2.9.1 At regular intervals through the research programme, the tool tips were checked for cracks using the Ardrox 985 fluorescent penetrant flaw detection process. Some cracks which initiated at, or reached the surface of the tip fluoresced clearly against the darkened background under ultra-violet light.

2.10 High Speed Photography

2.10.1 Machining at high speeds renders normal visual observation inadequate, and high speed photography offered the opportunity of viewing the process in slow motion. Several 100 ft lengths of 16 mm film were taken using a Hycam high speed camera model number K20S4E with a speed range of 20 frames per second to 11,000 frames per second. Uniform illumination was achieved with a bank of photo-flood lamps.

CHAPTER 3

OBSERVATIONS AND EXPERIMENTAL RESULTS

3:1 Steel Analysis

3.1.1 A typical analysis for test piece material is shown below - the specification for EN30(B)* is given for comparison:-

Element	Weight % EN30(B) Specification	Weight % Test Piece Composition
Carbon	0.26 - 0.34	0.26
Nickel	3.90 - 4.30	4.15
Chromium	1.10 - 1.40	1.27
Manganese	0.40 - 0.60	0.53
Molybdenum	0.20 - 0.40	0.20
Silicon	0.10 - 0.35	0.24
Sulphur	0.05 max.	0.028
Phosphorus	0.05 max.	0.020

3:2 Properties of the Tool Tips

3.2.1 In view of apparent differences, (see Section 3.2.2), in the "comb" cracking behaviour of tool tips used in the present work compared with those of Miles[11] and Webster[21], it was necessary to carry out a series of investigations into three categories of tip. Type SN37, purchased in 1973, was used in the present work, whereas type SN37 used by Miles[11] was purchased in 1968; they are designated SN37 (1973) and SN37 (1968) respectively. The tips used by Webster[21], SN56, were of the same material and area of cross-section but of reduced thickness.

3.2.2 An initial qualitative analysis of tips used in the present work showed the following composition:-

* Hardness 280 HV.

Major component - Aluminium oxide

Minor component - Calcium

Trace elements - Zirconium

Gallium

Manganese

Titanium

For comparison, a more precise analysis was carried out for all the tip types. Results are shown below:-

ELEMENT wt %

Tip Type	CaO	MgO	SiO_2	Fe_2O_3	Al_2O_3
SN56	0.1	0.28	0.10	0.07	Remainder
SN37 (1968)	0.03	0.31	0.10	0.07	Remainder
SN37 (1973)	0.21	0.1	0.06	0.20	Remainder

The following elements were also detected below 0.1%:- Manganese, sulphur, phosphorous, nickel, chromium, molybdenum, niobium, titanium, copper, zirconium and barium.

3.2.3 Bend tests were undertaken to ascertain the values of Young's Modulus for the three types of tool tips. Sixteen samples of each batch were tested and the averages are shown below, all of which lie within a band of 10%:-

Tip Type	E Value
SN56	3.27×10^3 N/mm^2
SN37 (1968)	4.74×10^3 N/mm^2
SN37 (1973)	3.37×10^3 N/mm^2

Figs.3.2.3(a) to (c) all show elastic behaviour up to the

point of fracture.

3.2.4 Differential Thermal Analysis carried out by Dr.J.Sharp of the Ceramics Department of Sheffield University revealed no phase changes occurring over the working temperature range, fig.3.2.4.

3.2.5 A Leitz micro-hardness testing machine was used in an attempt to determine hardness levels on the three types of tool tips. At loads below 20 grams no indentations were visible, but at loads greater than 20 g an irregular hole was obtained due to a total collapse of the material around the indentation, so giving unsatisfactory results, fig.3.2.5. Similar unsatisfactory results were obtained using a Vickers Pyramid hardness testing machine.

3.2.6 A number of miscellaneous thermal shock tests were carried out for the purpose of comparing the types of fracture:-

(i) Pekelharing[10] induced "comb" cracking by pouring molten steel onto the exposed corner of an alumina tool tip embedded in moulding sand. A similar test was carried out by melting a thin rod of low carbon steel by induction heating; the molten metal was directed onto the corners of several tool tips embedded in moulding sand. No "comb" cracking, or any other type of cracking, was observed.

(ii) Nine tips were heated uniformly in a furnace to temperatures ranging between 200°C and 1000°C, at temperature increments of 100°C, quenched in liquid nitrogen and subjected to light impact by dropping onto concrete from a height of 4 ft. No fracture or cracks were observed in any of the specimens.

(iii) Similar tests to those above were carried out by quenching in water and again dropping onto concrete from a height of 4 ft. The following results were obtained:-

Temperature °C	Result: Quenched in H_2O and dropped from 4 ft
200	Uncracked
300	Cracked
400	Broken in large pieces
500	Disintegrated
600	"
700	"
800	"
900	"
1000	"

Figs.3.2.6(iii) (a) and (b).

(iv) Two tool tips were broken catastrophically by passing the corner as rapidly as possible through a carbon arc, fig.3.2.6(iv).

(v) Similar results were obtained using an oxy-acetylene flame, fig.3.2.6(v).

(vi) Several tips were heated in the test rig using a four-coil inductance heater without the application of any load. During one test the susceptor melted, but no damage occurred to the tool tips.

3:3 Lathe Tests

3.3.1 Lathe tests were carried out in an attempt to induce "comb" cracking along the cutting edge of the alumina tool tips, based upon the work carried out by Miles[11], fig.3.3.1(a). The tool tips, tool-holder and test piece material were all of the same types used by Miles in order to reproduce as closely as possible similar machining conditions. Cutting velocities of between 500 and 2500 ft/min (150 to 760 m/min), were related to depths of cut ranging from 0.05 to 0.25 in

(1.25 to 6.25 mm) with a constant feed rate of 0.005 in/rev (0.125 mm/rev), fig.3.3.1(b). No "comb" cracks were observed, even at metal removal rates at over twice the Miles threshold.

3.3.2 The above tests were repeated with the feed rate doubled to the value of 0.010 in/rev (0.25 mm/rev). These tips also failed to exhibit "comb" cracks, fig.3.3.2.

3.3.3 Exhaustive lathe tests at machining rates above the "comb" crack threshold established by Miles, (see fig.3.3.1(a)), were repeated for each of the four possible chip-breaker positions at 0.010 in/rev (0.25 mm/rev) feed rates. No "comb" cracks were observed, fig.3.3.3.

3.3.4 Pekelharing[10] stated that "comb" cracks occurred during the first cut and only became visible when a second cut was taken with the same tip due to the fact that "steel was forced into them". Therefore, some selective lathe tests covering the entire range of cutting velocities, depths of cut, feed rates and chip breaker positions already used, were repeated in an attempt to reproduce Pekelharing's observations. These tips also failed to exhibit any cracking, fig.3.3.4.

3.3.5 Miles[11] also established a "comb" crack threshold by relating cutting velocities to feed rates whilst keeping a constant depth of cut, fig.3.3.5(a). Similar tests with cutting velocities between 500 and 2500 ft/min (150 to 760 m/min) were related to feed rates ranging from 0.005 to 0.03125 in/rev (0.125 to 0.794 mm/rev) at a constant depth of cut of 0.100 in (2.5 mm) at each of the four possible chip-breaker positions with no evidence of "comb" cracking, fig.3.3.5(b).

3.3.6 Using the variable parameters of cutting velocity and feed rate with the depth of cut constant, similar second cut tests to those carried out in section 3.3.4 showed no "comb" cracking.

3.3.7 During the tests carried out in section 3.3.6, however, catastrophic failure occurred on re-engagement when the feed rate was 0.028 in/rev (0.71 mm/rev) or above, at cutting velocities of 1000 ft/min (304 m/min), fig.3.3.7.

3.3.8 Several tests were carried out at a cutting speed of 4500 ft/min (1371 m/min) at a depth of cut of 0.050 in (1.25 mm) with a feed rate of 0.005 in/rev (0.125 mm/rev). Each corner was used twice over the entire 10 in (252 mm) length of test piece. No "comb" cracks were seen. Fig.3.3.8 illustrates swarf behaviour at high cutting speeds.

3.3.9 Catastrophic failure occurred on the first engagement when the feed rate was 0.035 in/rev (0.89 mm/rev) or above, at a cutting speed of 1000 ft/min (304 m/min) and depth of cut of 0.050 in (1.25 mm).

3:4 Dynamometer Tests

3.4.1 It was desirable to have some knowledge of the level of loading during the cutting process in order to ascertain any possible correlation with the modes of failure of the tool tips. A duplicate tool holder, fig.3.4.1, was reduced on the shank to suit a Mecalex two-force pneumatic dynamometer.

3.4.2 A number of tangential and axial force readings up to the value of 130 lbf (578N) were recorded for depths of cut between 0.30 and 0.70 in (0.75 to 1.75 mm) at a cutting velocity of 1000 ft/min (304 m/min) with a feed rate of 0.005 in/rev (0.125 mm/rev). Average values of force readings were plotted against depths of cut, fig.3.4.2(a) and against each other, fig.3.4.2(b). Reductions in the test piece diameters did not lead to any apparent change in the dynamometer force readings.

3.4.3 In another series of dynamometer tests the feed rate was doubled to a value of 0.010 in/rev (0.25 mm/rev) and the depth of cut varied to between 0.005 and 0.070 in/rev (0.125 and 1.75 mm/rev). Average force readings to values of 225 lbf (1000N) were plotted against depths of cut, fig.3.4.3(a), and against each other, fig.3.4.3(b).

3:5 Temperature Measurements

3.5.1 Several different methods of temperature measurement of the tool/chip interface during machining were tried. All of the results were unacceptable. (See Appendix II).

3:6 Interrupted Cutting

3.6.1 It was observed that catastrophic tool tip failure, (Reference 3.3.7), invariably occurred at the moment of re-engagement at a feed rate of 0.028 in/rev (0.71 mm/rev) or above, when the cutting velocity was 1000 ft/min (304 m/min). These results were unaffected by varying the depths of cut over a range of values from 0.050 to 0.150 in (1.25 to 3.75 mm) with cutting velocities between 750 ft/min and 1000 ft/min (228 m/min and 304 m/min). Tool tips were carefully checked for damage after the first cut by several different methods including the Ardrox 985 fluorescent penetrant flaw detection process, visual and microscopic examination. No evidence of cracking on the tip was ever detected. Fig.3.6.1.

3.6.2 Some interrupted cutting tests were undertaken using slotted test pieces, fig.3.6.2, with a 0.5 in slot between each journal. Feed rates ranging from 0.005 to 0.025 in/rev (0.125 to 0.625 mm/rev), (Ref. Table 1), all below the critical value of 0.028 in/rev (0.71 mm/rev), and depths of cut of 0.050 and 0.010 in (1.25 mm and 2.50 mm) were used. Catastrophic failure was not observed.

TABLE 1

Cutting Speed Ft/Min	Depth of Cut In	Feed In/Rev	No.of Cuts	Result
1000	0.050	0.005	2	Unbroken
"	"	0.010	2	"
"	"	0.014	2	"
"	"	0.020	2	"
"	"	0.025	2	"
"	0.10	0.005	2	"
"	"	0.010	2	"
"	"	0.014	2	"
"	"	0.020	2	"
"	"	0.025	2	"

3.6.3 During his research on "comb" cracking, Pekelharing[10] established that this phenomenon was not time-dependent. In order to ascertain whether there was a time-dependency between re-engagement and the incidence of catastrophic failure after disengagement of the first cut, a test piece was machined with slots 32, 16, 8 and 4 mm widths with standard 25 mm long journals between them, fig.3.6.3. An additional slot for the purpose of tool "run-out" was provided after each pair of 25 mm journals. Thus, it was possible to machine a 25 mm length of test piece and then permit the tool tip to traverse a known slot length before engagement with the next 25 mm long journal, followed by "run-out" at the next slot if failure did not occur. Interrupted cutting tests were carried out at a velocity

of 1000 ft/min (304 m/min) with a feed rate of 0.03125 in/rev (0.79 mm/rev) at 0.050 in (1.25 mm) depth of cut to conserve material.

Cutting velocity	=	1000 ft/min
Speed of 4 in diameter workpiece	=	15.9 rev/sec
Feed	=	0.0312 in/rev
Tool tip traverse in 1 second	=	15.9 x 0.03125
	=	0.497 in
Time for tool to traverse 0.16 in slot	=	$\frac{0.16}{0.497}$
	=	0.322 seconds.

Results showed that catastrophic failure on re-engagement was not time-dependent to a value of 0.322 seconds, the time taken for the tool to traverse the 0.160 in wide slot.

3:7 Taper Turning

3.7.1 Interrupted cutting tests, (Ref.Section 3.6.3), showed that catastrophic failure on re-engagement was not time-dependent to the time scale of the narrowest slot and it was apparent that an alternative method would be necessary to establish at which point tool tip damage occurred. Since there was no facility for changing the feed rate during machining on the lathe, an alternative method of changing the metal removal rate with the cutting speed and feed rate held constant was to reduce the depth of cut. Previously prepared tapered test pieces were used to provide a means of accurate control over the cutting cycle. Three test pieces were machined, tapering in diameter over the length of journal C, at 0.060 in (1.5 mm), 0.080 in (2.0 mm) and 0.10 in (2.5 mm) respectively. Each test piece was machined at 1000 ft/min (304 m/min) with a feed rate of 0.03125 in/rev (0.79 mm/rev) with an initial depth of cut of 0.050 in (1.25 mm) over the

entire 10 in length. Re-engagement in each case was successful on the now parallel journals, which were machined over the whole length, and in each case catastrophic failure occurred when another cut was attempted. Tests were repeated using a 0.1 in taper on diameter over 10 in and 5 in lengths of journal, with the same result. Journal C was gradually reduced in length, whilst the 0.1 in taper was maintained, and failure on the first re-engagement occurred consistently at lengths of 1.25 in and below. Results are shown in Table 2.

TABLE 2

Taper In	Angle Degrees	1st Cut Taper	2nd Cut Parallel	3rd Cut Parallel
0.03 in 10	0° 10'	Unbroken	Unbroken	Fail
0.04 in 10	0° 14'	"	"	Fail
0.05 in 10	0° 17'	"	"	Fail
0.05 in 5	0° 34'	"	"	Fail
0.05 in 2.5	1° 9'	"	"	Fail
0.05 in 2	1° 26'	"	"	Fail
0.05 in 1.75	1° 38'	"	"	Fail
0.05 in 1.5	1° 54'	"	Fail	-
0.05 in 1.25	2° 17'	"	Fail	-
0.05 in 1	2° 52'	"	Fail	-
0.05 in 0.75	3° 49'	"	Fail	-
0.05 in 1.5	1° 54'	"	Unbroken	Fail
0.05 in 1.5	1° 54'	"	"	Fail
0.05 in 1.25	2° 17'	"	Fail	-
0.05 in 1.25	2° 17'	"	Fail	-

3.7.2 The foregoing results indicated that tool life might be increased by a gradual reduction of the cutting forces and, hence, a much less drastic rate of cooling prior to disengagement. To test this theory, two test pieces were prepared with three consecutive 0.1 in tapers on 3 in journal lengths, fig.3.7.2(a). The cutting speed, depth of cut and feed rates were kept constant at 1000 ft/min, 0.050 in and 0.03125 in/rev respectively. All three tapers were successfully

machined without interruption, fig.3.7.2(b), and a thorough examination of the tool tip corner revealed no damage. Results are shown in Table 3 below:-

TABLE 3

Taper In	Angle Degrees	1st Cut Taper 1	2nd Cut Taper 2	3rd Cut Taper 3
0.05 in 3	0° 57'	Unbroken	Unbroken	Unbroken
0.05 in 3	0° 57'	"	"	"

3:8 Test Rig

3.8.1 A series of investigations were carried out on the test rig in which the tool tips were subjected to loads ranging between 14 lbs and 70 lbs and temperatures from 240°C to 1100°C. Heating was achieved by induction using a variety of coils. Figs.3.8.1(a) to 3.8.1(e) illustrate the thresholds of failure for each coil. Figure 3.8.1(f) shows a typical tool tip failure. The modified test rig is referred to in Appendix 2.

3:9 Shaping Machine

3.9.1 Tests carried out on a shaping machine were at a fixed cutting speed of 25 ft/min (7.6 m/min) with depths of cut ranging between 0.010 in (0.25 mm) and 0.040 in (1.0 mm) and in-feed ranging from 0.010 in (0.25 mm) and 0.040 in (1.0 mm). Fig.3.9.1 shows a relationship between the number of cutting strokes and the area of cross-section of cut.

3:10 Crack Detection

3.10.1 Some cracks on the corners of the tool tips could not be

detected using the dye penetrant and ultra-violet light method. In such cases it was discovered that macroscopic examination with background illumination revealed the presence of a crack by a shadowing effect due to a break in the translucency of the alumina around the edges.

3:11 Electron Microscopy

3.11.1 A selection of electron micrographs are shown in figs. 3.11.1(a) to 3.11.1(h), showing a number of different characteristics.

CHAPTER 4

DISCUSSION

The incidence of "comb" cracking in alumina tool tips during turning on a lathe appears to be a common phenomenon. Pekelharing[10] et al established well-defined thresholds above which all of the tips exhibited "comb" cracks when certain values of the cutting velocity and feed rate were exceeded. He defined the critical value as a "rubbing energy" equivalent to 1kW on the rake face of the tool, in the region of the wear crater where the cracks appeared.

During attempts to establish how the cracks originated and at which stage of the machining cycle they occurred, he first examined the effects of cutting times. Extended machining as a possible cause of cracking was eliminated when the cutting cycle was reduced to a period of five seconds which, however, did not prevent the formation of "comb" cracks. It appeared that cracking occurred either at the commencement of cutting due to the ultra rapid heating of the tool tip corner whilst the remainder of the tool was relatively cold, or during cooling by a reversal of the heating sequence after disengagement from the workpiece.

Pekelharing retarded the cooling rate by means of a gas flame of "appropriate temperature" directed on to the tool tip at the moment of disengagement, followed by a "tea-cosy" of insulating material placed over the tip. This did not prevent the formation of cracks. Cutting was then commenced with a lower temperature start and finish by means of a reduction in the feed rate at engagement and disengagement to values below the "comb" crack threshold. The centre section

of the test piece was machined above the threshold value, but "comb" cracking of the tips still occurred.

Pekelharing deduced that plastic deformation had taken place in the surface layers of the tips within a few milli-seconds of cutting when the temperature difference between the upper and lower regions was at a maximum. Cracking subsequently occurred in the weakened surface structure on cooling due to the tensile stress which developed when the temperature difference between the upper and lower regions was again at a maximum. The cracks were thus confined to the surface layers and resulted from both plastic and elastic deformation.

El-Zahry and Dugdale[22] established "comb" crack thresholds for three types of alumina tool tips, (two grades), during machining tests on four types of alloy steel, tempered to six discrete hardness values between the range 127 and 650 VPN. They showed that "comb" cracking occurred at lower cutting speeds as the hardness of the workpiece increased. They also investigated the effects of increasing the negativeness of the rake angle with other machining parameters held constant. It was established that the number of cracks increased as the negative rake was increased.

Pekelharing [10] described the physical dimensions of "comb" cracks in terms of length, depth and spacing, although as yet no-one appears to have determined whether they were intergranular or transgranular, or a combination of both. The direction of the cracks did not appear to be influenced by the approach angle of the tool and, hence, the direction of sliding of the chip, since they were always perpendicular to the cutting edge. Sibley and Allen[8] produced similar cracks in various ceramic and cermet materials during their work on friction

and wear behaviour at high sliding velocities and temperatures. In these cases the cracks were always perpendicular to the direction of sliding, although they appeared to be longer and deeper than "comb" cracks in the tool tips and were specified as being transgranular. Whether or not "comb" cracks contribute directly to catastrophic failure has yet to be established. It is reasonable to assume that any crack or flaw in the structure must be considered as undesirable when the ultimate strength of the tool tip is considered.

In the present work the SPK type SN37 (1973) tool tips used failed to exhibit "comb" cracks when machining at rates some four times greater than the threshold value defined by Miles[11]. Catastrophic failure occurred and other types of cracks were sometimes found, but never "comb" cracks. Chemical and "stiffness" analyses were undertaken in an attempt to elucidate these differences.

Chemical analyses of the tool tips revealed that CaO was the major additive, but in the tool tips used by Miles[11] and Webster[21] MgO was identified, (See Appendix IV). Both magnesia and calcia are known to be grain growth inhibitors. In the Al_2O_3-CaO system a liquid phase of the compound $3CaO5Al_2O_3$ occurred at 1680°C whereas in the Al_2O_3-MgO case a liquid phase only appeared at temperatures in excess of 1800°C. As sintering was carried out at 1750°C, the presence of a liquid phase may well be a possible explanation for the apparent change in properties of the tool tip that inhibited the formation of "comb" cracks.

According to Kingery[23], when a liquid phase is present during sintering a re-arrangement of the solids occurs such that the structure approaches the densest packing of the crystallites by their

sliding on the liquid film which separates them. If this occurs and the grain growth is also effectively retarded by the calcia-alumina phase, then it would seem reasonable to expect changes in some of the mechanical properties of the tool tips. It is generally accepted that the strongest tool tips have a fine uniform grain size and approach the theoretical density of α-Al_2O_3. However, it is doubtful if a liquid phase would bring about any marked improvement in the crystal symmetry of the structure which is usually of a low order in sintered products. Neither would it be anticipated that the random orientation of the grains would show a more ordered arrangement. It seems reasonable, therefore, to assume that tool tips manufactured by these sintering processes would be subjected to the same degree of residual stress from anisotropic thermal contraction of individual grains on cooling, with or without the presence of a liquid phase. In any event, the ultimate strength of the tool tips would probably be limited to the strength of the grain boundary material. It may be that the "compact" intergranular compound formed from the solidification of a liquid phase is stronger than the probably discontinuous intergranular medium $MgAl_2O_4$ produced as a result of solid sintering. It is suggested that the presence of the intergranular phase inhibited the formation of "comb" cracks.

To eliminate the possibility that phase changes occurred in the tool tips during machining, a differential thermal analysis of the tool tip material was carried out. No changes were revealed up to a temperature of 1340°C.

Stiffness values are significant in terms of thermal and mechanical stress behaviour within the elastic range. Young's modulus of elasticity for the three types of SPK tool tips was lower than the value specified[2] by two orders of magnitude. Whilst this difference was excessive, and probably attributable to the method of testing, the individual values were reasonably uniform and were all derived from the same test regime. The average E value for the 1968 (Miles) tips was 41% higher than the figure for the 1973 (Telfer) tips and 45% higher than the SN56 (Webster) type, (See Appendix IV).

Stress induced by thermal differences is given by the equation:-

$$\sigma = E \alpha \delta T$$

where α is the co-efficient of linear expansion and δT the temperature interval. Thermal stress was also enhanced by high thermal gradients in the tool tip corners due to the low conductivity of alumina[24]. Assuming that the conductivity and expansion values of the 1968 and 1973 materials were not dissimilar, the lower E value of the latter type would allow the absorption of a higher stress for the same value of strain.

From the instant of engagement the tool tips were subjected to mechanical and thermal stresses and during machining a state of dynamic equilibrium was achieved. Thus, cutting over an indeterminate length was possible whilst the dynamic balance was not upset until the point of disengagement.

It was suspected that abrupt disengagement when the feed rate was in excess of 0.028 in/rev was the likely source of trouble responsible for tool failure at re-engagement. This was more evident when previously prepared tapers were machined off and re-engagement

was successful. The cutting process was, therefore, equivalent to one in which the depth of cut was gradually decreased to zero over a prescribed length. After a taper was machined off and a second cut was taken on a now parallel journal, tool failure occurred again when a third cut was attempted. These findings were substantiated when interrupted cutting was carried out on three consecutive tapers without tool failure. A careful examination of the tool tip corners revealed no cracks or any other visible damage, although at the engagement of the second and third tapers the tool tips were subjected to the same conditions as those encountered on re-engagement of parallel journals, or when the length of the taper was 1.25 in or less, which had always resulted in catastrophic failure.

It would appear from the above that the strains arising from the balanced stresses during cutting, (i.e. mechanical and thermal), did not exceed the elastic limit of the material when they were diminished slowly and simultaneously. However, abrupt disengagement introduced imbalance to the system by the sudden removal of the stresses due to the cutting forces, whilst the stresses from the thermal effects were still active. Under these conditions it was possible that plastic deformation in the continuous grain boundary network, or in the crystallites, occurred beneath the surface layers. This would account not only for the absence of visible "comb" cracking but also for catastrophic failure at re-engagement.

El-Zahry and Dugdale[22] developed a model, fig.4.1, which illustrated a mechanism for crack formation when stress reversal occurred at disengagement. Cracks were the result of compressive yield in the alumina when the chip/tool interface temperature

exceeded 600°C during cutting and the cooling slope passed through the tensile fracture line. It would appear from the model that the rate of cooling did not affect the final result once compressive yield had taken place. If, however, the rate of cooling was a critical factor, as was indicated from the interrupted taper turning, then plastic yield could only have occurred immediately after disengagement provided that the temperature attained at the tool tip was of a sufficiently high value.

The E value of the tool tips would also be affected to some extent by the degree of porosity and its distribution., (see Appendix V). Three types of pore were identified in the micrographs of the fractured SN37 1973 tips. The smallest, which was characteristic of sintered α-alumina, was densely concentrated in some crystallites where it formed patterns of radial and straight parallel lines. Fracture was influenced in such cases and cleavage had followed through the pore patterns. This is typified in figs.4.2(a) and 4.2(b), which show the terraced plateau effects and the accompanying porosity.

The second type of pore, fig.4.3, was evident at grain boundaries and appeared to have formed as a semicontinuous "phase" parallel to the boundaries. This is, however, contrary to the generally accepted theory for sintered alumina in which diffusion processes tend to leave grain boundaries and adjacent areas relatively free from pores, Coble and Burke[25] et al.

The remaining type appeared to be isolated spherical crystals, (positive or negative?), surrounded completely or partially by a chain of smaller interconnected pores, reminiscent of the negative crystal pores which form in urania during sintering, (ref.Kingery[23],

p.204), figs.4.4(a) and (b). These pores were numerous but randomly distributed in fracture surfaces and at grain boundaries.

Well defined tool tip failure thresholds were established for each of the five different induction coils used on the test rig. Tool tip failure for a given combination of load and temperature was not affected by the rate at which the heat was applied. Levels of failure were the same whether the anvil was pre-heated or at room temperature prior to contact with the tool tip. Failure was almost identical to the type of fracture obtained during machining on the lathe. Fig.4.5 illustrates the modes of failure. Crack initiation was at the point between the active and inactive parts of the tool tip edge across the 20° chamfer. Differences in loading and thermal gradient would in all probability have rendered this part of the cutting edge of the tool tip most vulnerable to cracking as a precursor to catastrophic failure. Propagation from the edge crack followed a path across the corner of the rake face and down into the body of the tip to roughly halfway, in a plane parallel to the vertical corner. From this point to the bottom face, cleavage curved on a plane away from the corner, traversing an increasing area of cross-section. This fracture configuration occurred frequently and was aptly referred to as the "classic" failure.

On occasions a single crack only was observed, either on the front or on the side edge of the tool across the chamfer. Some tips exhibited both cracks and others were cracked across the rake face connecting both edge cracks without fracturing completely, see figs. 4.6(a) and (b). Detection was sometimes difficult and, in such cases, the use of a fluorescent dye was ineffective since it would not

penetrate the crack. These obscure cracks were detected by careful examination with a low-powered eye-glass, using daylight as background illumination. Cracks could be seen as a break in the translucency of the alumina near the edge where the cross-section was at its narrowest. They could not be detected by optical microscopy.

Examination of the broken tip surfaces by transmission electron microscopy showed a combination of intergranular and transgranular fracture, although propagation via the grain boundaries was predominant. Fracture through the crystallites, unaffected by pore concentrations, revealed a system of three-dimensional mutually perpendicular cleavage planes, (see fig.1.1). All of the micrographs showed brittle fracture with no evidence of plastic flow. There was also much evidence of entrapped pores of the types previously mentioned which, according to Coble[17], is attributable to high grain boundary mobility during sintering. The pores, which were originally irregular voids during the cold pressing stage of manufacture, have subsequently changed to symmetrical hollow spheres. The symmetrical shape of the pores was presumably the result of energy balance since there would be different energy levels in the irregular shape of the original voids from cold-pressing. In some micrographs the concentration of pores were of a high order and from their presence in some fracture surfaces it would seem that cleavage had taken place through them in preference to other planes. It is significant that where fractures revealed the "classic" three-dimensional cleavage planes there was little evidence of entrapped pores. The presence of pore concentrations in some of the crystallites would probably have resulted in a reduction in the strength of the tool tips and enhanced the fracture mechanism.

Clearly, the control of "end point" density in alumina tool tips manufactured by a sintering process is a difficult problem which is influenced by a host of variable parameters such as original grain size, temperature, sintering time and additional constituents, etc.

Cutting forces show differing trends for the tangential and axial components. The tangential force graphs resulted in gentle uniform curves with a near linear relationship to the depth of cut. The equations developed by Miles[11] were based on a linear relationship between the power dissipated and the depth of cut which, although disproportionate for shallow cuts due to the corner radius of the tool, provided a satisfactory correlation between theory and practice for deeper cuts.

Tool tip failure on the lathe did not appear to be influenced by the depth of cut. For a criterion of cutting velocity and feed rate, failure still occurred when the depth of cut was reduced drastically, (i.e., halved). In practical terms, the incidence of tool failure was more sensitive to the feed rate than the depth of cut. Miles also suggested that "the cutting velocity carried the most weight in the cracking criterion since its index was more than twice the value of the other two variables". He concluded that a reduction in the cutting velocity could be compensated for by an increase in the depth of cut to maintain a given metal removal rate whilst reducing the incidence of "comb" cracking. Whereas the foregoing comments are probably valid for tool tips in terms of a "comb" cracking criterion, the evidence from this work is in contradiction in terms of metal removal and tool failure. It was found that metal removal rates could be boosted by increasing the cutting velocity and the depth of cut, provided that the choice of feed rate was not greater than the

critical value. Two sets of values of the cutting variables, in terms of metal removal rates, are shown in Appendix VI.

CHAPTER 5

CONCLUSIONS

1. The use of calcia as the main sintering auxiliary, with its associated liquid phase, was thought to be responsible for the following characteristics of the SN37 (1973) tool tips:-

   (i) an increase in thermal shock resistance.

   (ii) the formation of different types of pores and their distribution influenced the mode of fracture.

   (iii) catastrophic failure occurred prior to attainment of conditions necessary to induce "comb" cracking.

2. Provided feeds were below 0.028 in/rev, repeated cuts could be made.

3. Higher feed rates were possible on a single pass above the critical feed rate of 0.028 in/rev but re-engagement would result in the probable loss of the complete tool tip.

4. Repeated passes were possible above the critical feed rate of 0.028 in/rev when a tapered run-out was provided at the end of the cut.

5. Damage was sustained at the instance of abrupt disengagement and on short tapers of 1.25 in long, or less.

6. Fractures on the lathe and test rig initiated at the junction between the active and inactive parts of the tool tip corner.

7. Observations using the test rig showed that both loading and heating were simultaneously required to produce failure.

8. These findings lend support to the view that the major problem associated with the practical utilisation of alumina tool tips is at disengagement rather than at the commencement of or during the machining cycle.

Recommendations for Further Work

In closing, the following recommendations for further research are suggested in the areas of this work which were inconclusive:-

1. Measurement of cutting forces at higher metal removal rates.
2. Correlating the incidence of catastrophic failure to normal and polished tool tips.
3. Correlating the incidence of "comb" cracking to catastrophic failure.
4. Investigating the problem of re-engagement at variable feed rates and cutting speeds.
5. Examination of the fractures obtained in terms of porosity and mode of failure.
6. Re-appraisal of practical methods of temperature measurement.

In view of the significant differences in the properties and performance of the tool tips currently used when compared with those purported to be of the same type, it would seem to be a wise precaution to ensure that subsequent supplies of tool tips were all of the same batch.

Fig.1.1. Typical transgranular fracture. Note the three dimensional mutually perpendicular cleavage planes in the absence of pore concentrations. 20,000 X.

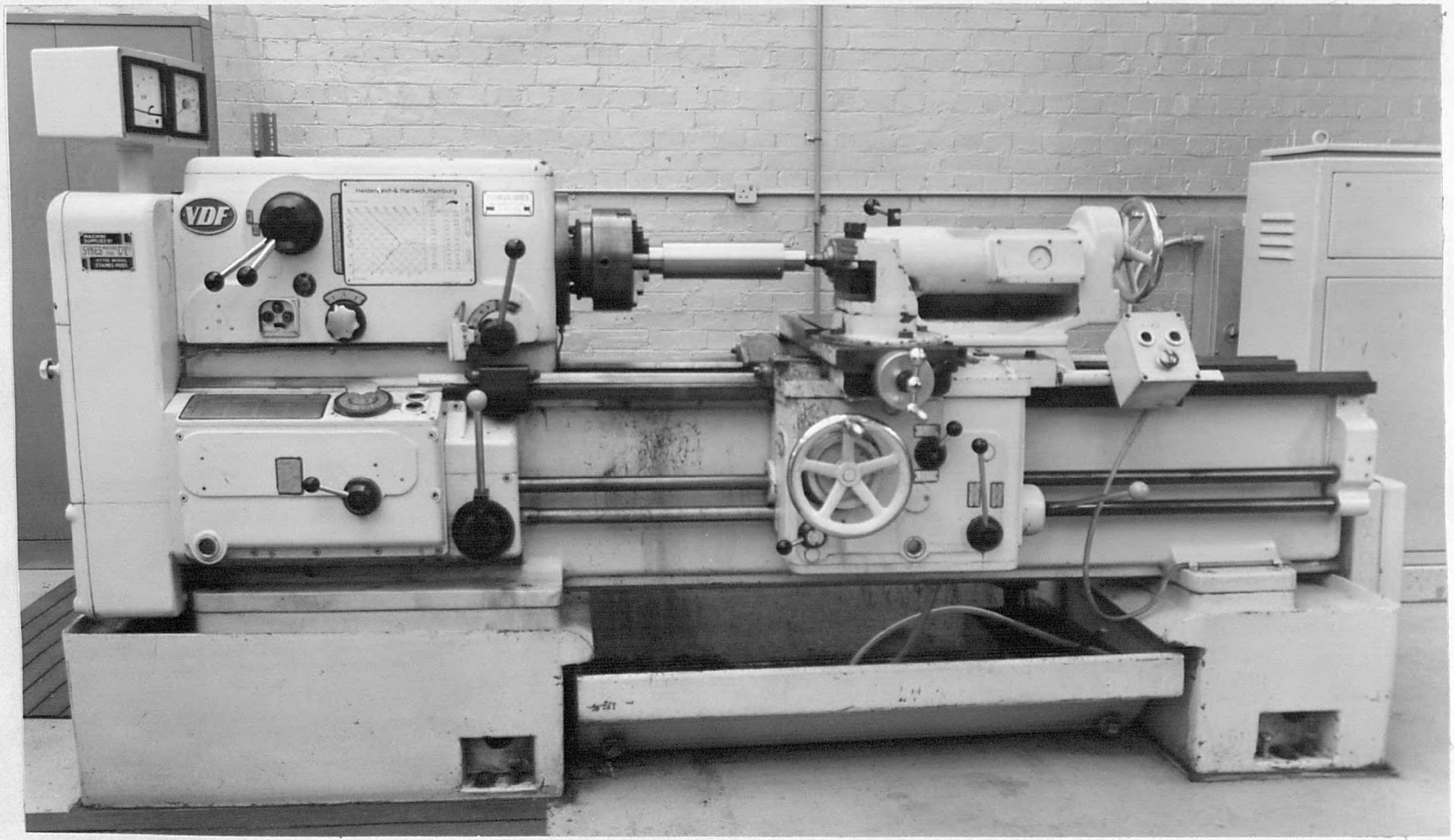

Fig.2.1.1. VDF Lathe.

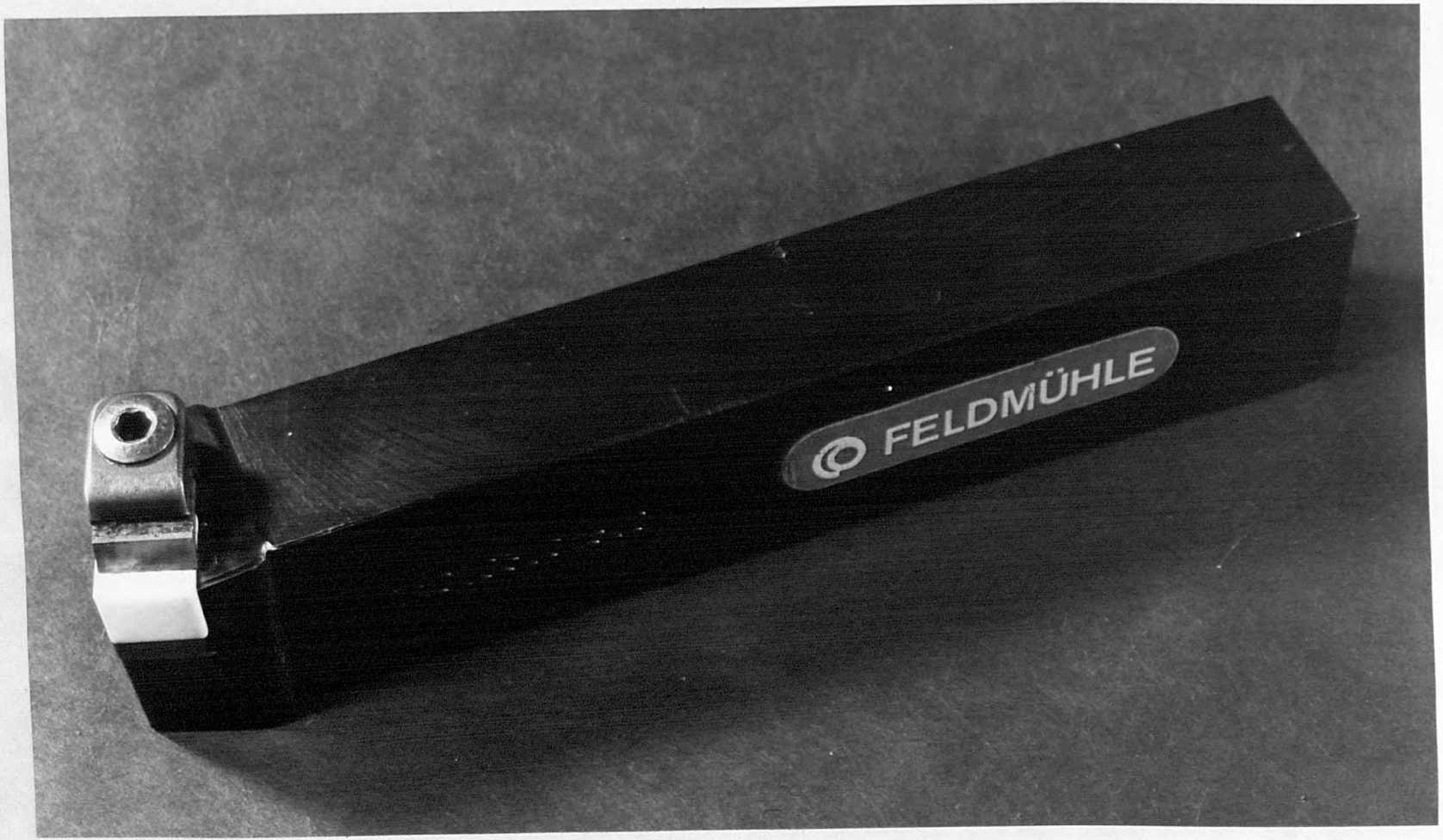

Fig.2.2.1. SPK Tool Holder.

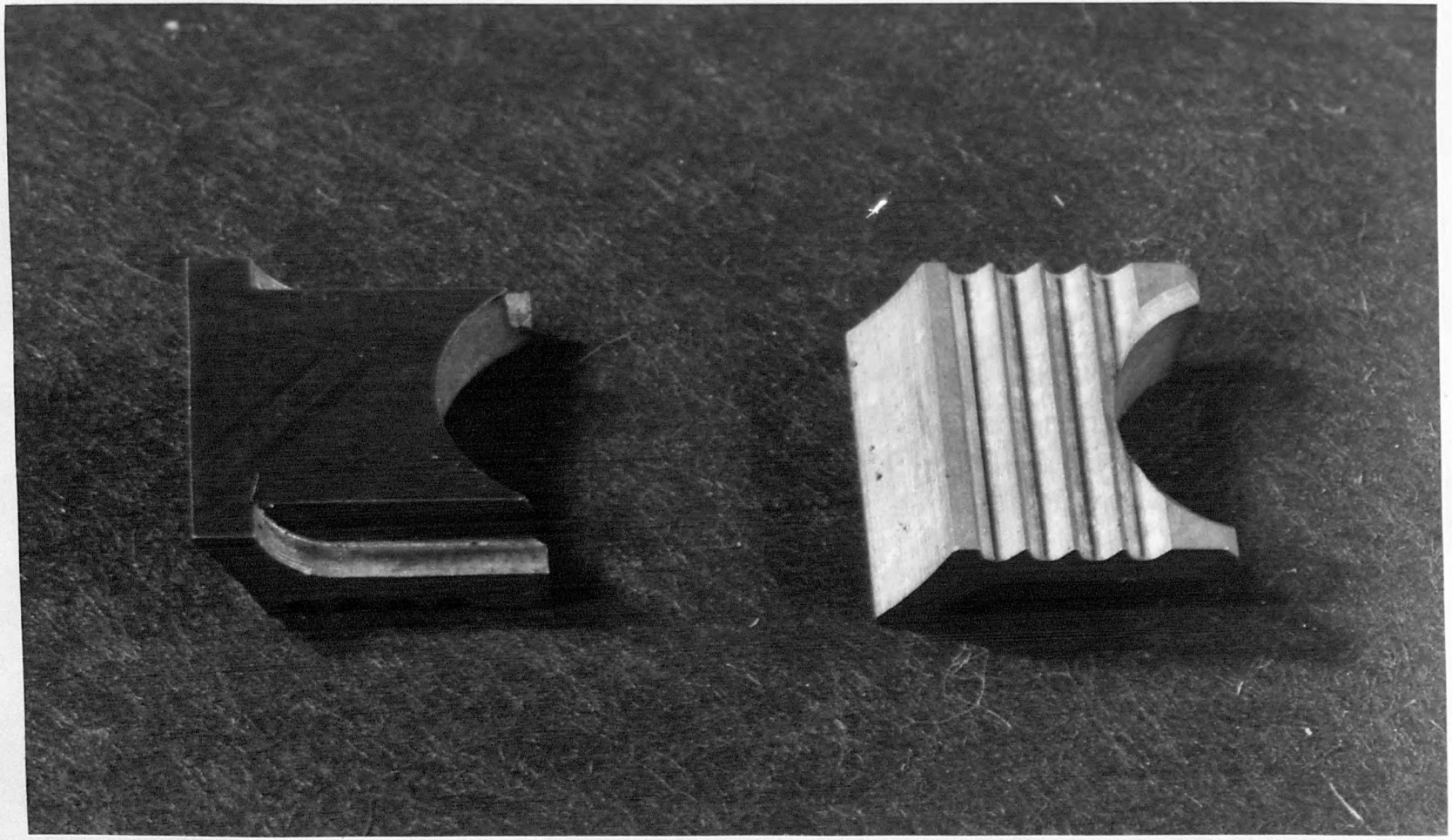

Fig.2.2.2. Tool Clamp/Chip-Breaker. Grooves on top face for adjustment relative to cutting edge. Underside flat for clamping tool tip. Recesses for location of retaining spring.

Fig.2.2.3. TOOL GEOMETRY

Dimensions in mm.

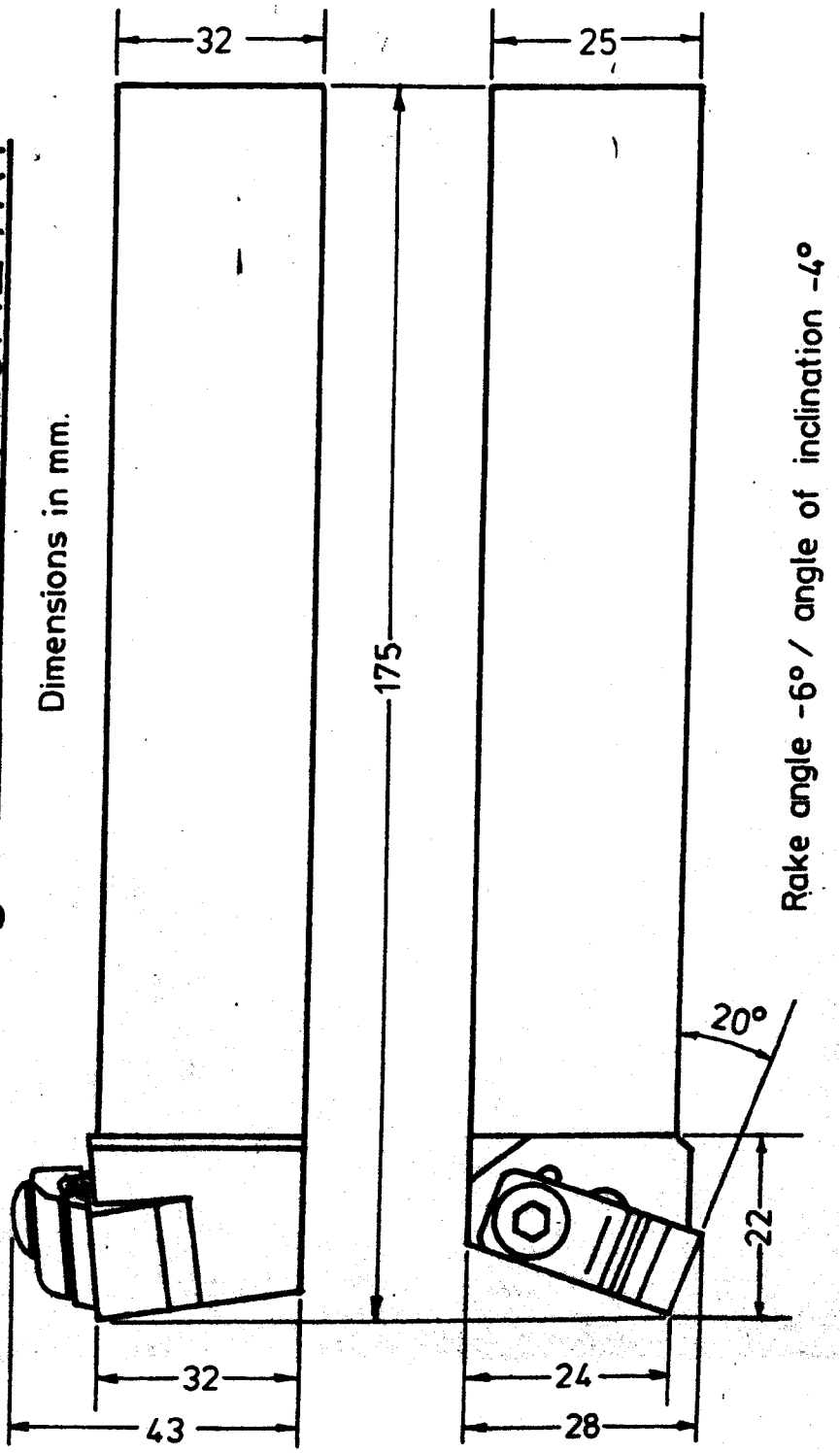

Rake angle -6° / angle of inclination -4°

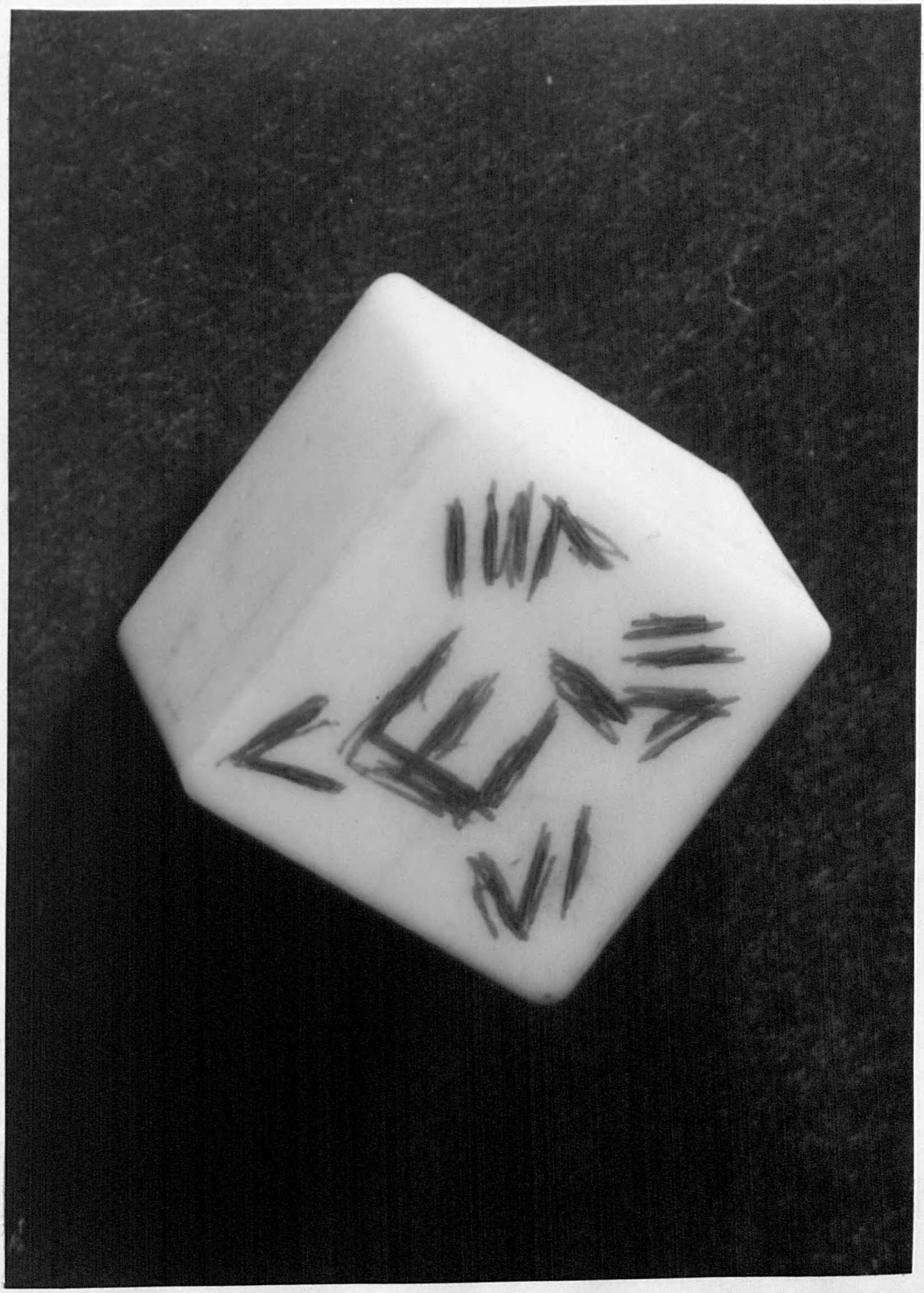

Fig.2.3.1. Alumina Tool Tip.

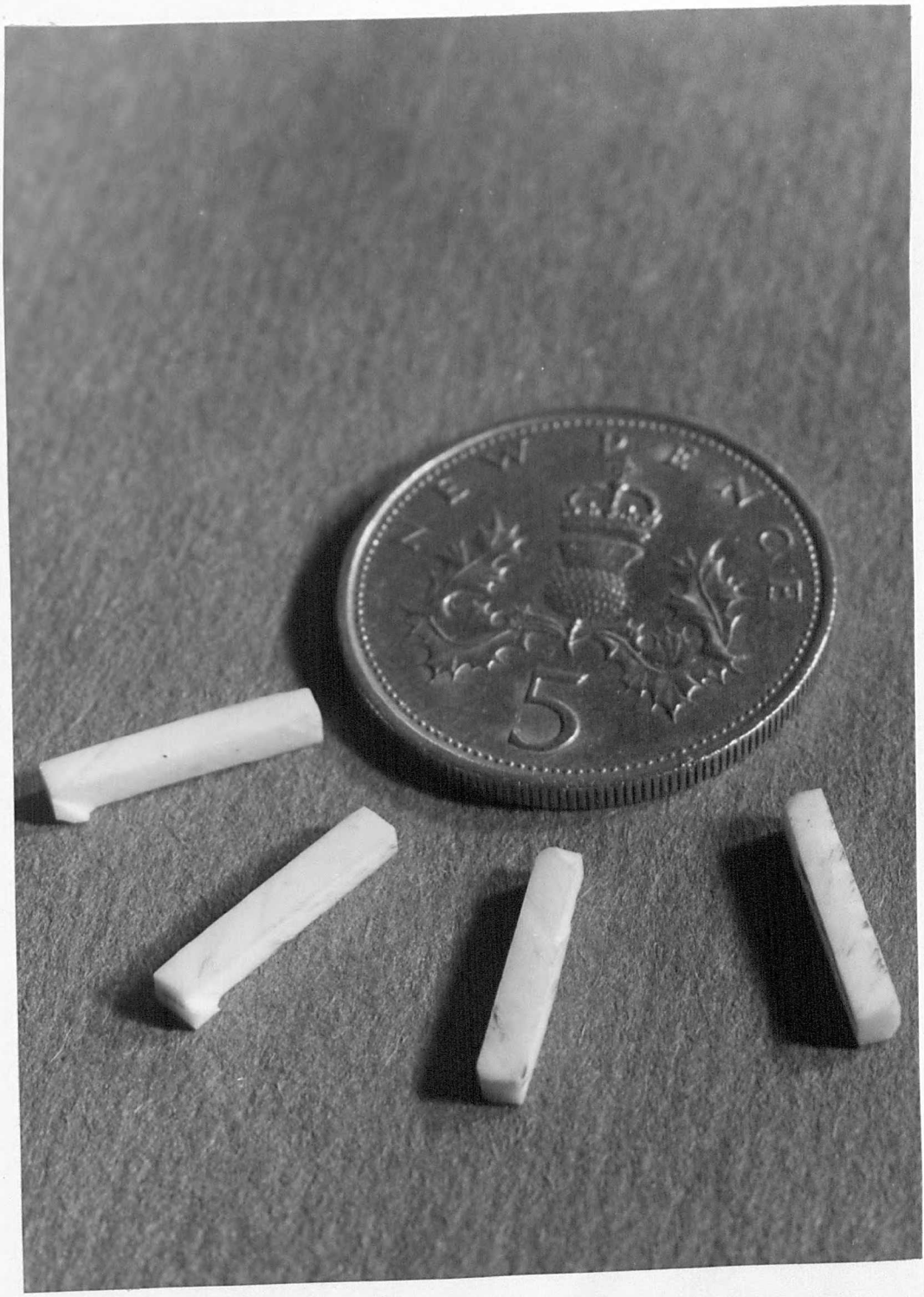

Fig.2.3.3(a). Alumina Prisms.
Cut from tool tips for stiffness tests.

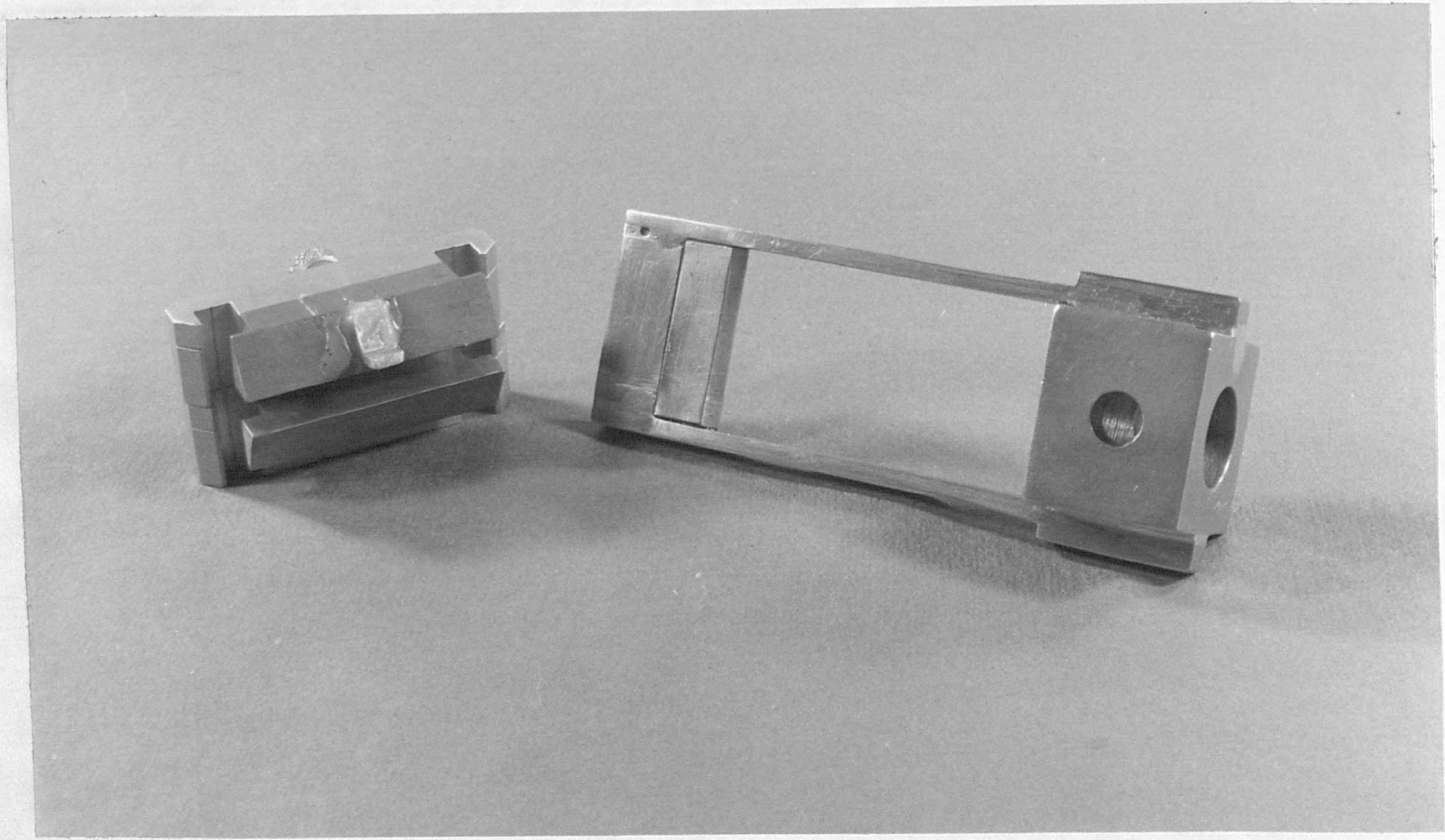

Fig.2.3.3(b). Adaptors for Hounsfield Tensometer to accommodate 12.7 mm long alumina prisms.

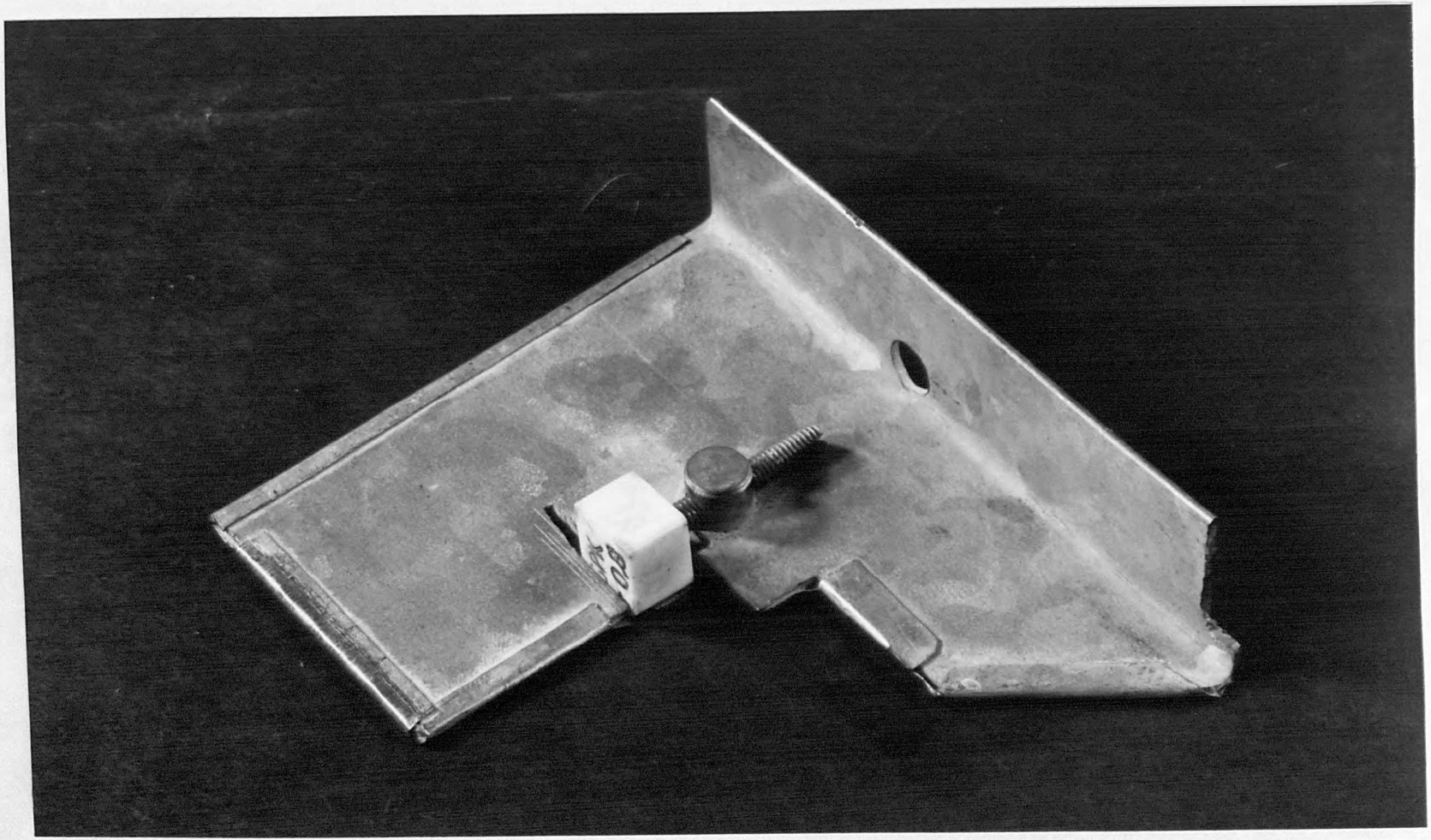

Fig.2.3.4. Jig for slitting tool tips into prisms.

Fig. 2.4.1.

Dimensions in inches.

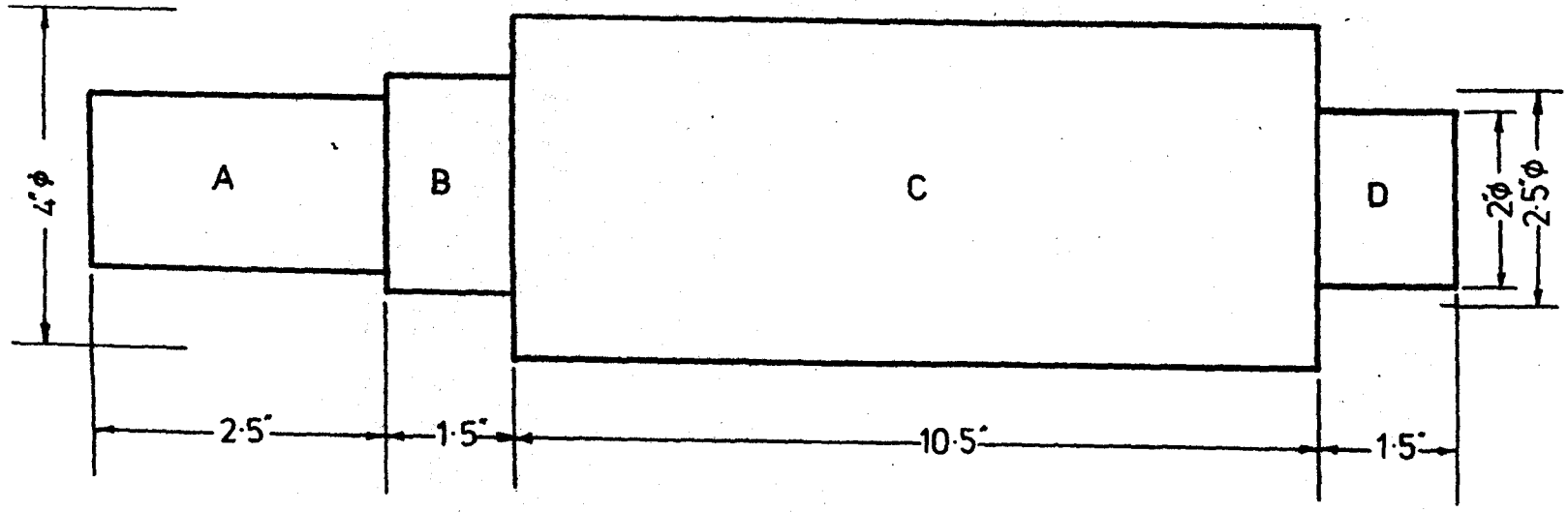

Standard test piece machined from EN30B supplied in the 'AS ROLLED' condition.

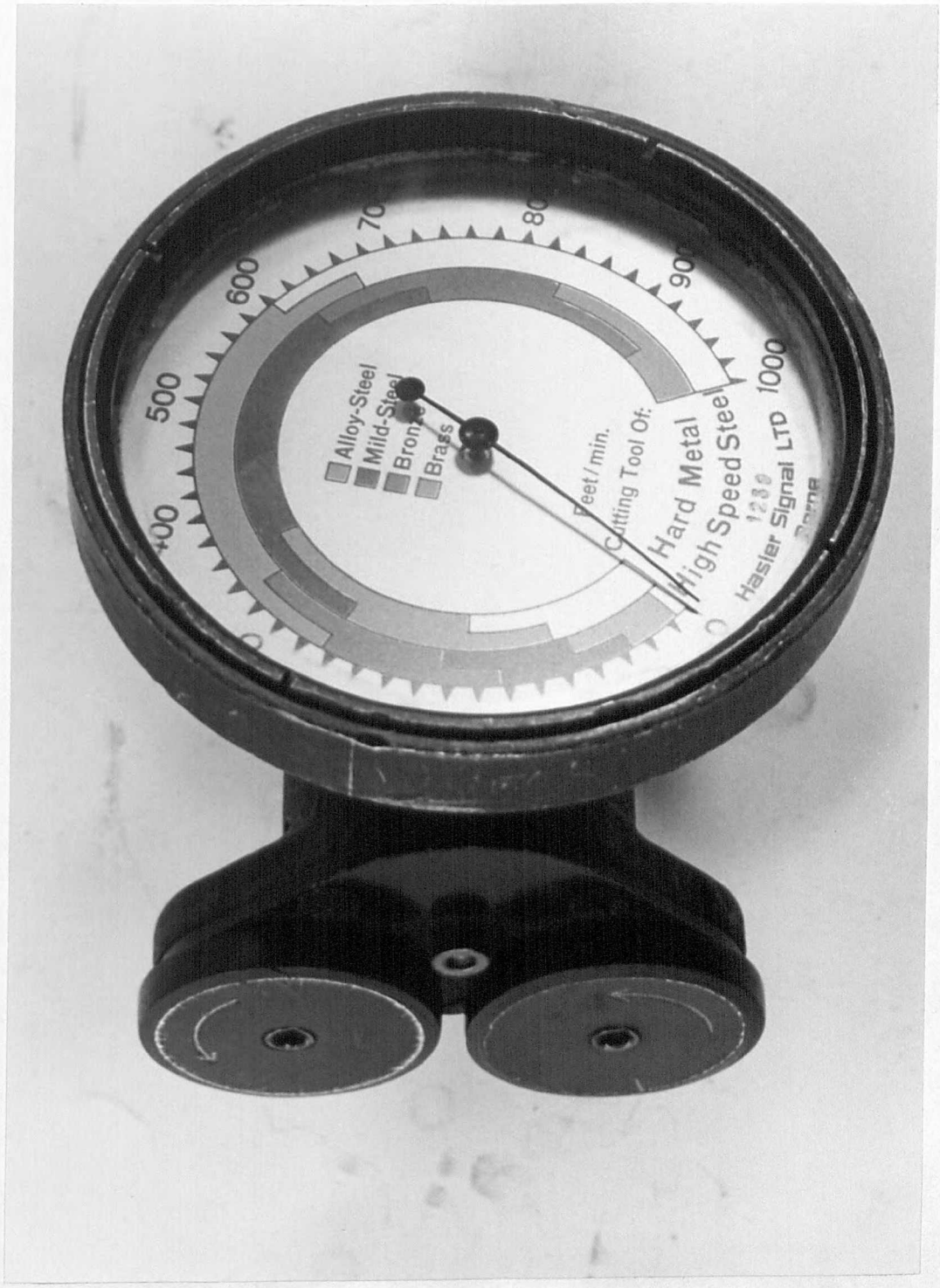

Fig.2.4.2. Hasler Surface Speed Meter.

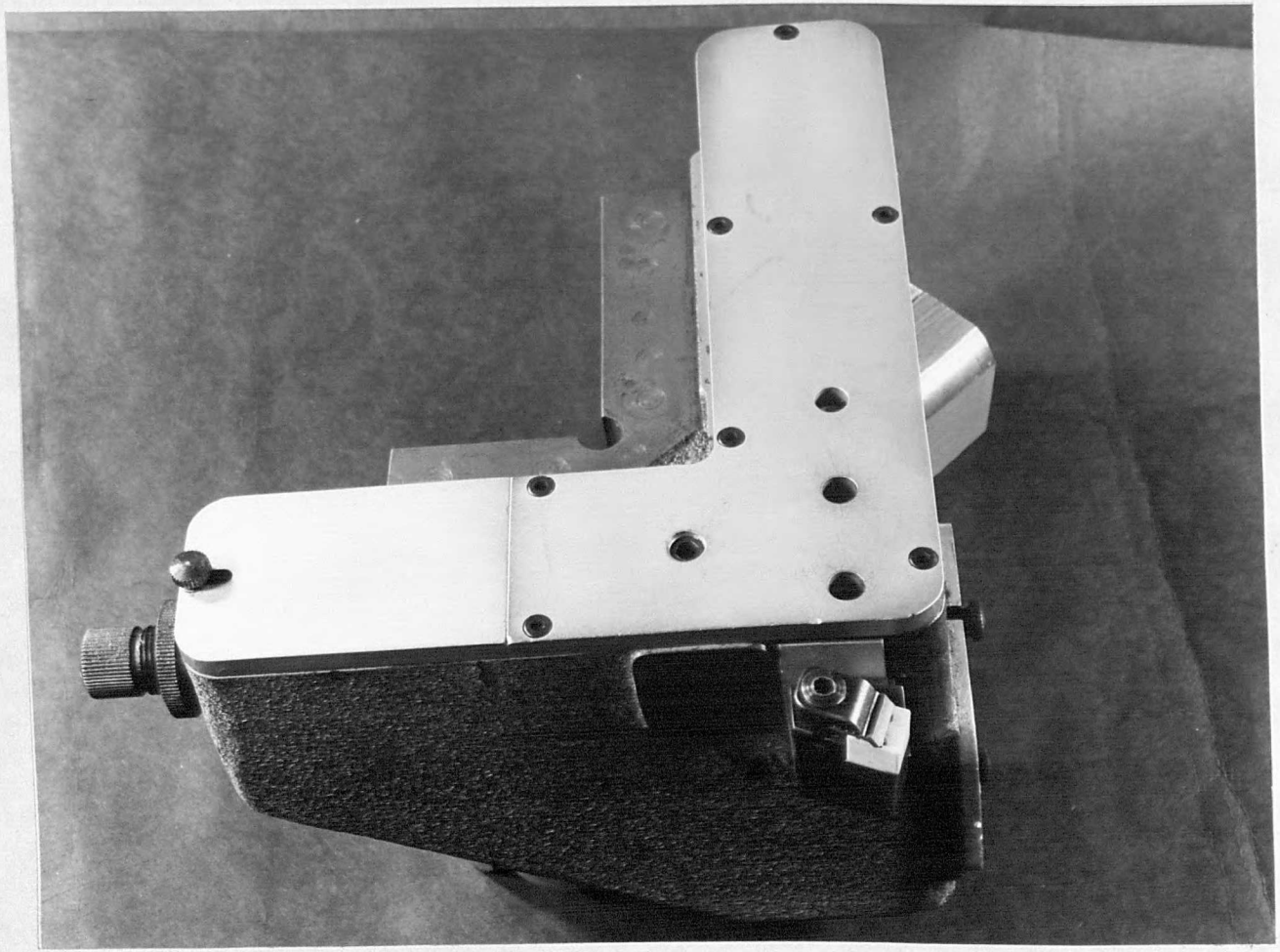

Fig.2.4.3. Mecalex Two-Force Pneumatic Dynamometer.

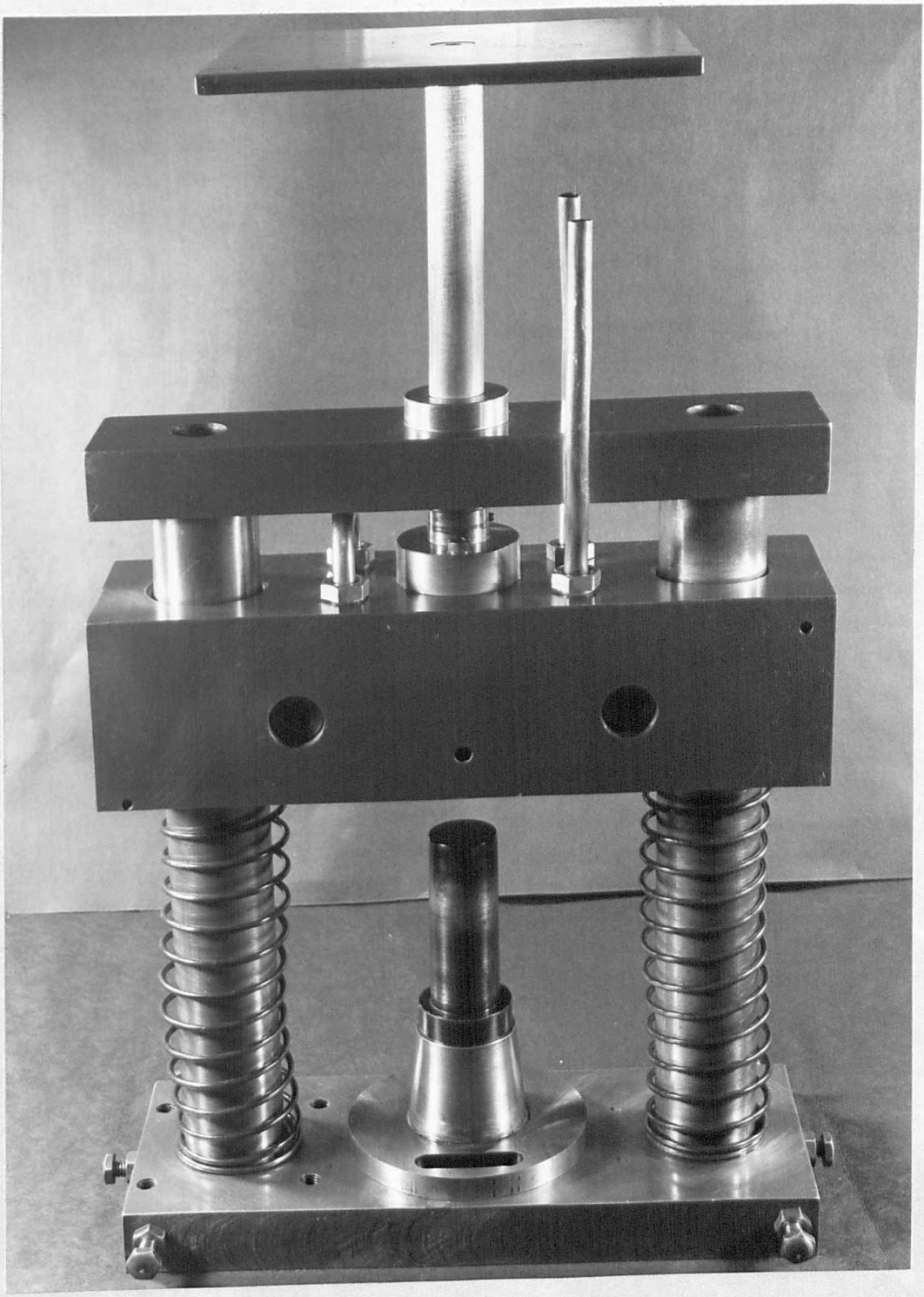

Fig.2.5.1(a). Test Rig.

Fig.2.5.1(b). Split spherical tool tip holder.

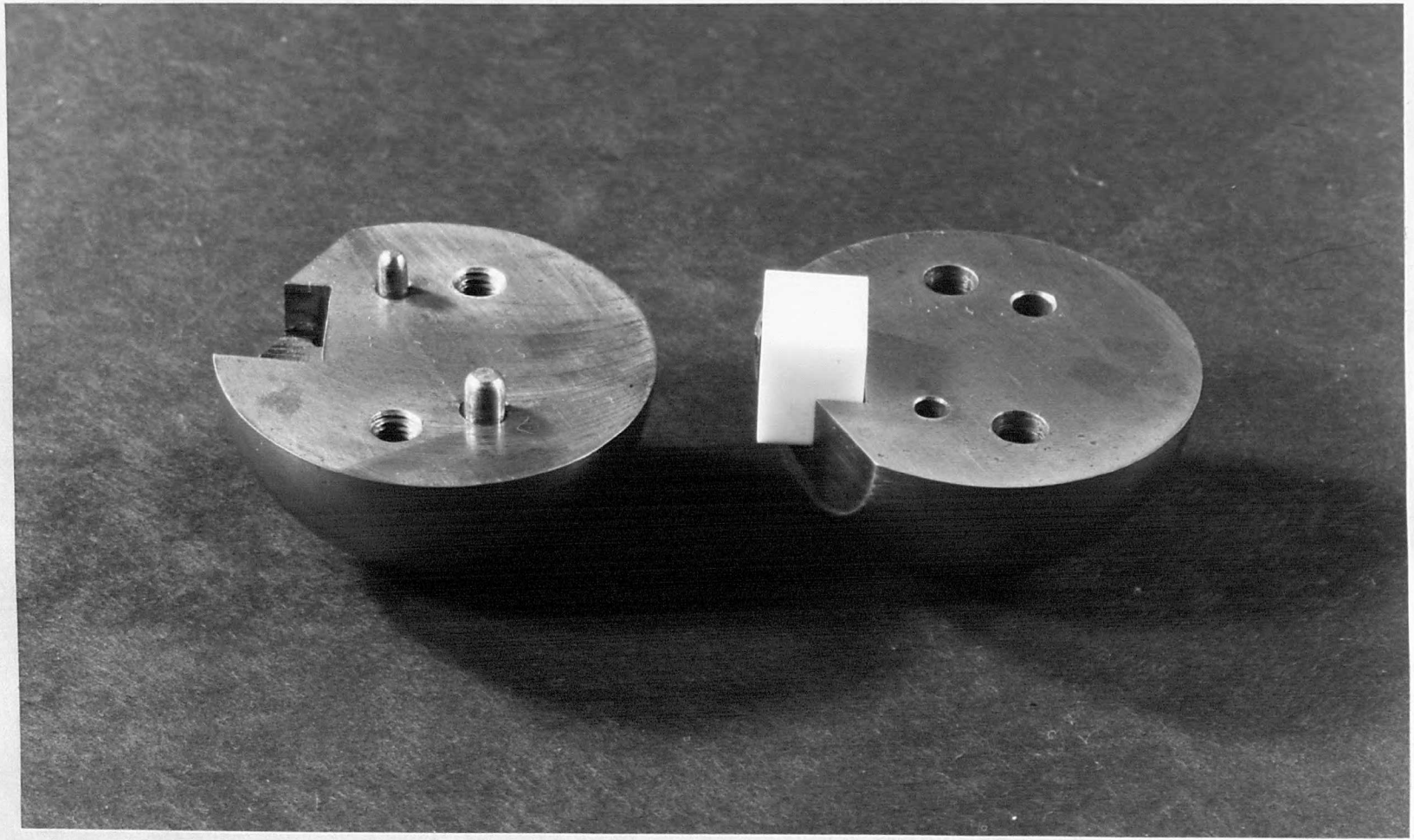

Fig.2.5.1(c). Split spherical tool tip holder showing detail.

Fig.2.5.1(d). Tool Tip Setting-Piece with top face of -6° rake and -4° angle of inclination.

Fig.2.5.2. Stellite 80 Anvil.

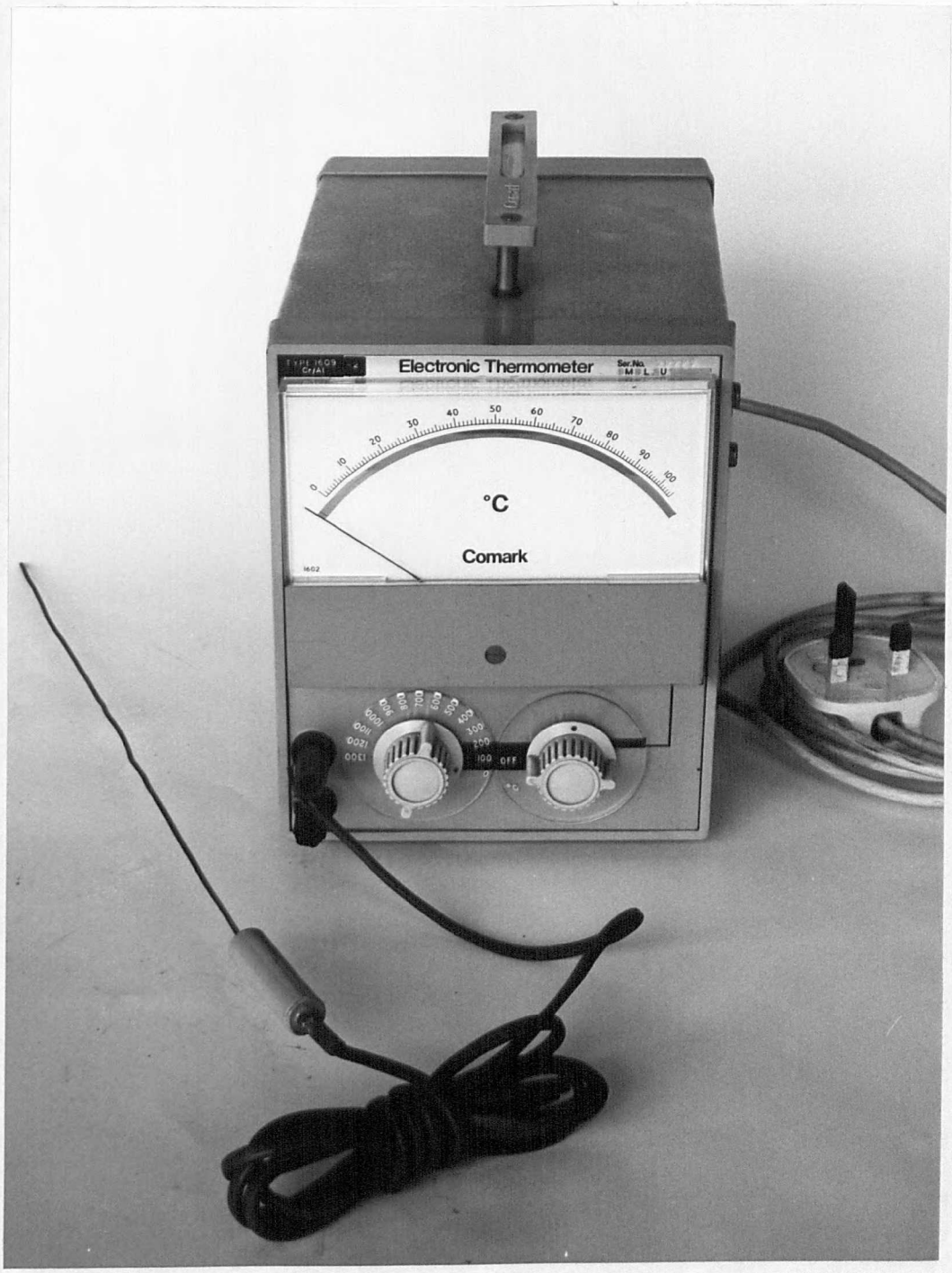

Fig.2.5.3. Comark Electronic Thermometer and Thermo-Couple.

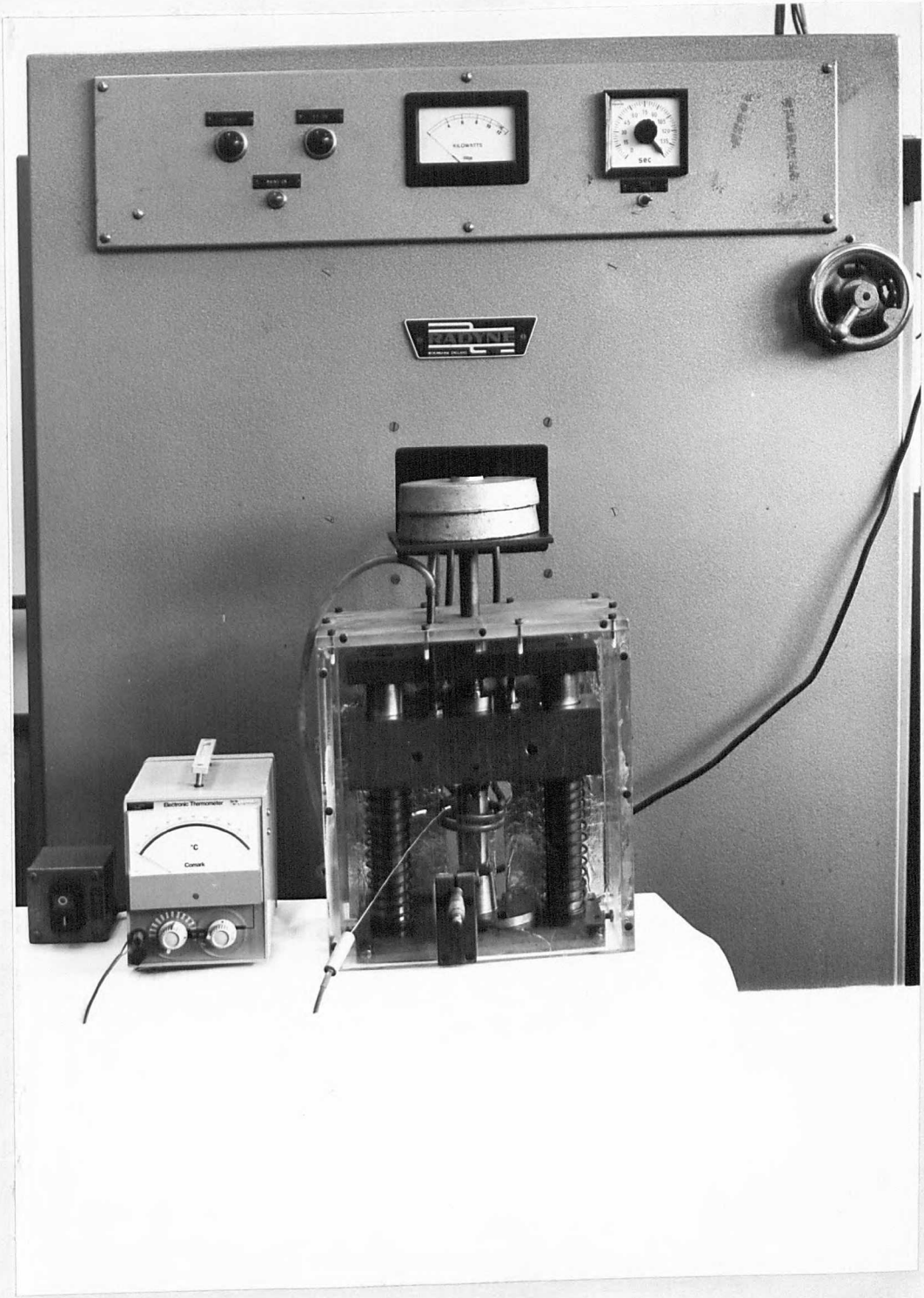

Fig.2.5.5. Test Rig with perspex cover in position ready for purging.

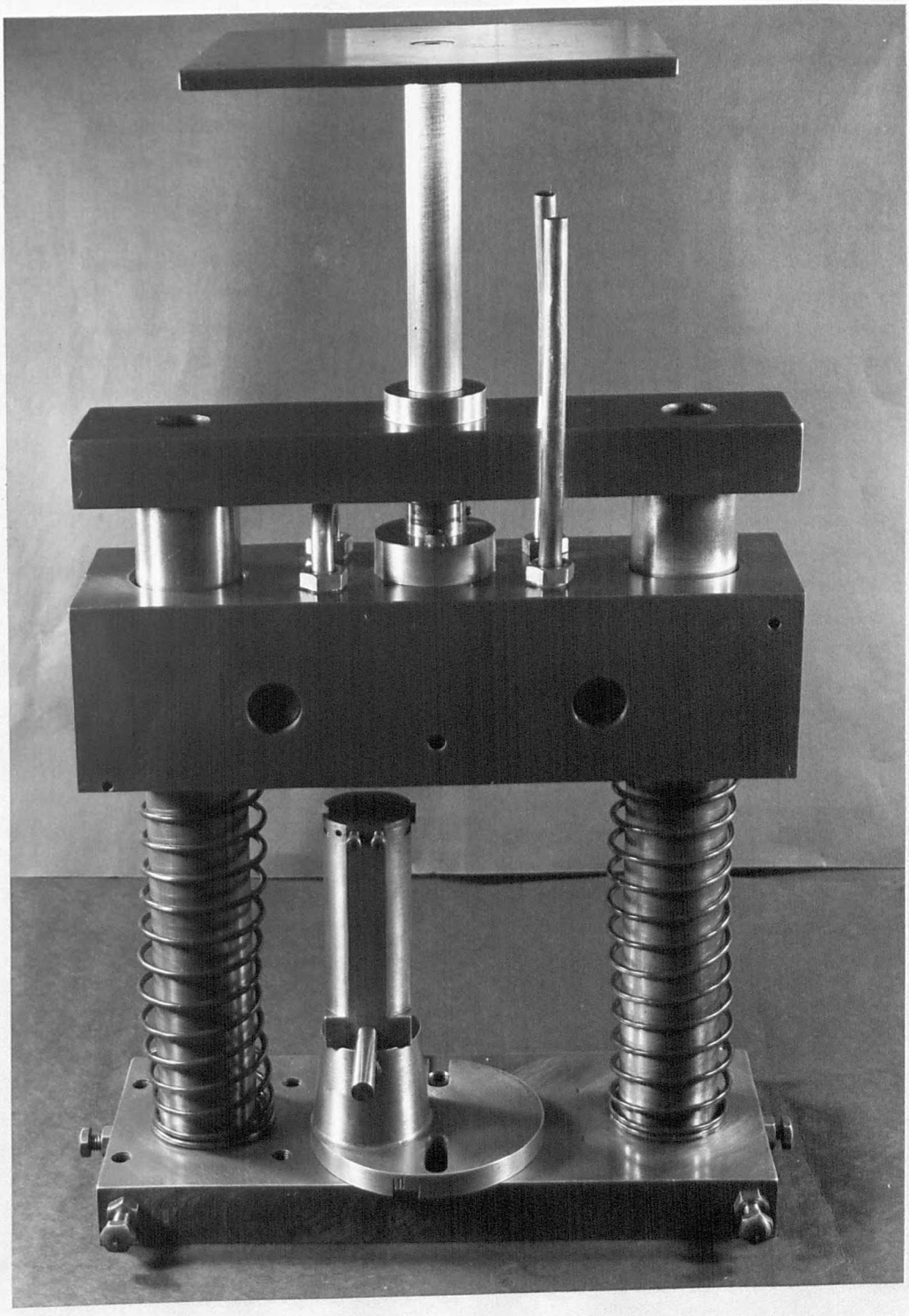

Fig.2.6.1(a). Modified Test Rig.

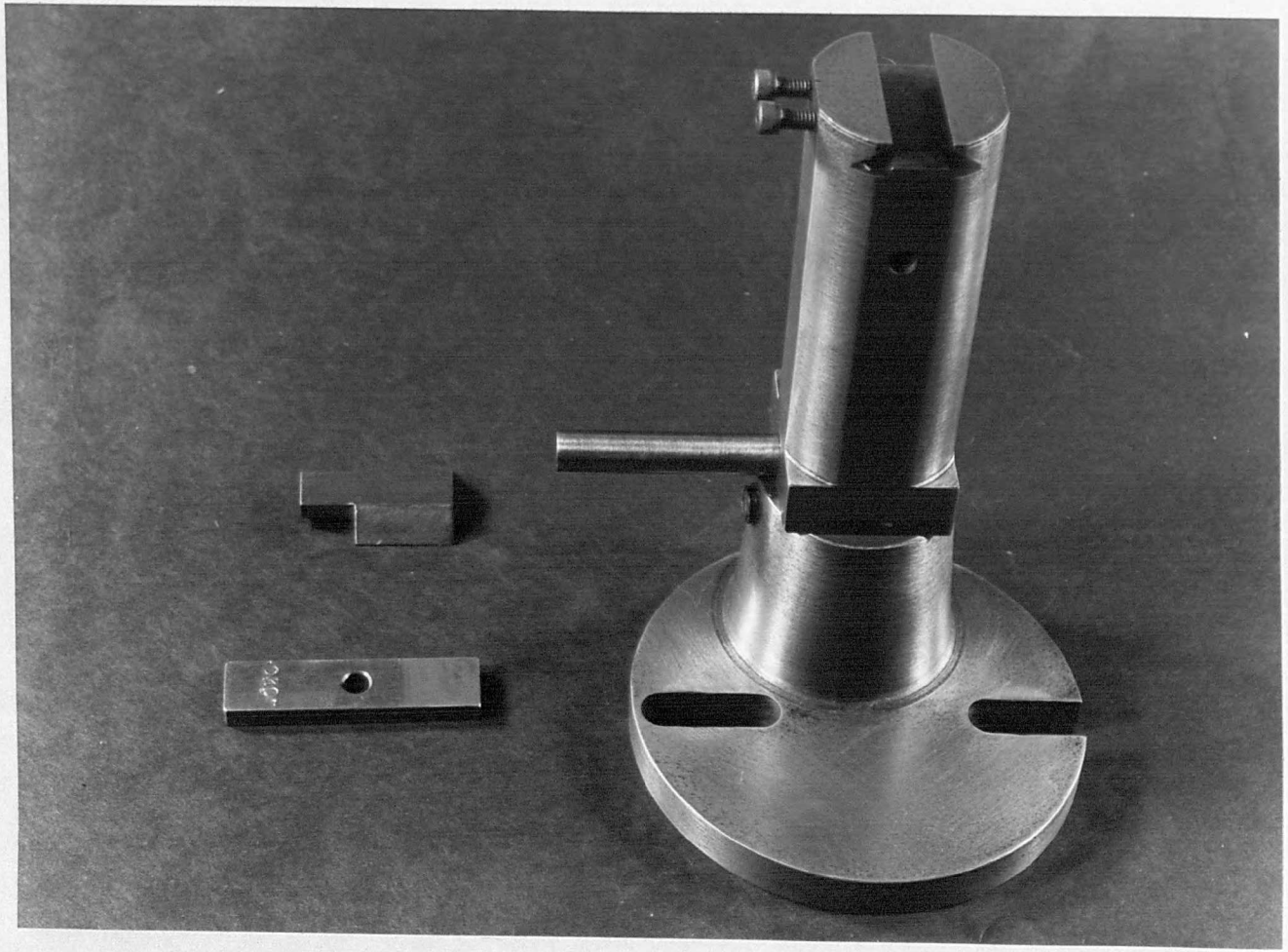

Fig.2.6.1(b). Redesigned Susceptor with dove-tail test piece and setting gauge.

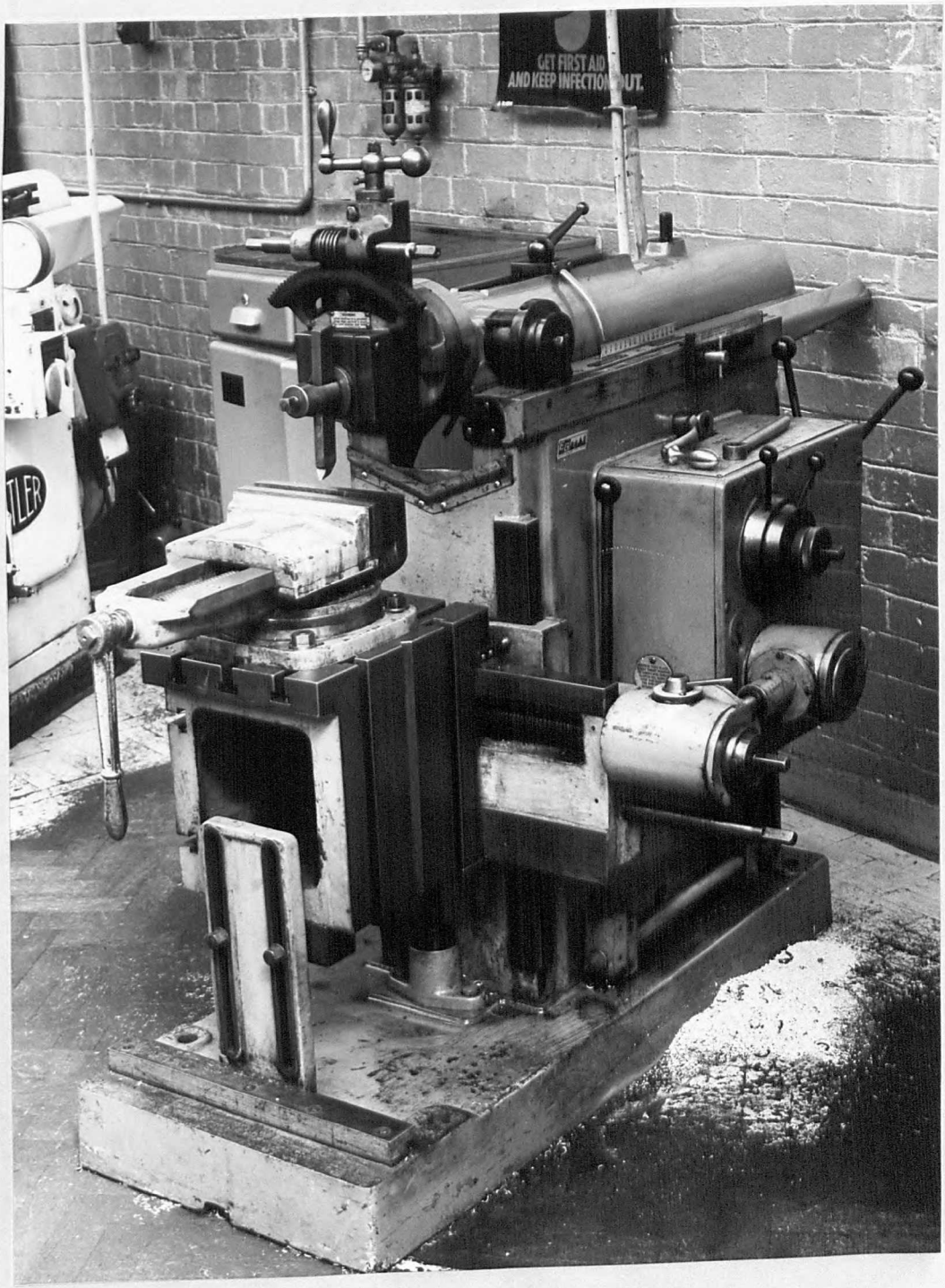

Fig.2.7.1. Butler 14 in Shaping Machine.

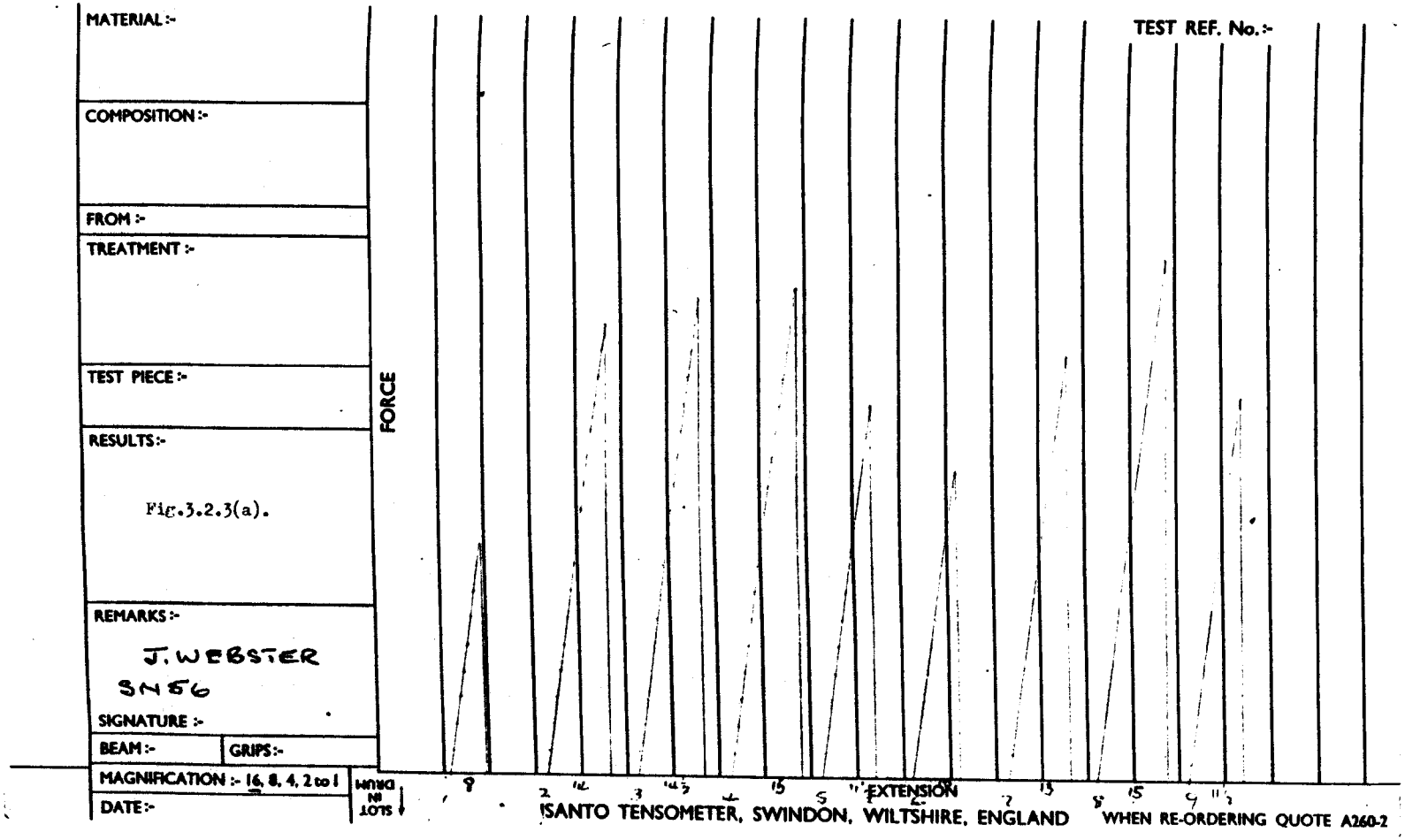

Fig.3.2.3(a). Bend test graph of SN56 prisms.

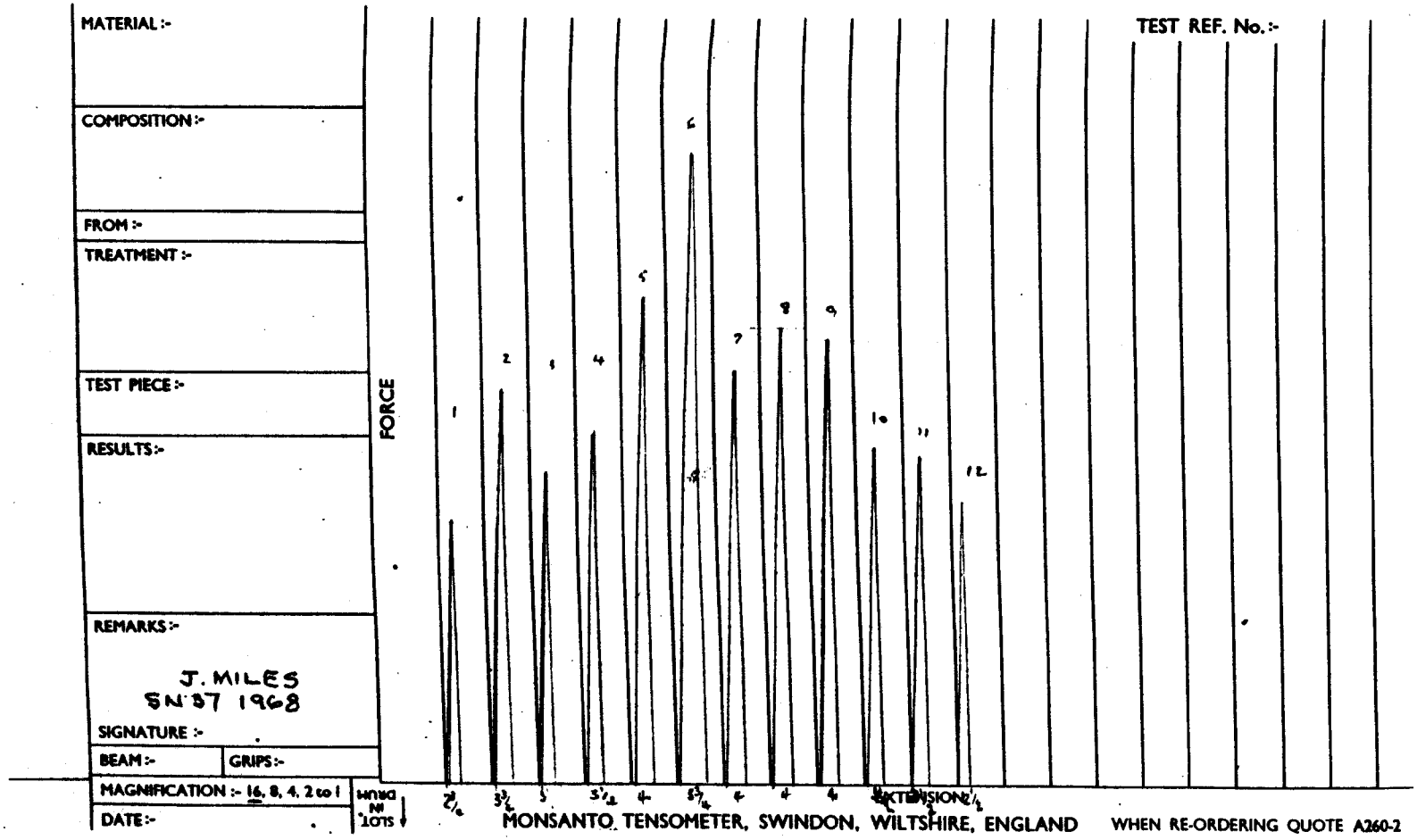

Fig.3.2.3(b). Bend test graph of SN37 (1968) prisms.

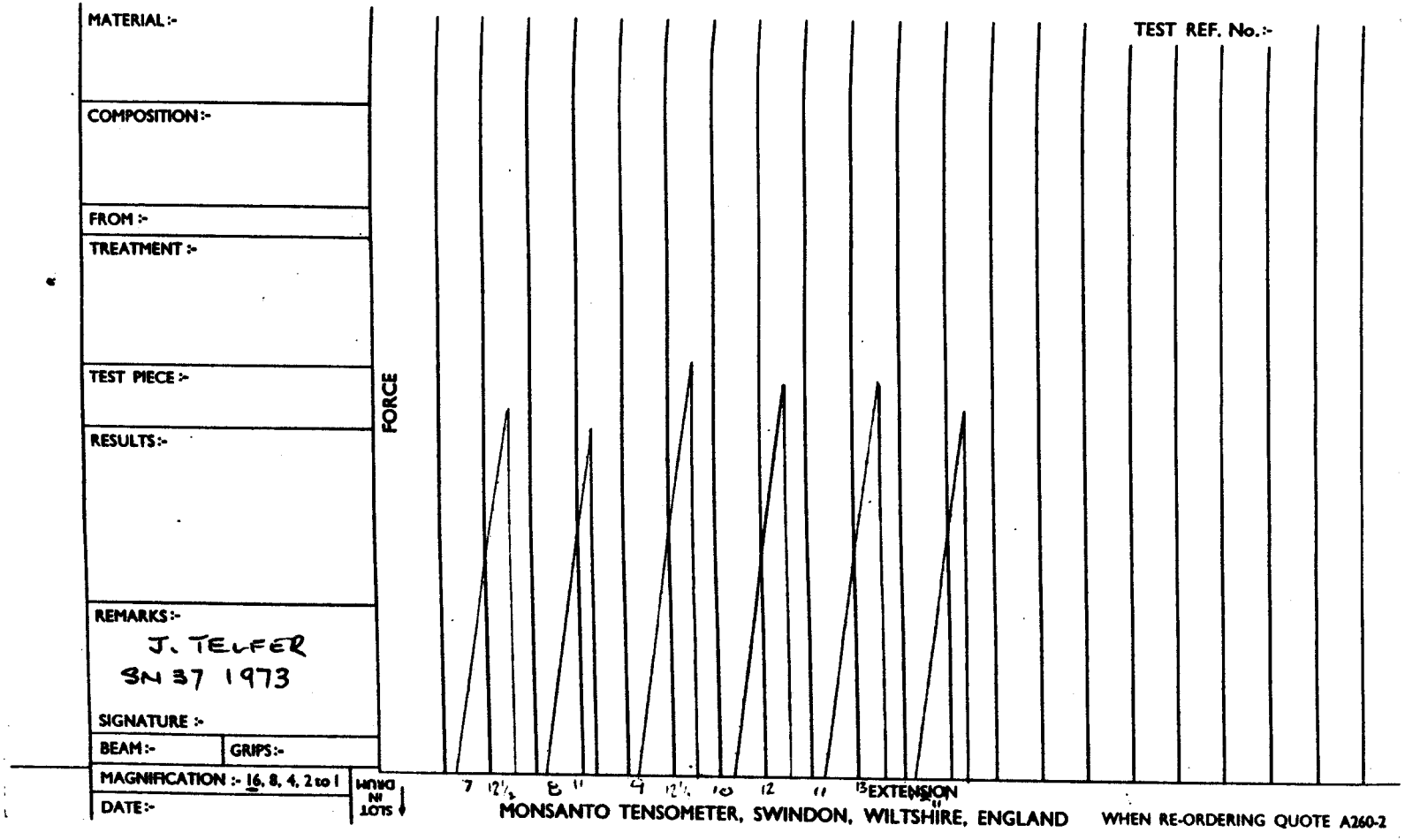

Fig.3.2.3(c). Bend test graph of SN37 (1973) prisms.

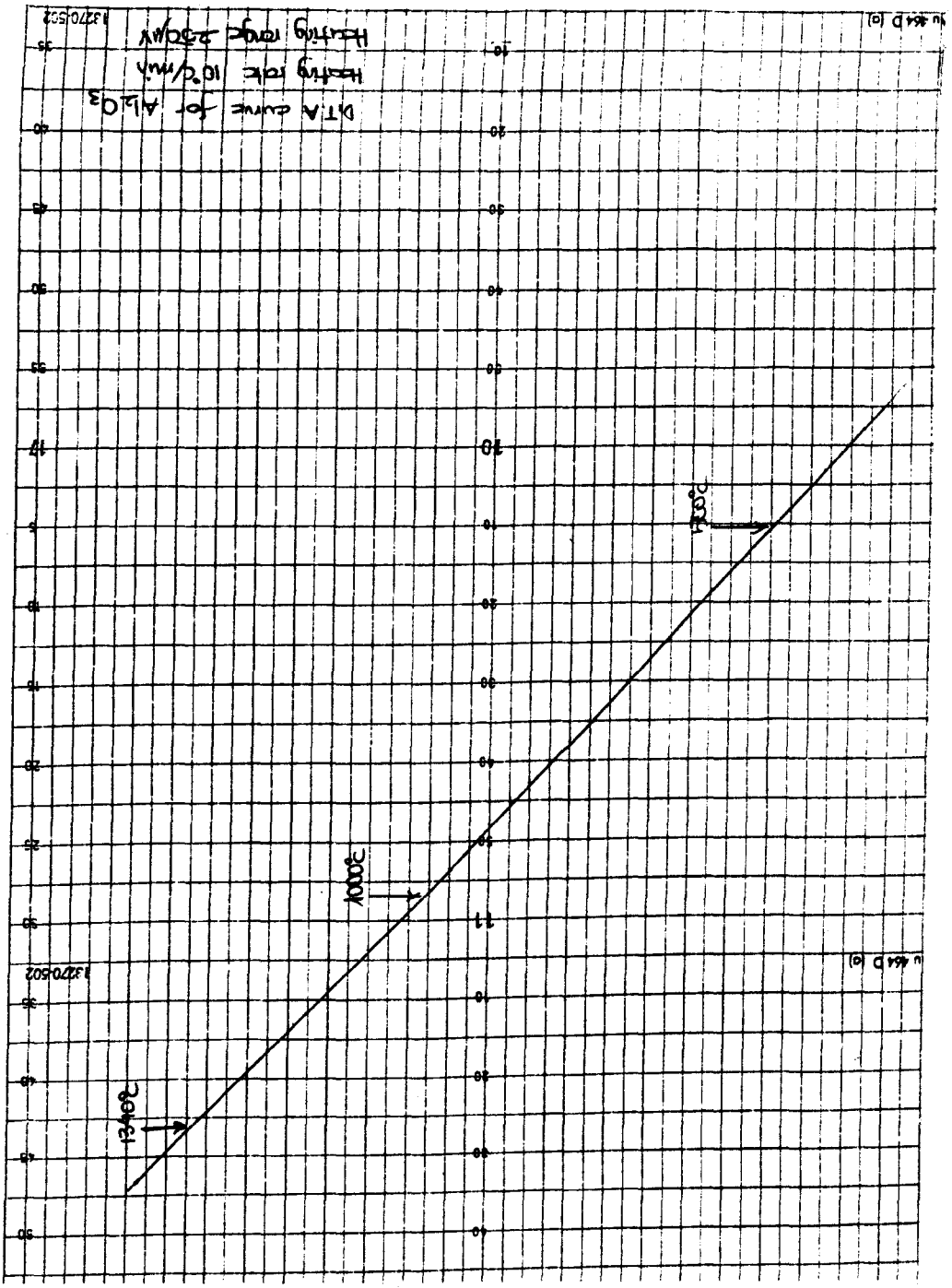

Fig.3.2.4. D.T.A. curve for tool tip material.

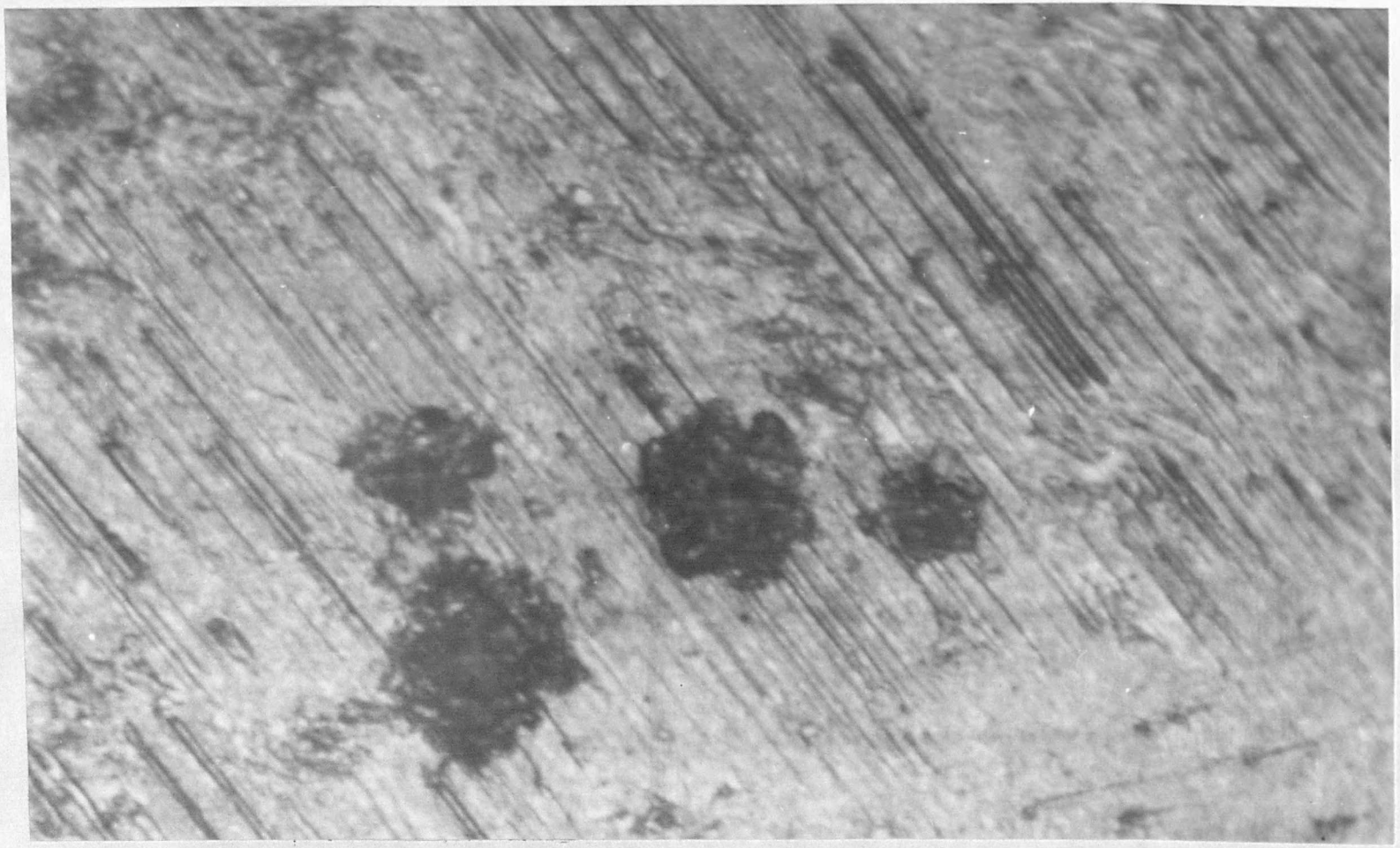

Fig.3.2.5. Leitz Micro-Hardness Indentations at loads of 25g, 50g and 100g.

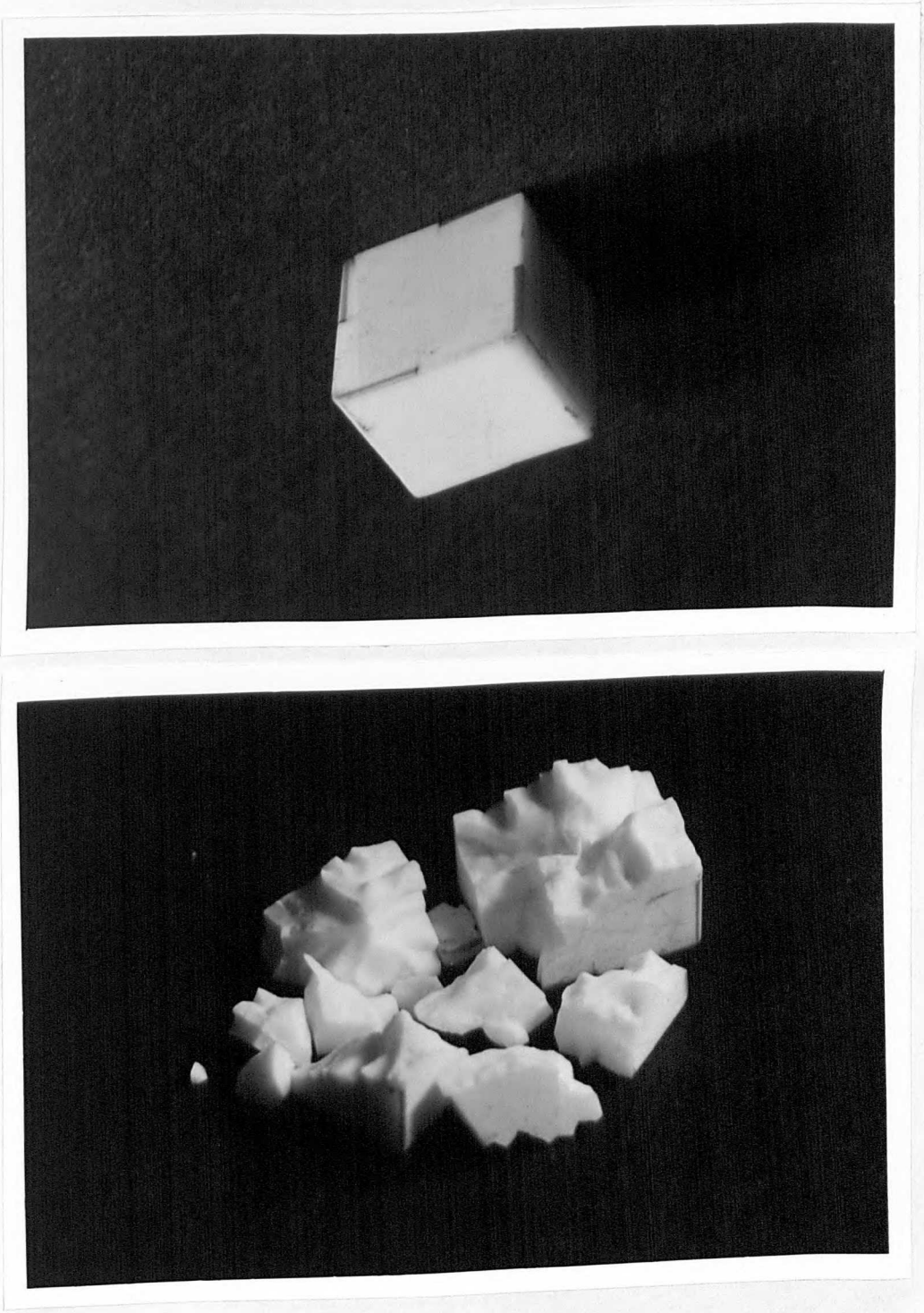

Figs.3.2.6(iii) (a) and (b). Thermal shock effects on tool tips quenched in H_2O from (a) 300°C and (b) 700°C.

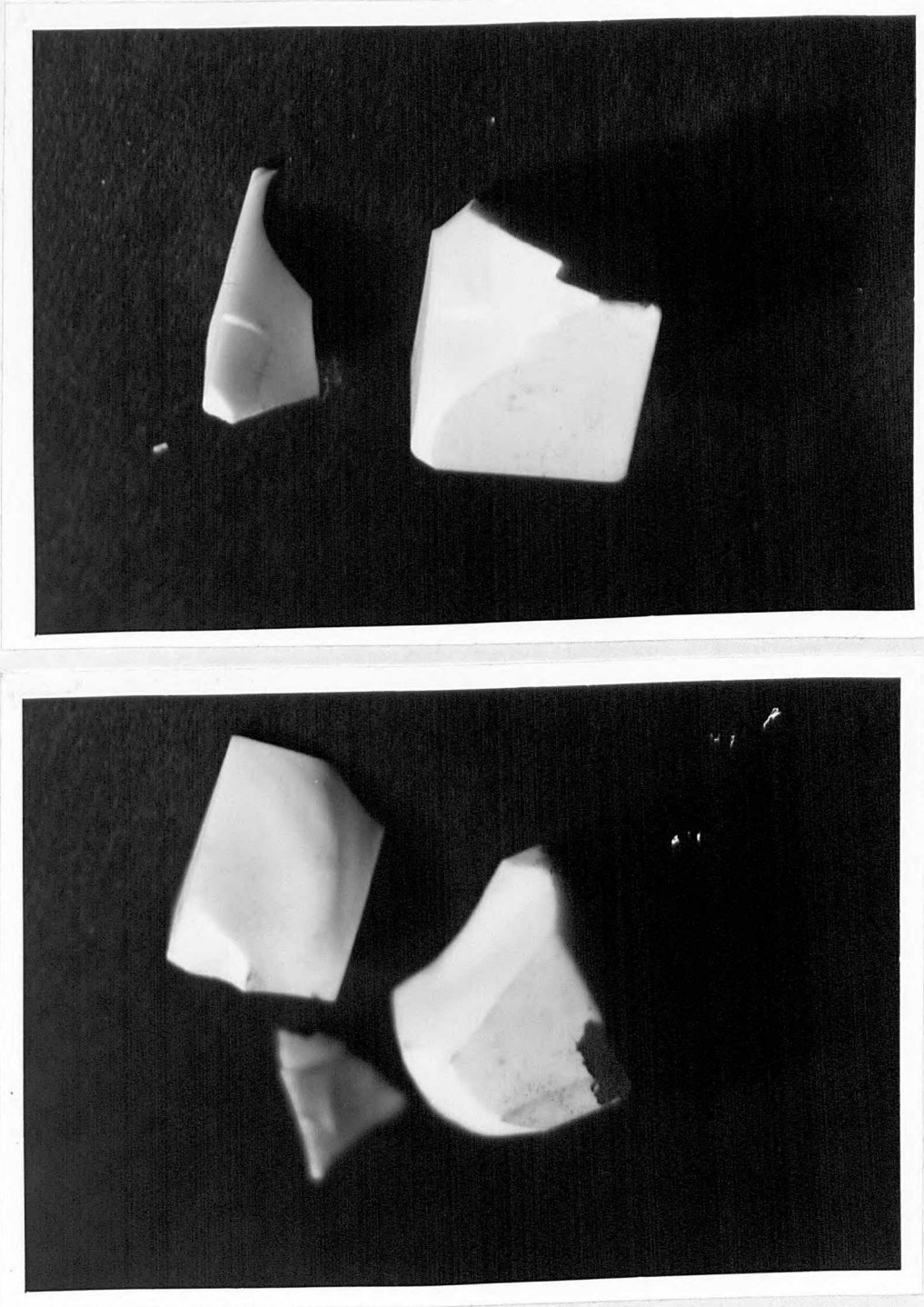

Fig.3.2.6(iv) and (v). Thermal shock effects of heating tool tip corner momentarily in (iv) a carbon arc and (v) oxy-acetylene.

Fig.3.3.1.A

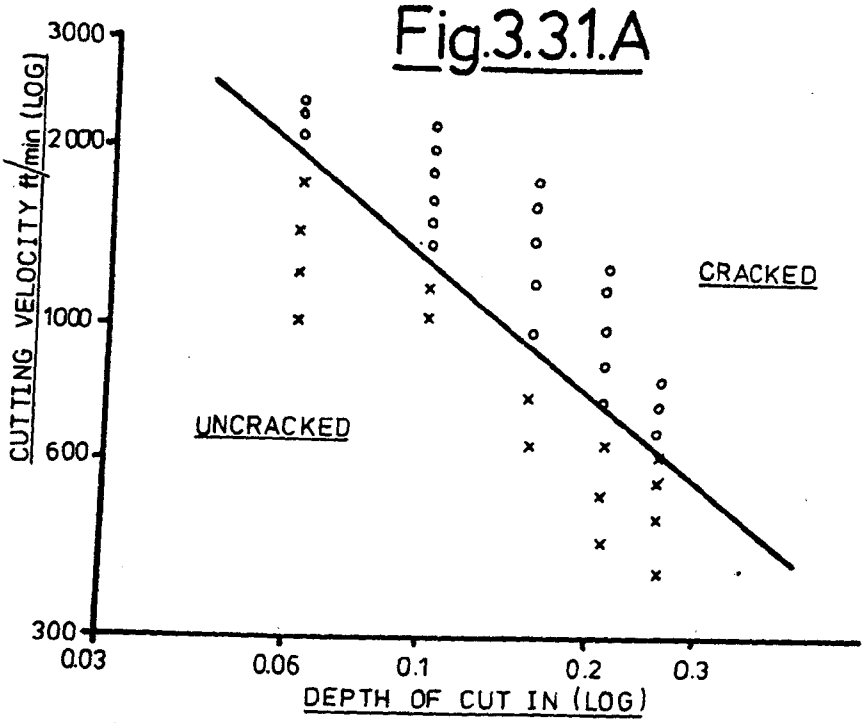

"COMB-CRACK" THRESHOLD OBTAINED BY MILES AT CONSTANT FEED RATE OF 0.006 in/rev.

Fig.3.3.1.B

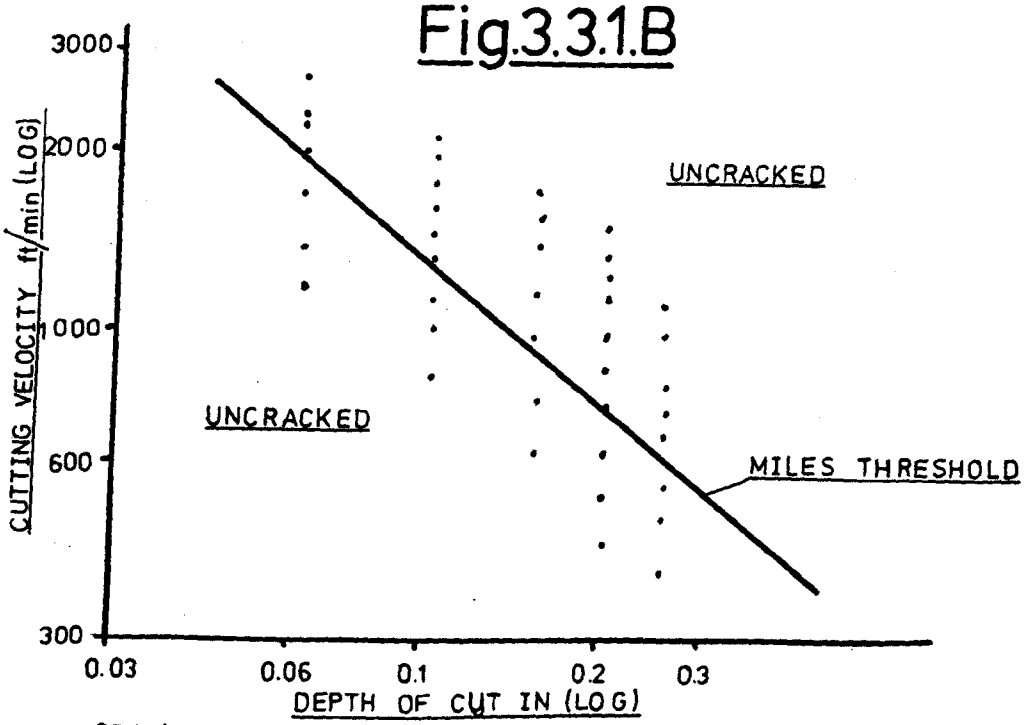

GRAPH COMPARING MACHINING PARAMETERS WITH MILES-FEED RATE CONSTANT AT 0.005 in/rev. NO 'COMB' CRACKS OBSERVED.

Fig.3.3.2.

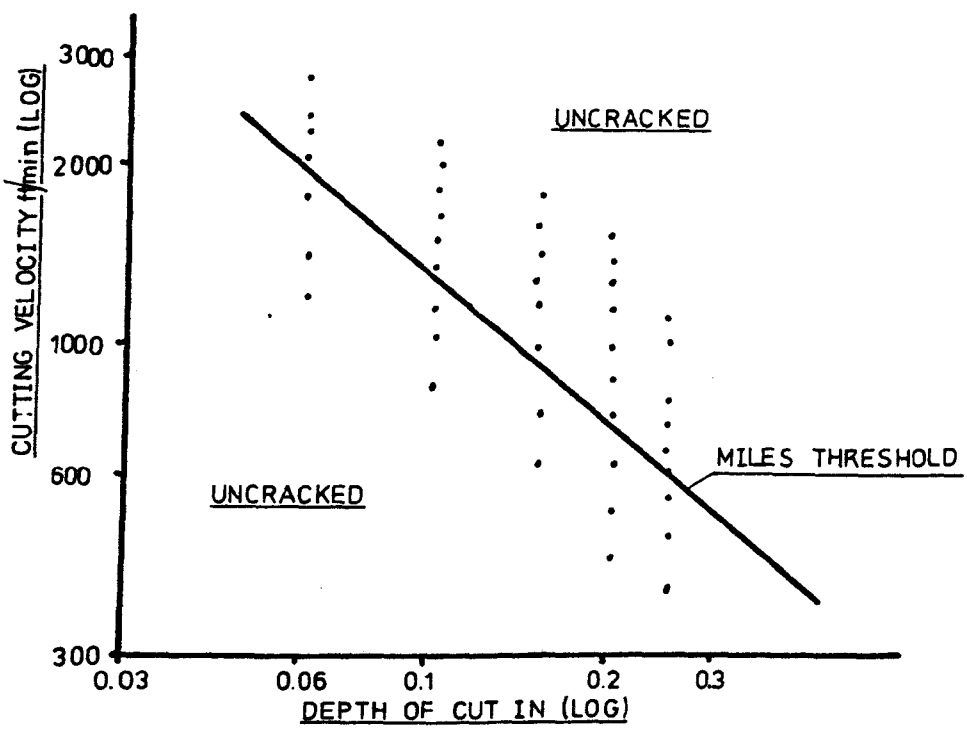

GRAPH COMPARING MACHINING PARAMETERS WITH MILES NO COMB-CRACKS OBSERVED. FEED RATE CONSTANT AT 0.010 in rev. TWICE THE RATE USED IN THAT OF FIGS 3.3.1A AND 3.3.1B.

Fig 3.3.3.

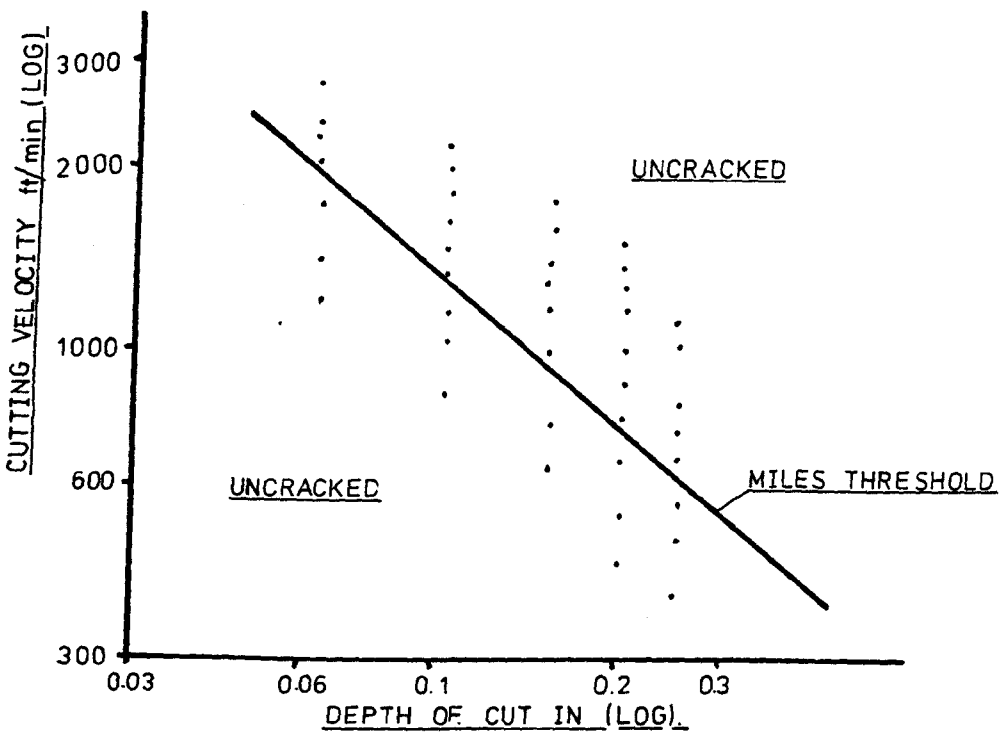

GRAPH COMPARING MACHINING PARAMETERS WITH MILES - FEED RATE CONSTANT AT 0.010 in/rev. CHIP BREAKER POSITIONED IN EACH OF FOUR POSSIBLE LOCATIONS. NO 'COMB' CRACKS OBSERVED.

Fig 3.3.4.

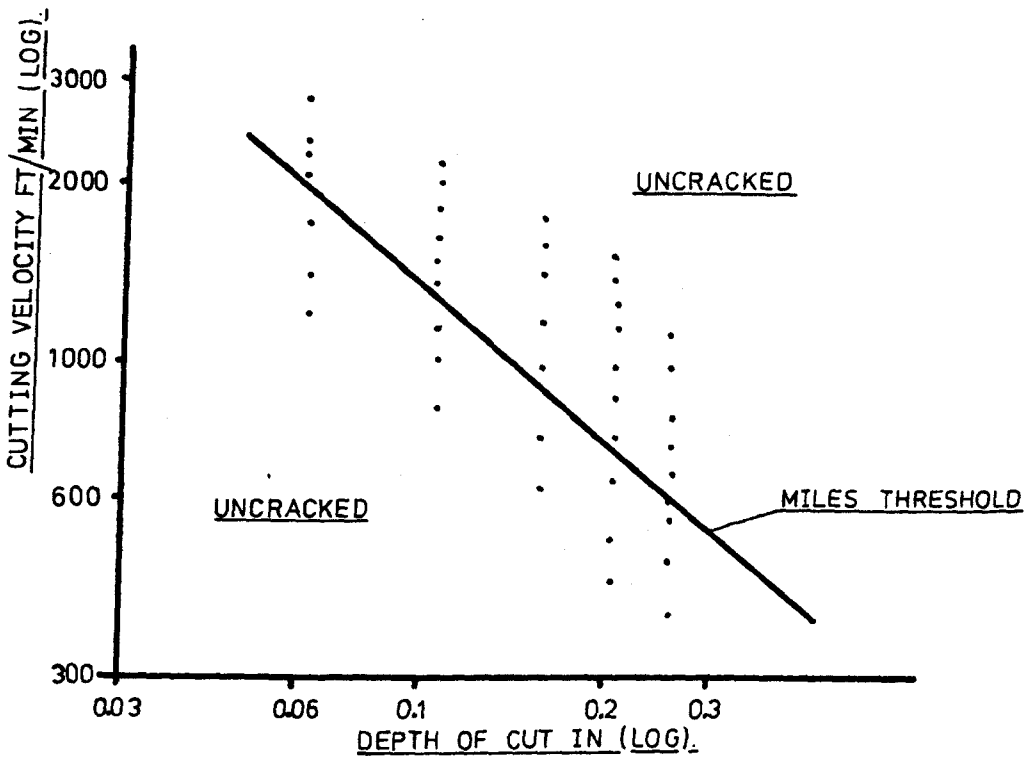

GRAPH COMPARING MACHINING PARAMETERS WITH PEKELHARING AND MILES. EACH TOOL TIP CORNER USED TWICE AT FEED RATES OF 0.005 AND 0.010 in/rev. WITH CHIP BREAKER IN VARIOUS POSITIONS. NO 'COMB' CRACKS OBSERVED.

Fig. 3.3.5.A

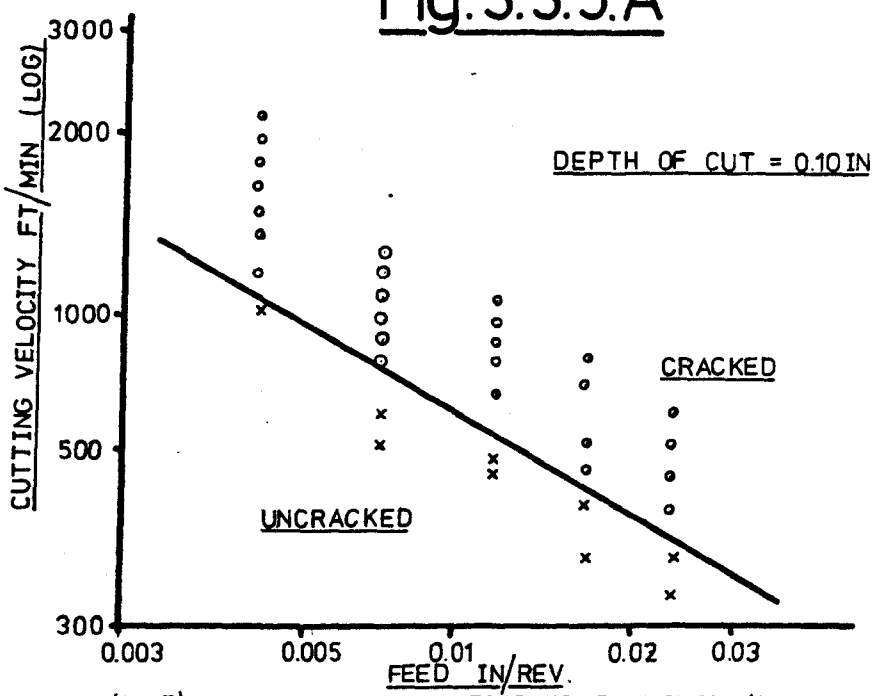

'COMB' CRACK THRESHOLD OBTAINED BY MILES AT CONSTANT DEPTH OF CUT.

Fig. 3.3.5.B

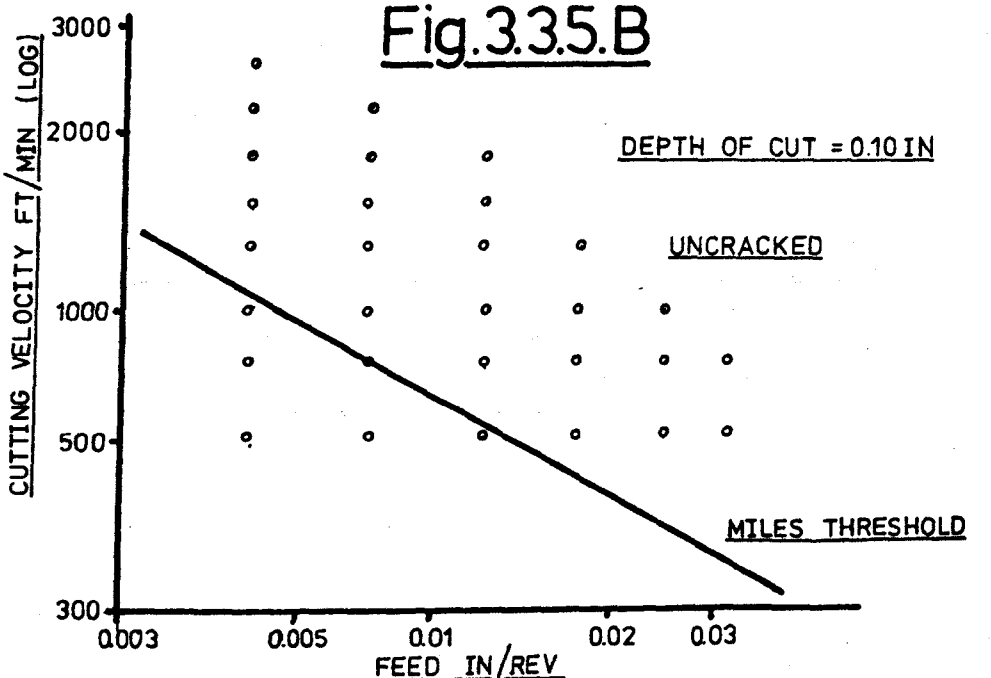

GRAPH COMPARING VALUES WITH FIG. 3.3.5.A NO COMB CRACKS OBSERVED.

Fig. 3.3.7.

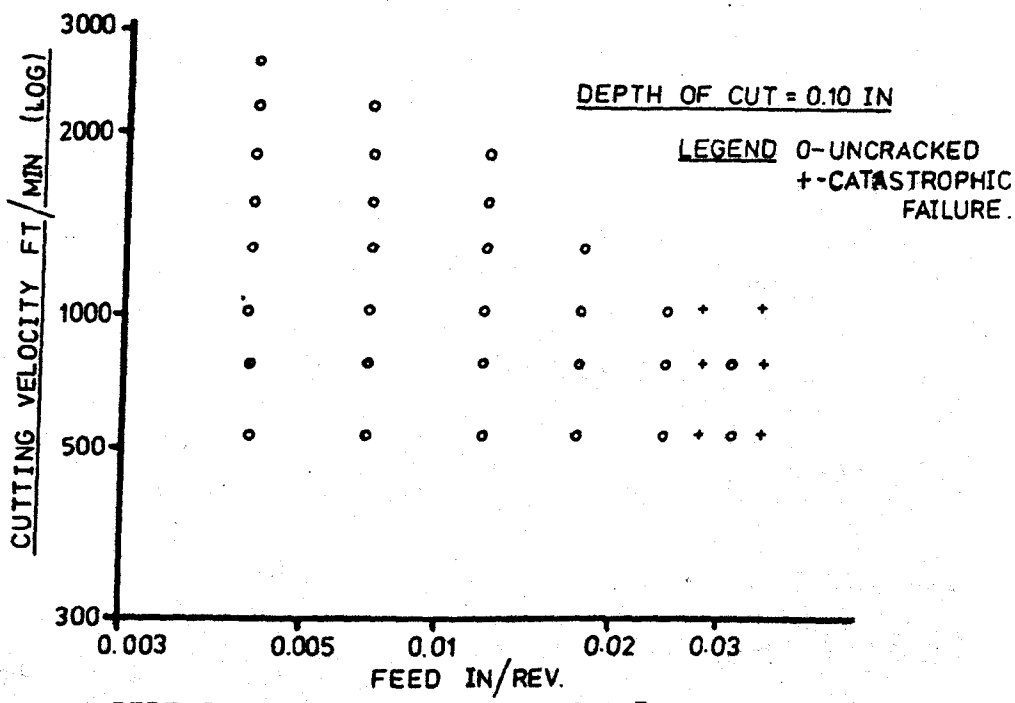

REPEAT OF GRAPH 3.3.5B SHOWING RE-ENGAGEMENT FAILURES AT FEEDS OF 0.028 IN/REV AND ABOVE.

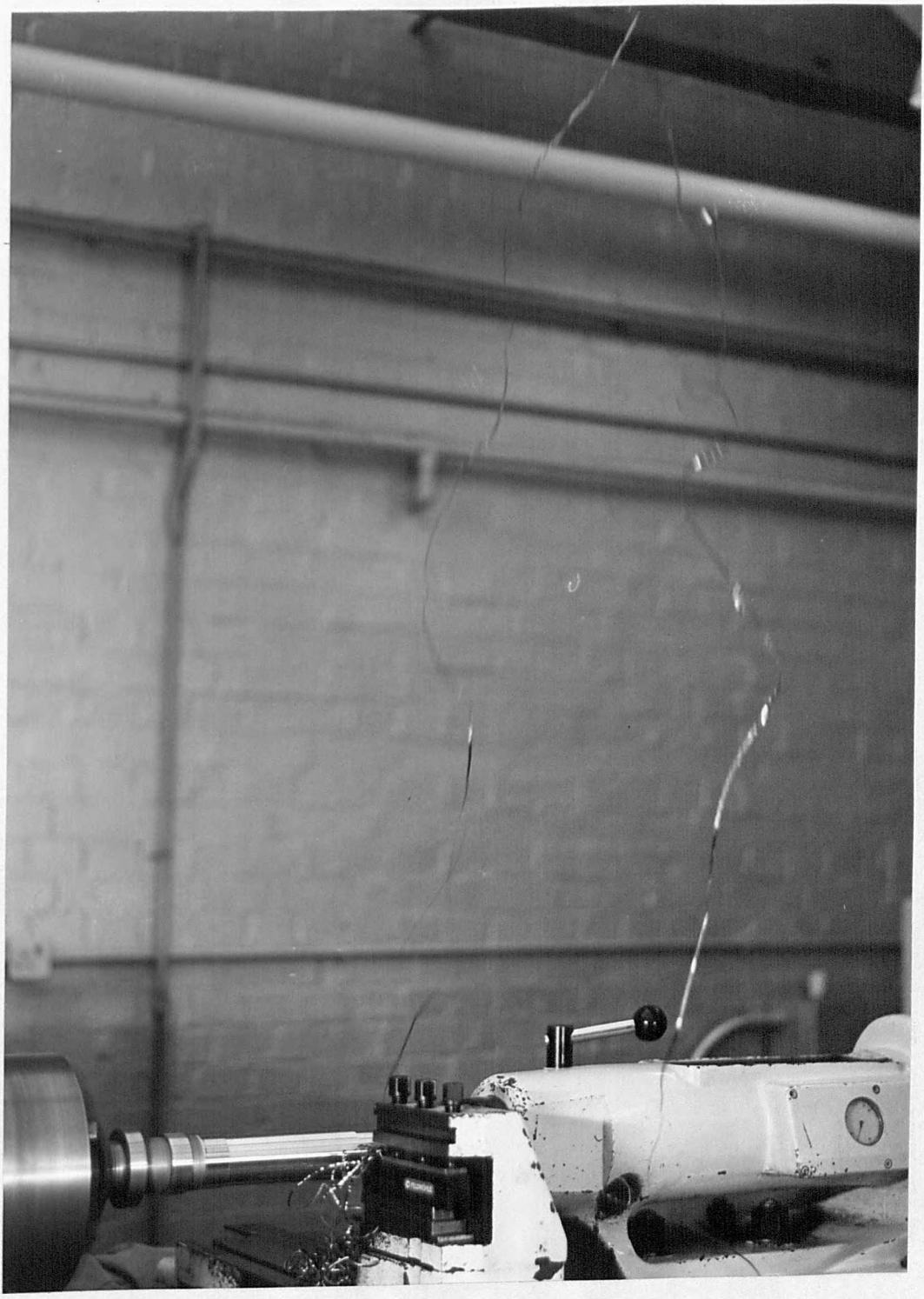

Fig.3.3.8. Swarf behaviour at cutting speed of 4500 ft/min with depth of cut 0.05 in and feed rate of 0.005 in/rev.

Fig.3.4.1. Duplicate tool holder reduced on shank to suit Mecalex dynamometer.

Fig 3.4.2A

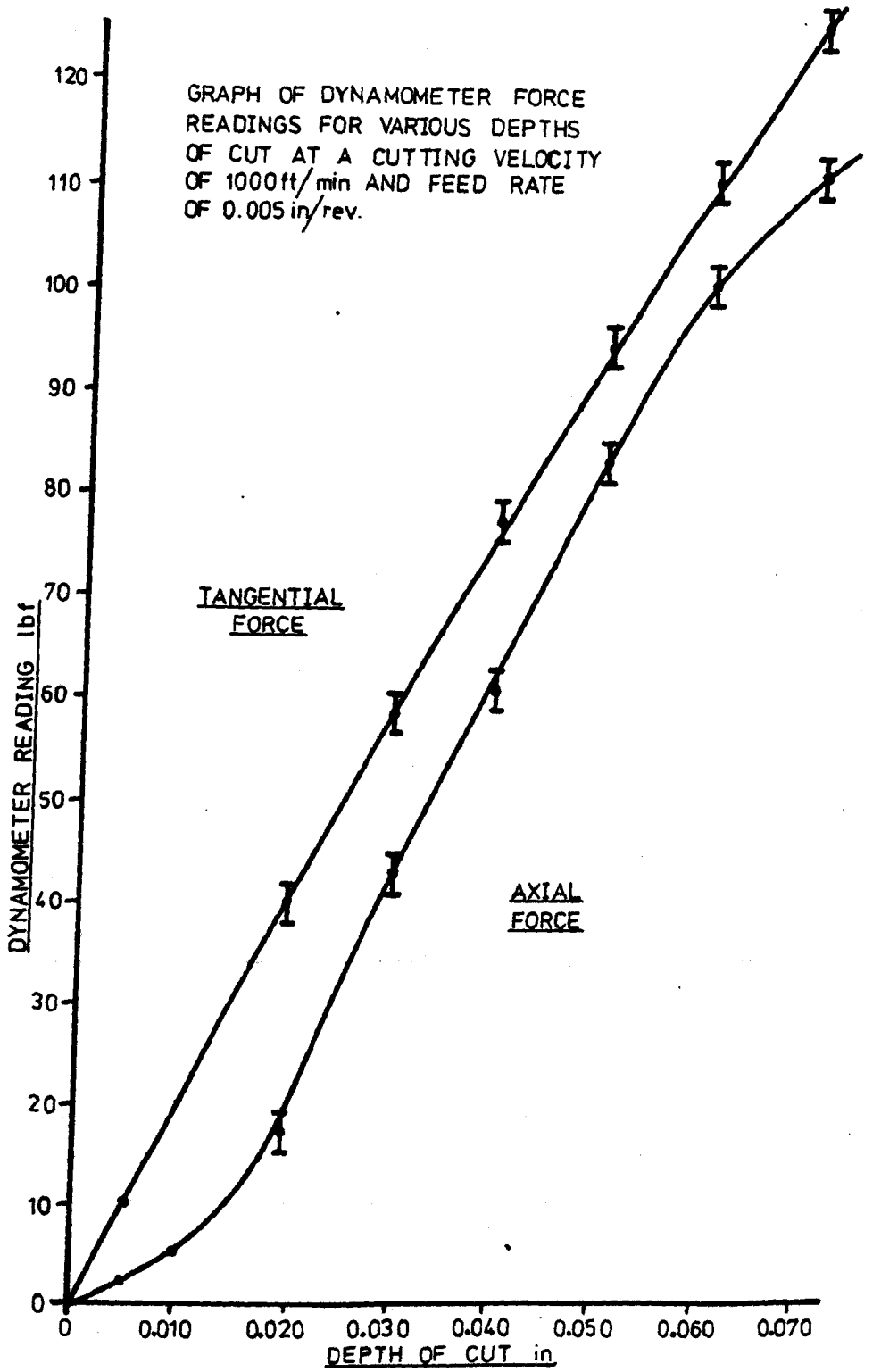
GRAPH OF DYNAMOMETER FORCE READINGS FOR VARIOUS DEPTHS OF CUT AT A CUTTING VELOCITY OF 1000 ft/min AND FEED RATE OF 0.005 in/rev.
TANGENTIAL FORCE
AXIAL FORCE
DYNAMOMETER READING lbf
DEPTH OF CUT in
0
10
20
30
40
50
60
70
80
90
100
110
120
0.010
0.020
0.030
0.040
0.050
0.060
0.070

Fig. 3.4.2B

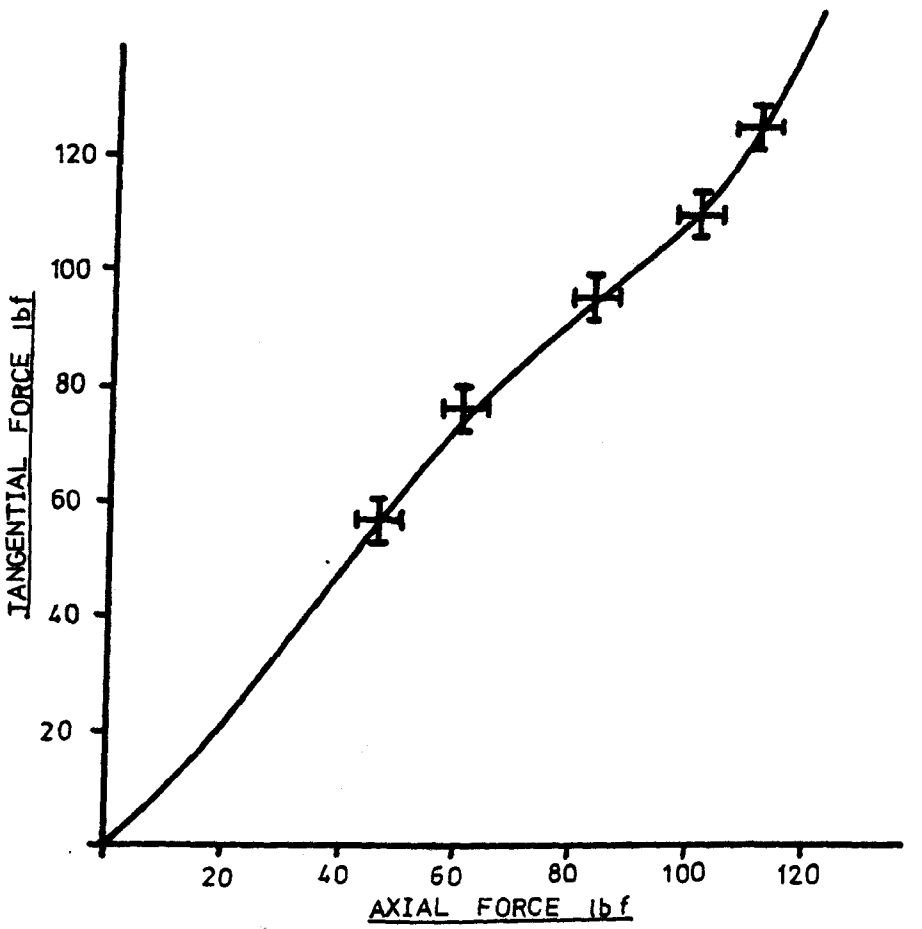

RELATIONSHIP BETWEEN DYNAMOMETER FORCES FOR VARIOUS DEPTHS OF CUT AT A CUTTING VELOCITY OF 1000 ft/min AND FEED RATE OF 0.005 in/rev.

Fig. 3.4.3A

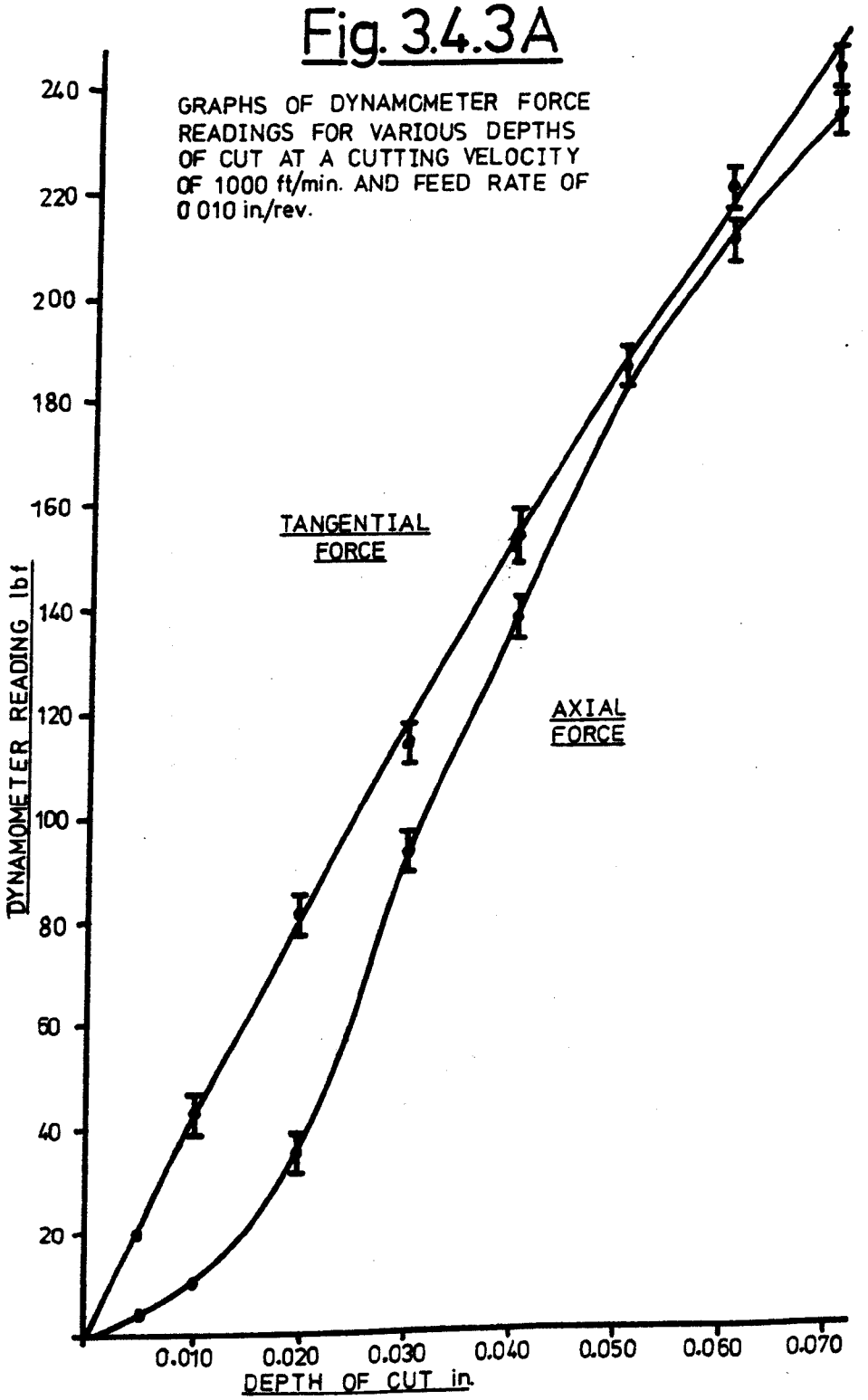
GRAPHS OF DYNAMOMETER FORCE READINGS FOR VARIOUS DEPTHS OF CUT AT A CUTTING VELOCITY OF 1000 ft/min. AND FEED RATE OF 0 010 in./rev.
TANGENTIAL FORCE
AXIAL FORCE
DYNAMOMETER READING lbf
240
220
200
180
160
140
120
100
80
60
40
20
0.010
0.020
0.030
0.040
0.050
0.060
0.070
DEPTH OF CUT in.

Fig. 3.4.3B

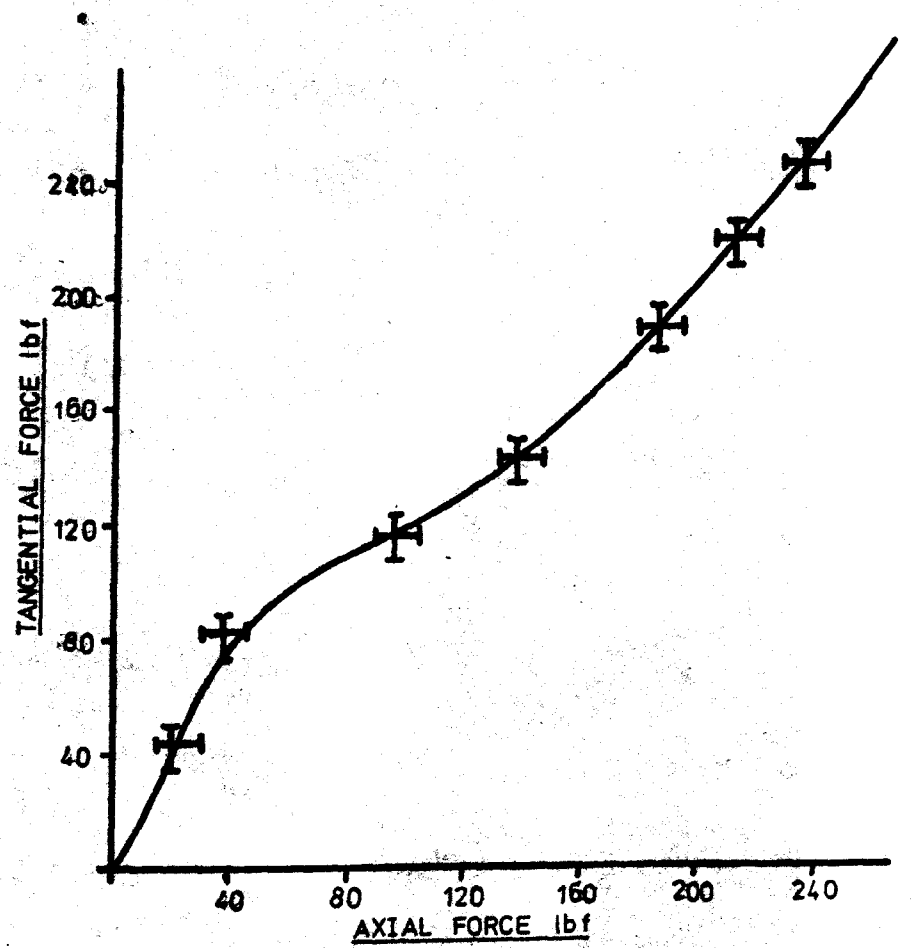

RELATIONSHIP BETWEEN TWO DYNAMOMETER FORCES FOR VARYING DEPTHS OF CUT AT CUTTING VELOCITY OF 1000 ft/min. AND FEED RATE OF 0.010 in/rev.

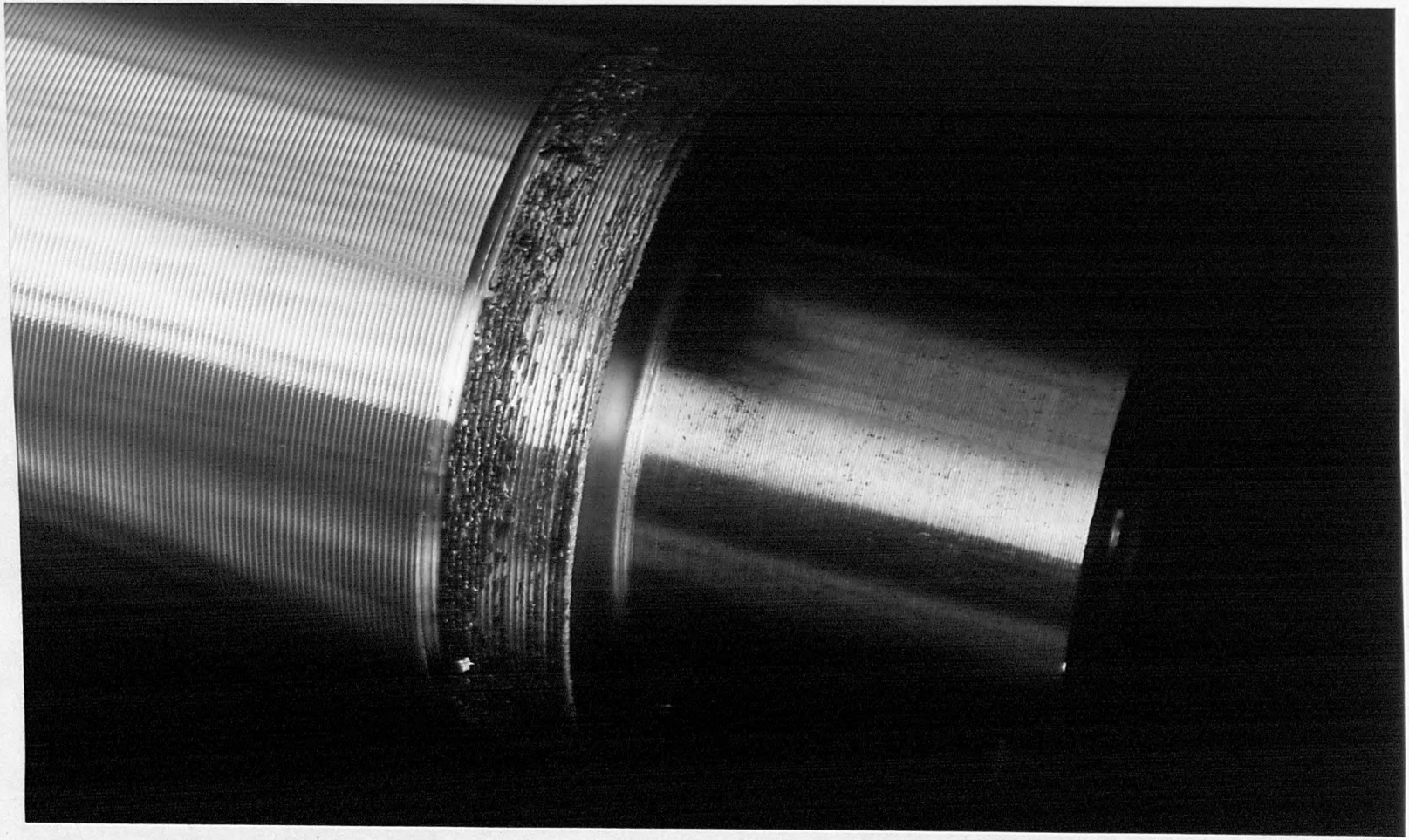

Fig.3.6.1. Illustration of re-engagement tool failure on test piece with feed rate of 0.028 in/rev at cutting speed of 1000 ft/min.

Fig.3.6.2

Dimensions in inches.

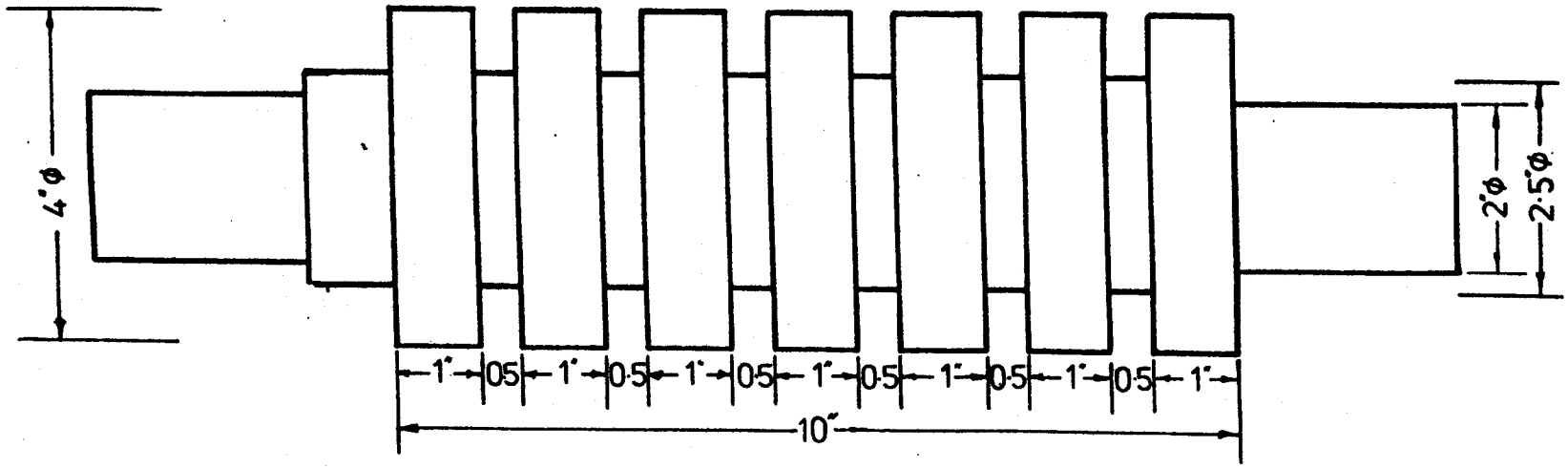

Test piece for interrupted cutting below critical feed rate of 0·028in/rev. at depths of cut between 0·05 and 0·1 in. Cutting velocity 1000 ft/min.

Fig. 3.6.3.

Dimensions in mm.

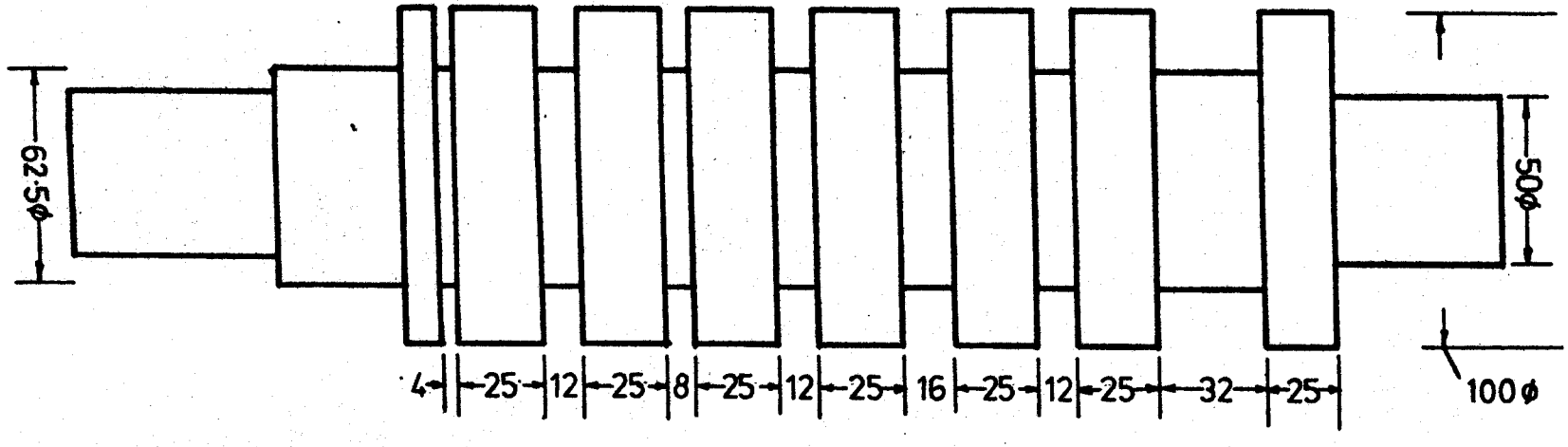

Slotted test piece used to check time dependency of catostrophic failure on re-engagement. Feed rate 0·03125 in/rev. and cutting velocity 1000 ft/min.

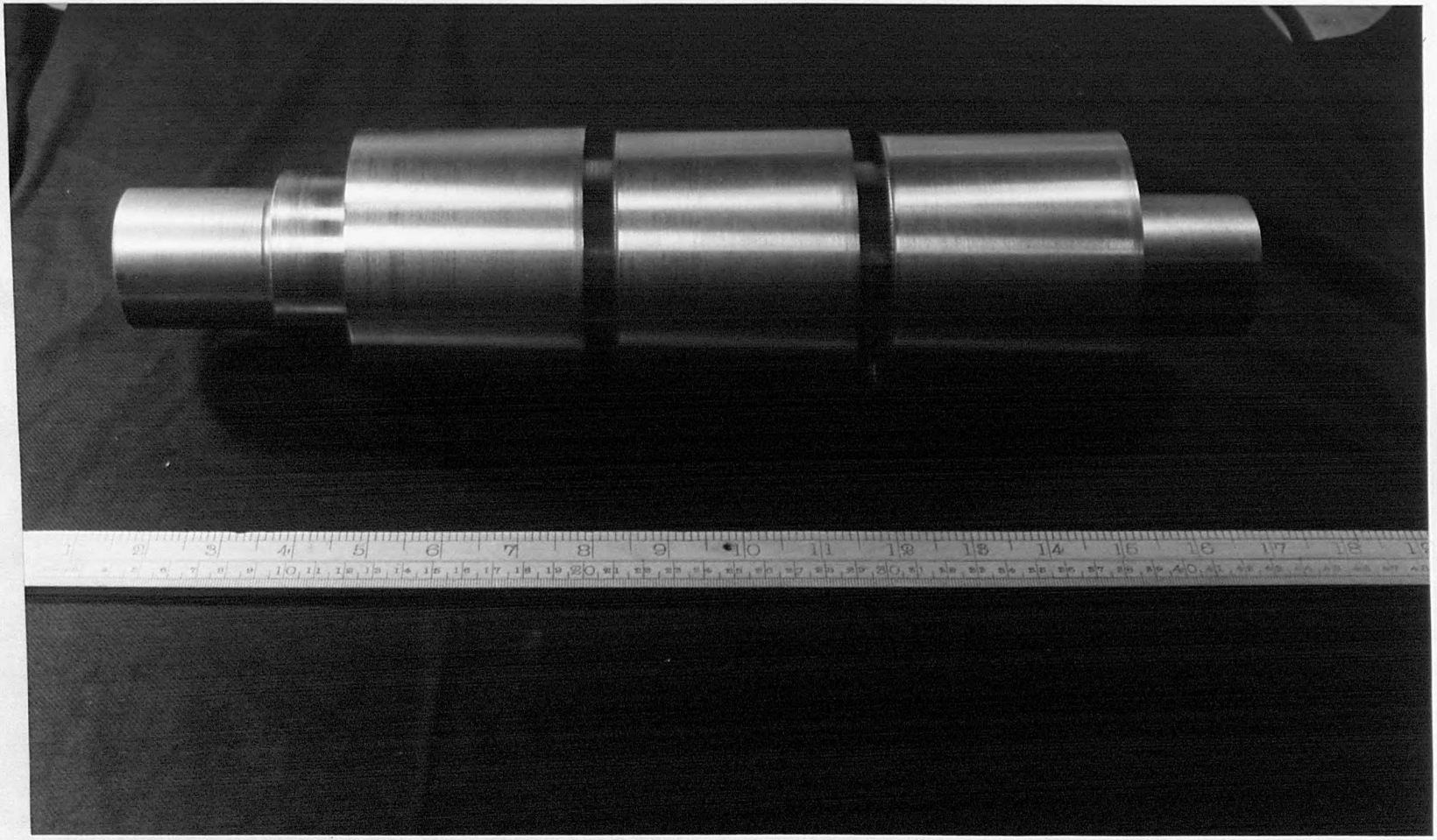

Fig.3.7.2(a). Test piece with three consecutive 3 in journals tapering 0.1 in on diameter.

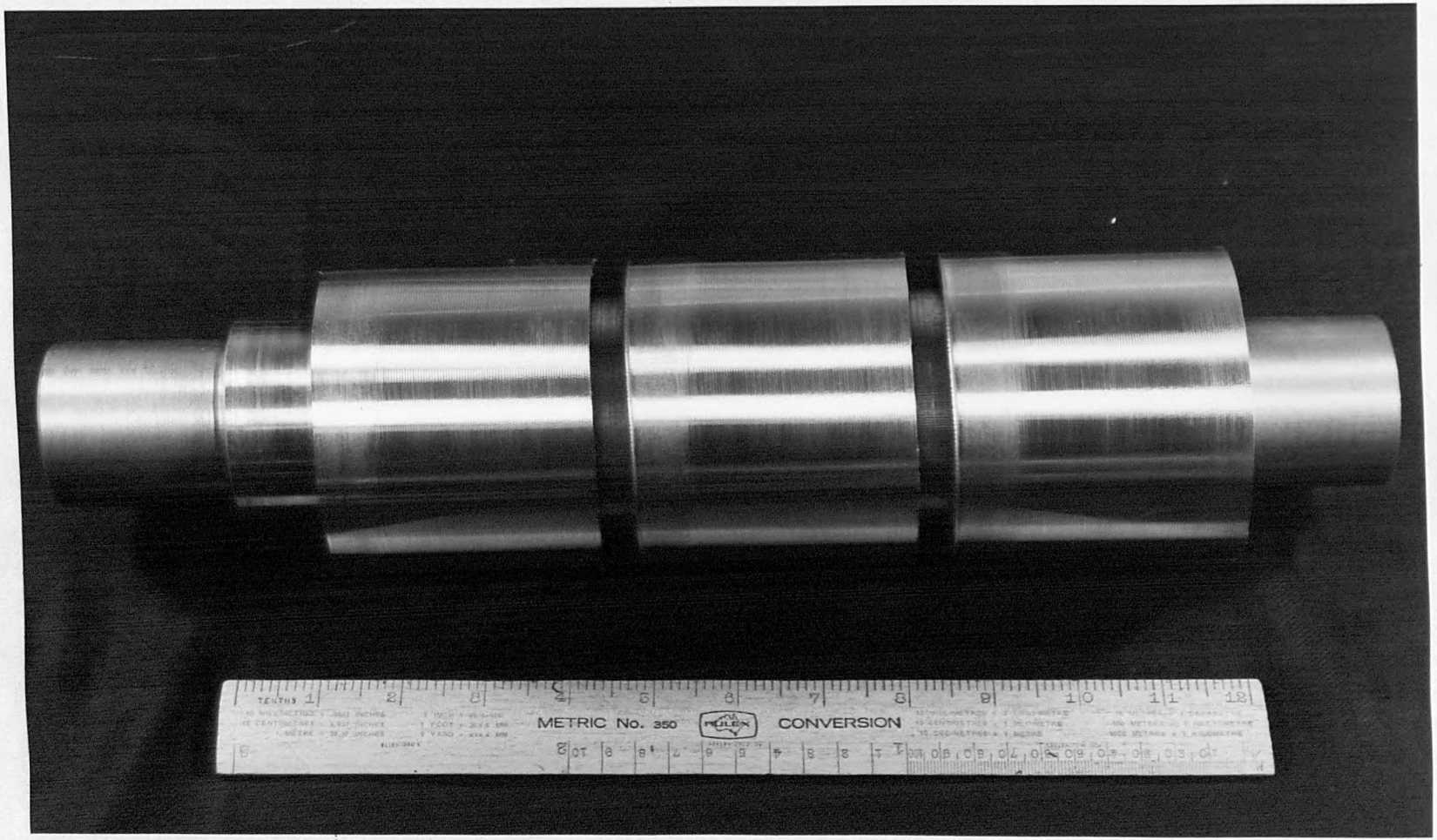

Fig.3.7.2(b). Test piece shown in fig.3.7.2(a) with tapers machined off in one pass at a cutting speed of 1000 ft/min and feed rate of 0.03125 in/rev.

1 COIL INDUCTOR

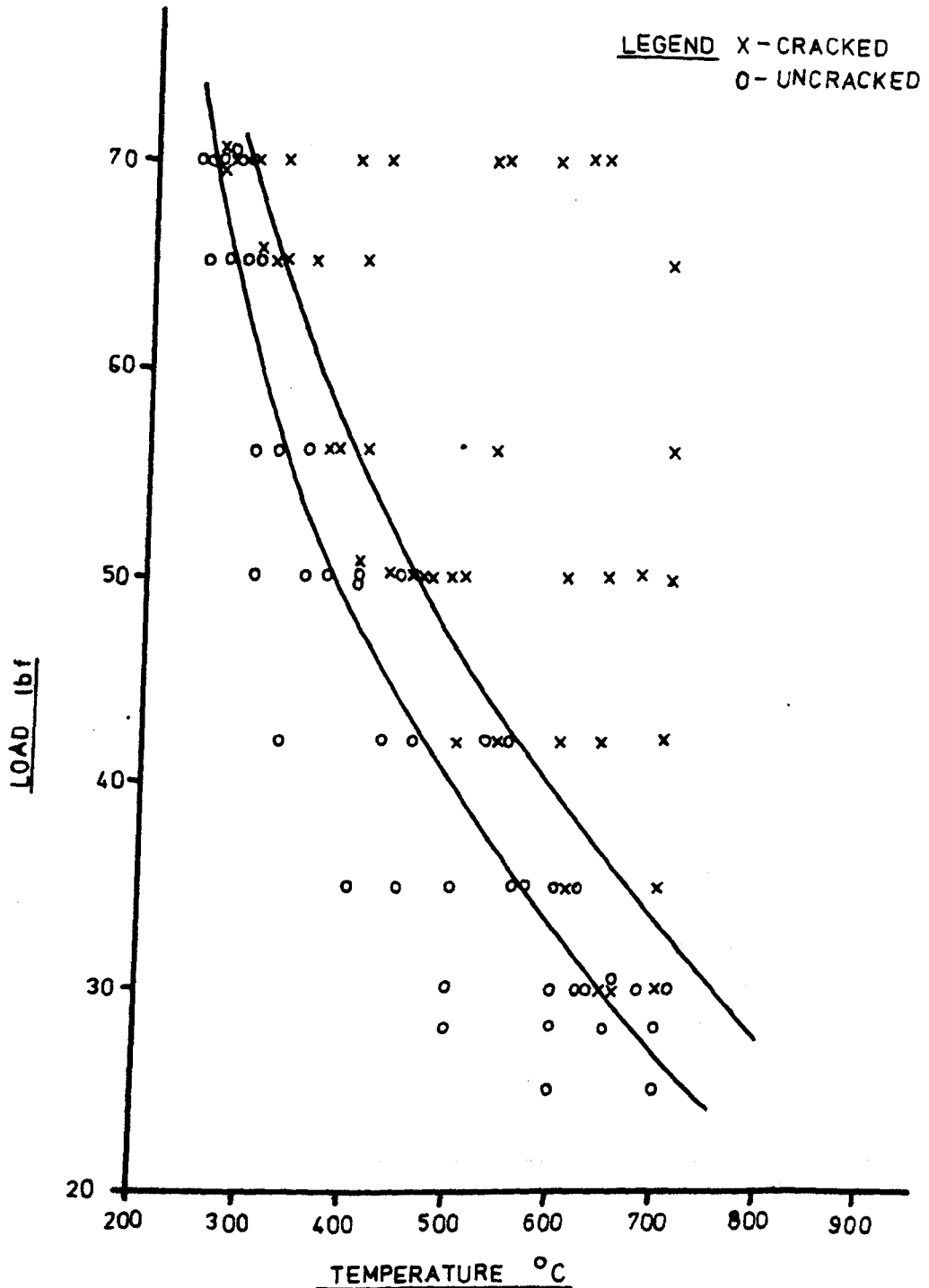

FIG. 3.81(A) FAILURE THRESHOLD FOR 1 COIL INDUCTOR

2 COIL INDUCTOR

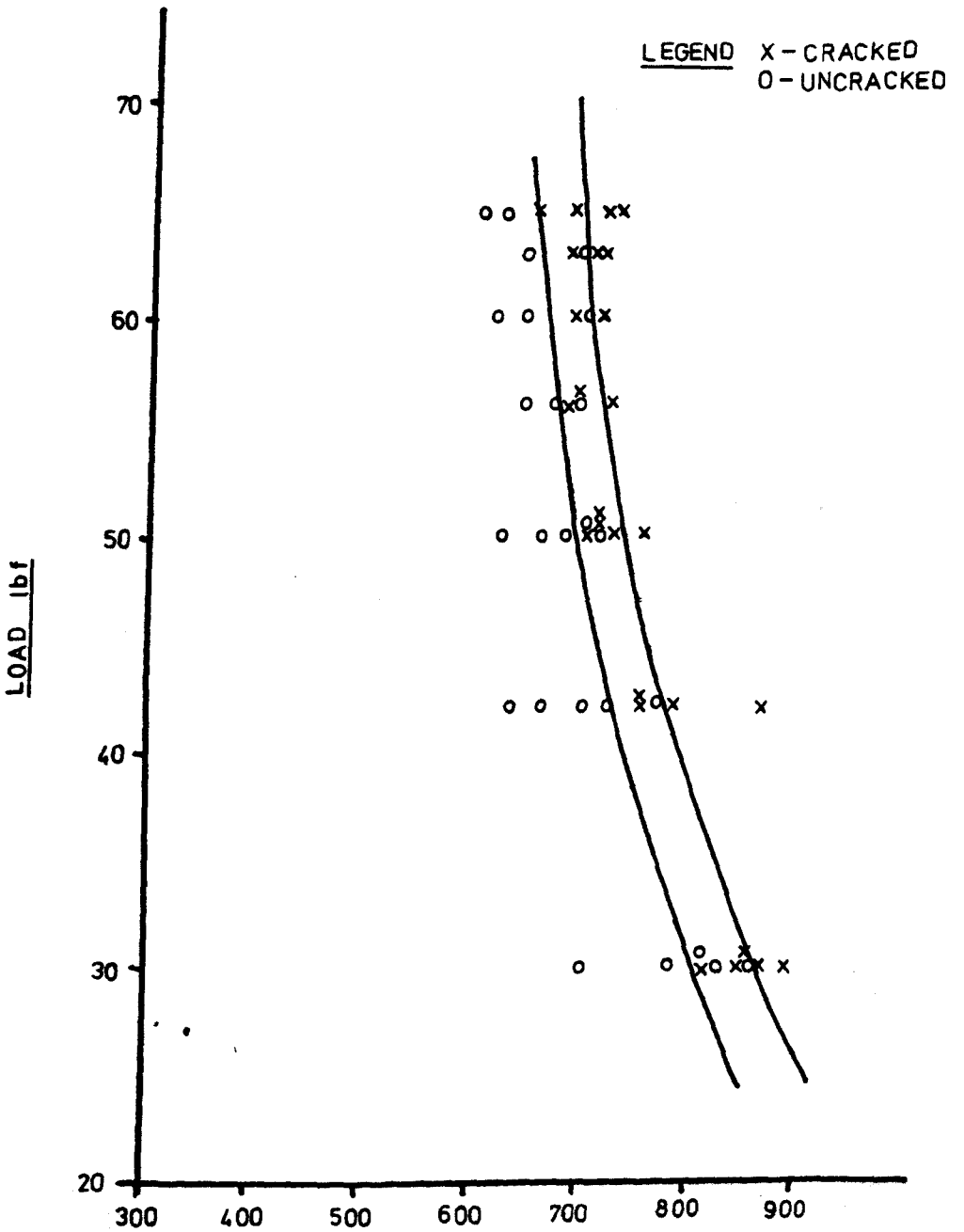

FIG. 3.81(B) FAILURE THRESHOLD FOR 2 COIL INDUCTOR

3 COIL INDUCTOR

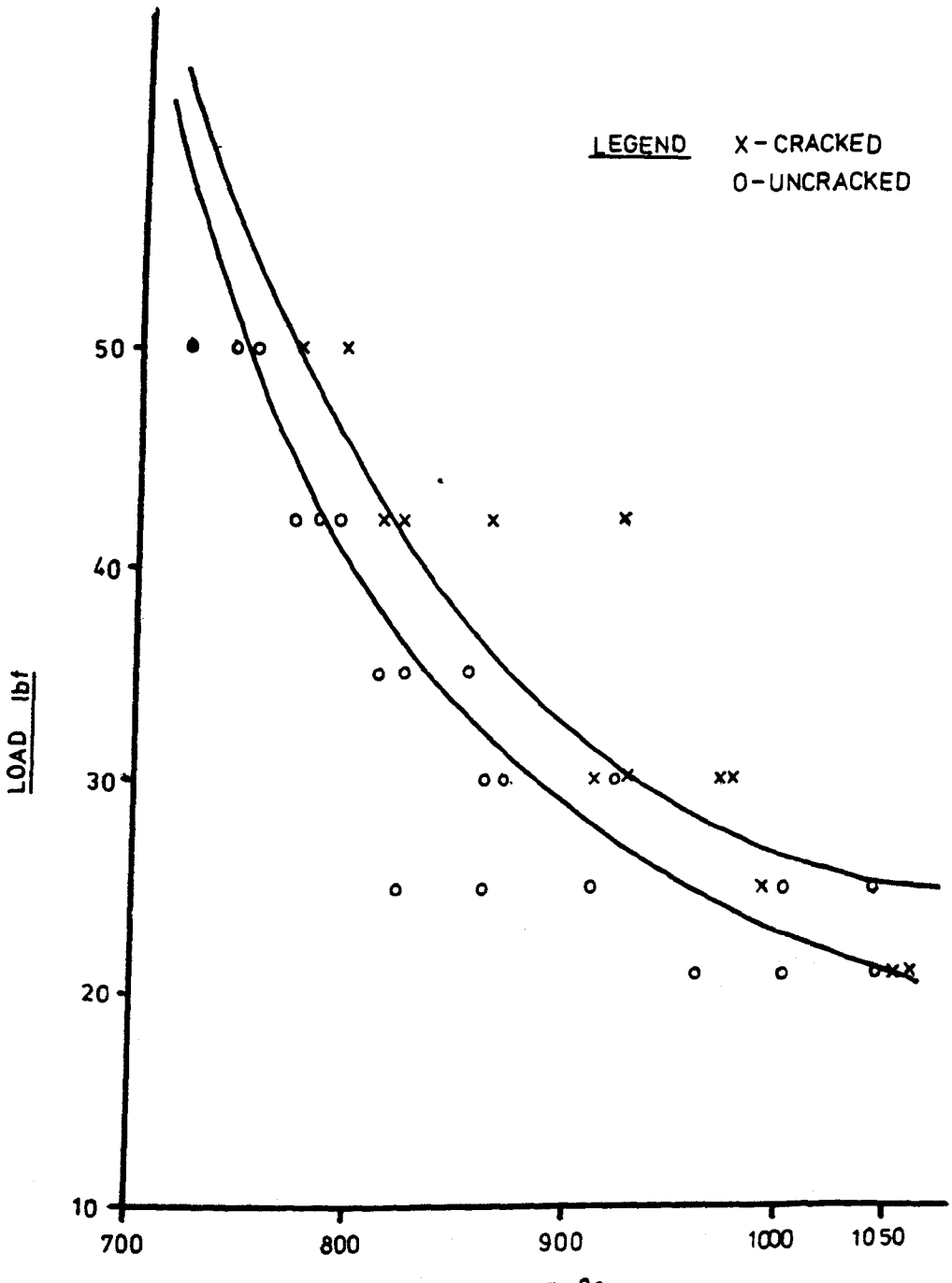

FIG .3.8.1(C) FAILURE THRESHOLD FOR 3COIL INDUCTOR

4 COIL INDUCTOR

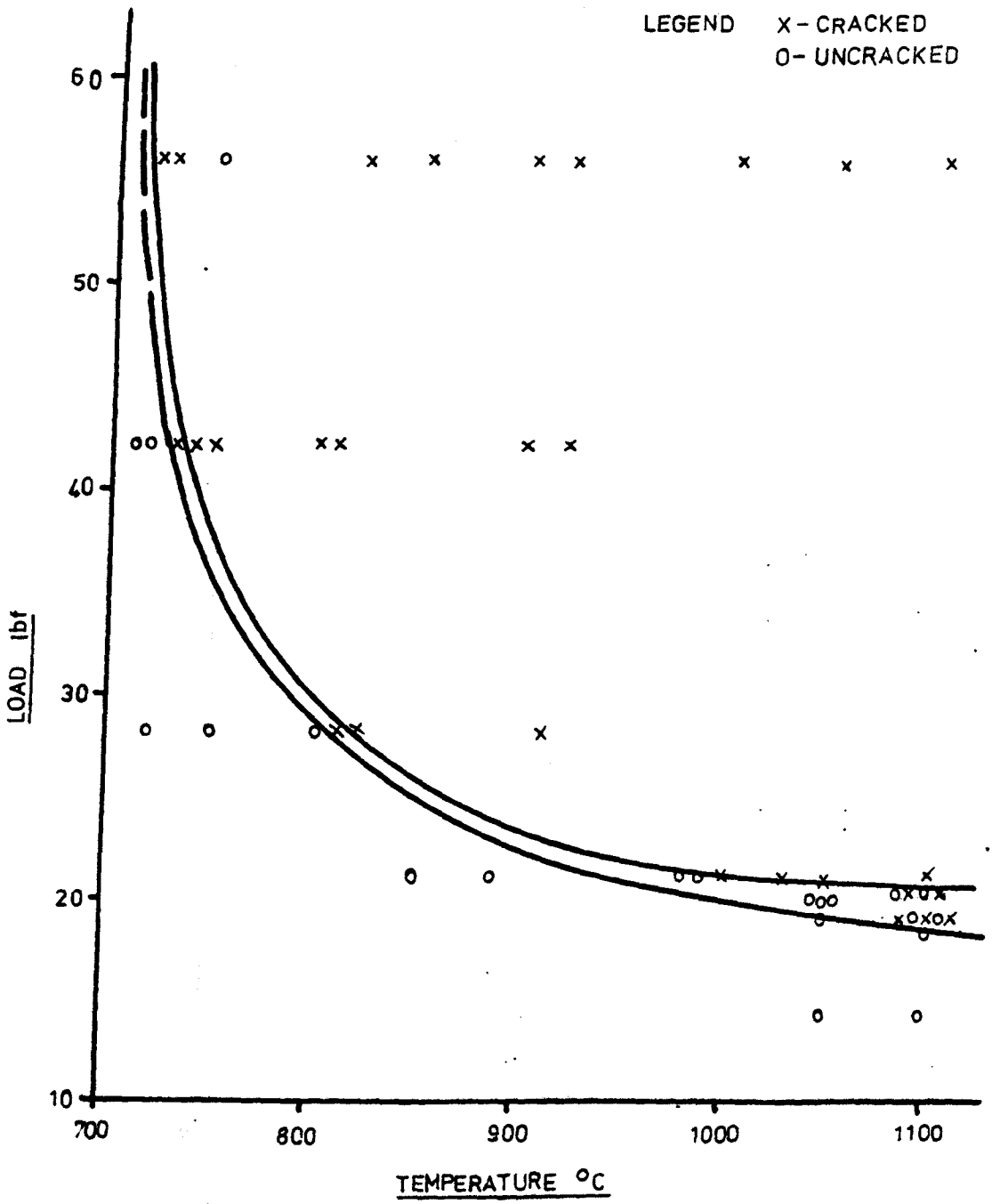

FIG. 3.8.1 (D) FAILURE THRESHOLD FOR 4 COIL INDUCTOR

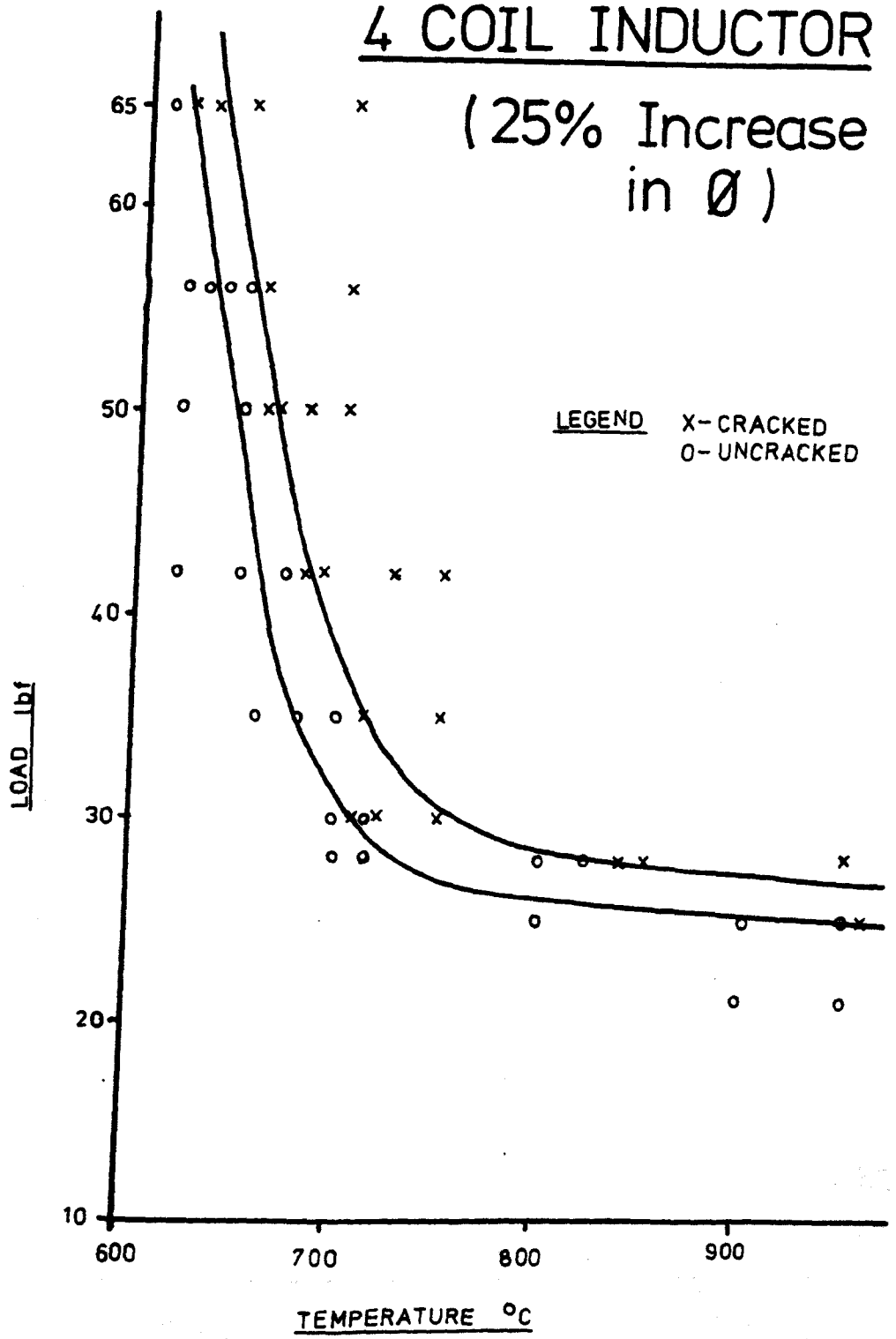

FIG. 3.8.1(E) FAILURE THRESHOLD FOR LARGE 4COIL INDUCTOR.

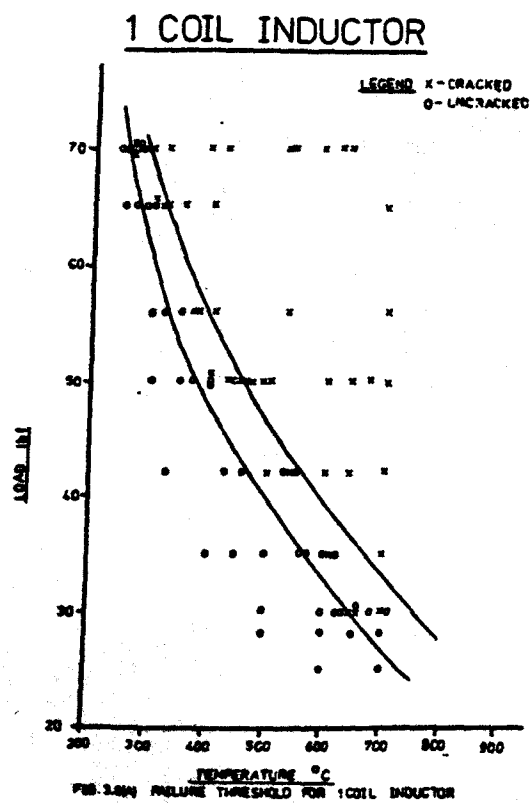

FIG.3.8(A) FAILURE THRESHOLD FOR 1COIL INDUCTOR

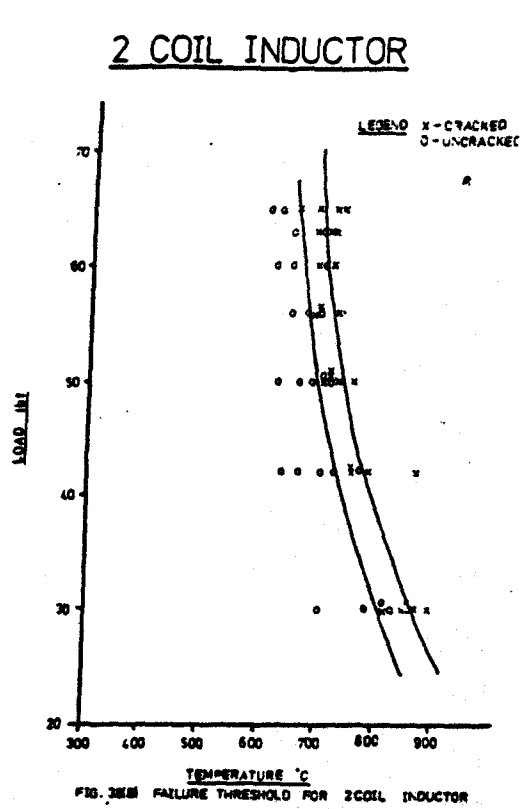

FIG. 3.8(B) FAILURE THRESHOLD FOR 2COIL INDUCTOR

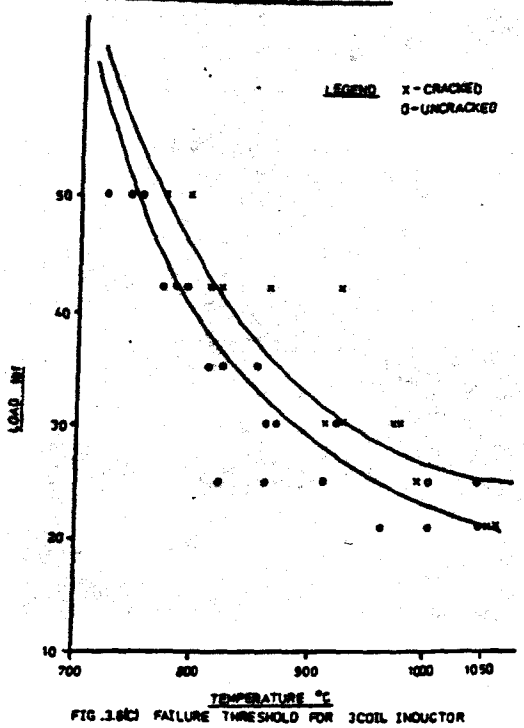

FIG.3.8(C) FAILURE THRESHOLD FOR 3COIL INDUCTOR

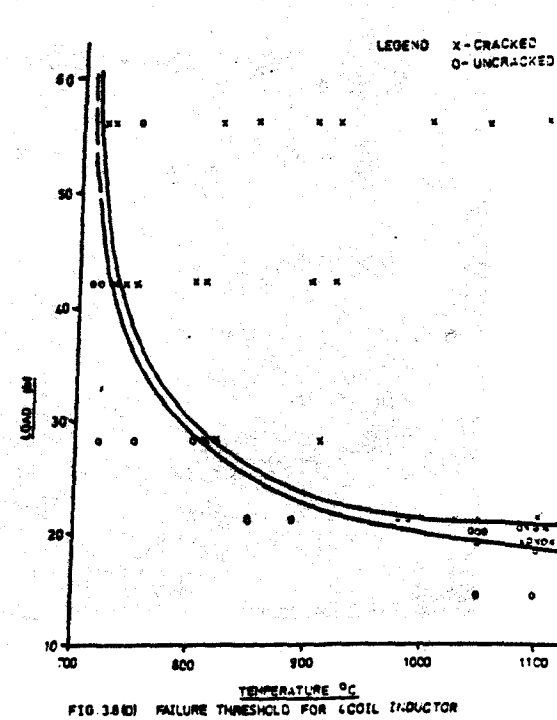

FIG.3.8(D) FAILURE THRESHOLD FOR 4COIL INDUCTOR

FIG.3.8.1 (A) to (D) THRESHOLD FAILURES OF SAME DIAMETER INDUCTORS FOR COMPARISON.

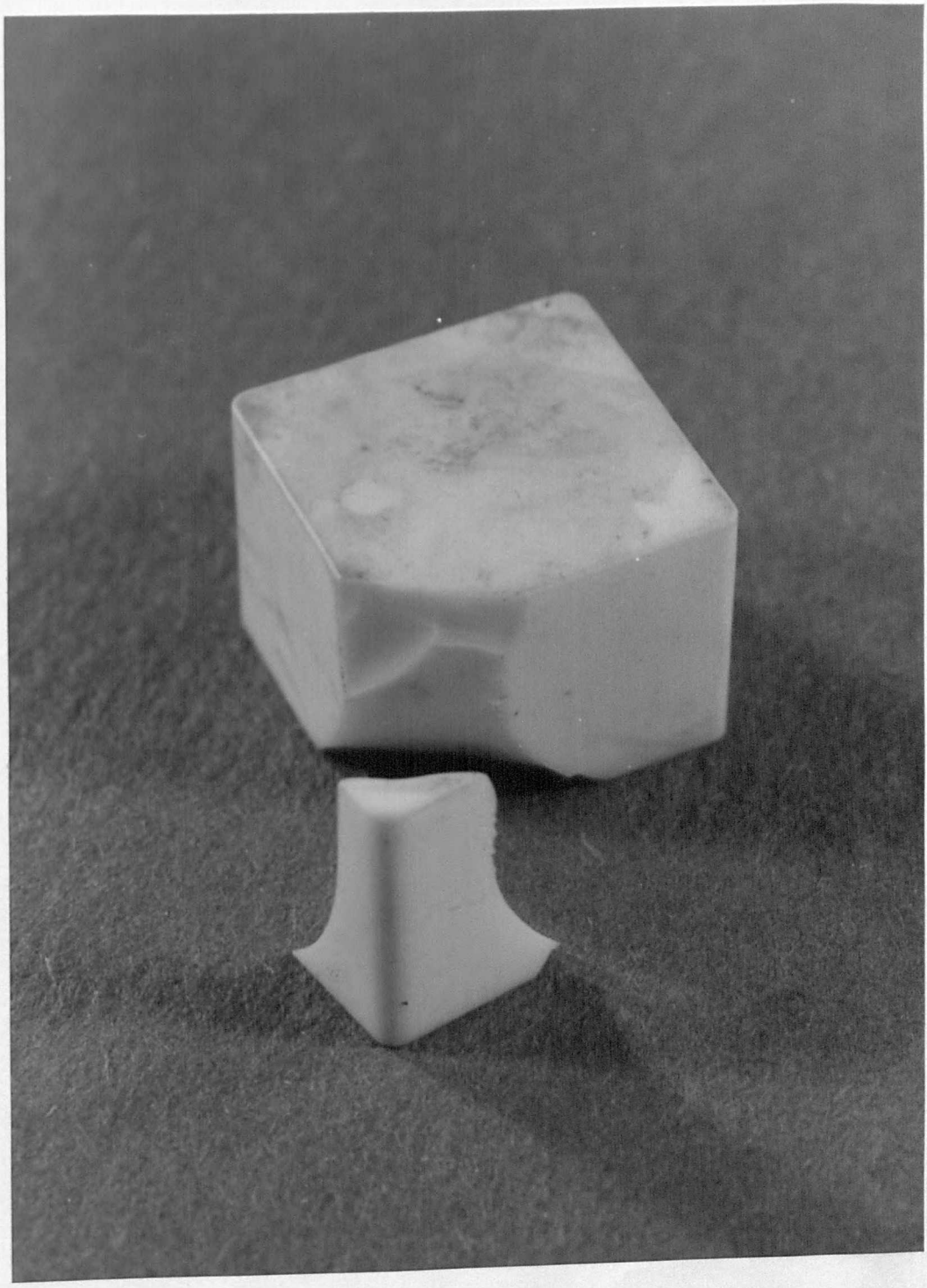

Fig.3.8.1(f). Typical test rig tool tip failure.

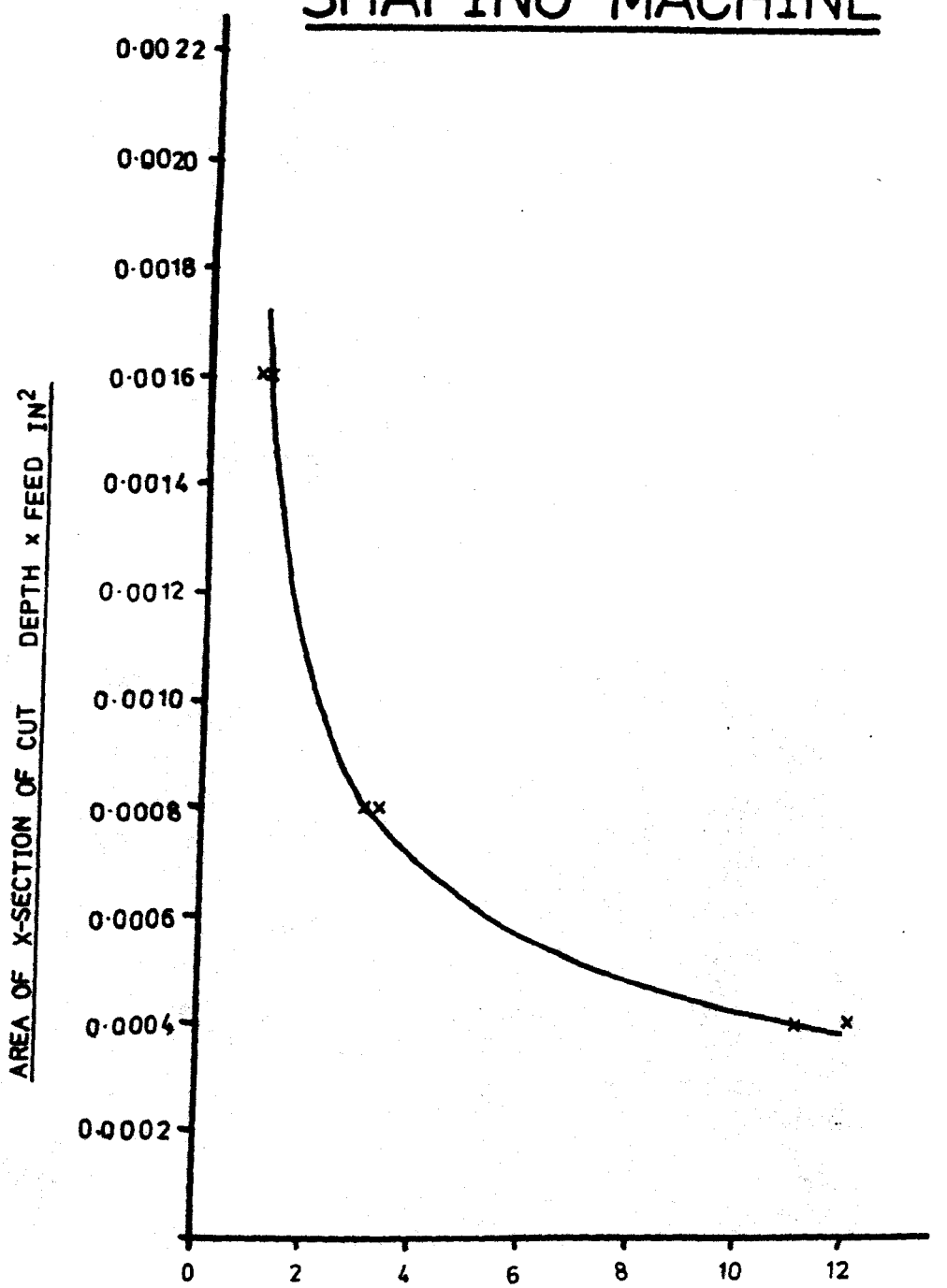

FIG. 3.9.1 RELATIONSHIP BETWEEN AREA OF CUT AND NUMBER OF CUTTING STROKES BEFORE FAILURE.

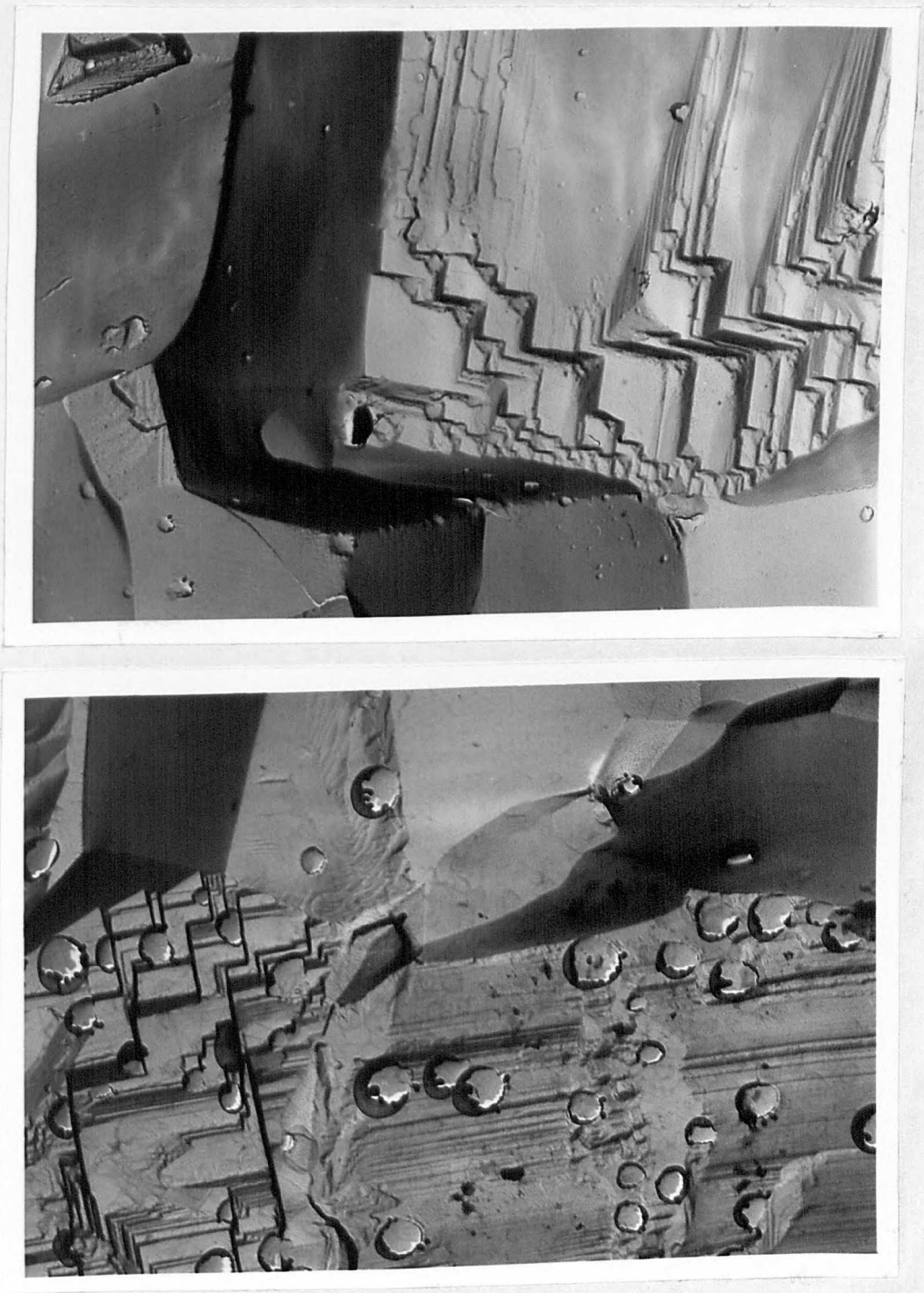

Fig.3.11.1. Micrographs of tool tip fracture surfaces. 8000X.
(a) Intergranular and transgranular fracture. (b) Porosity.

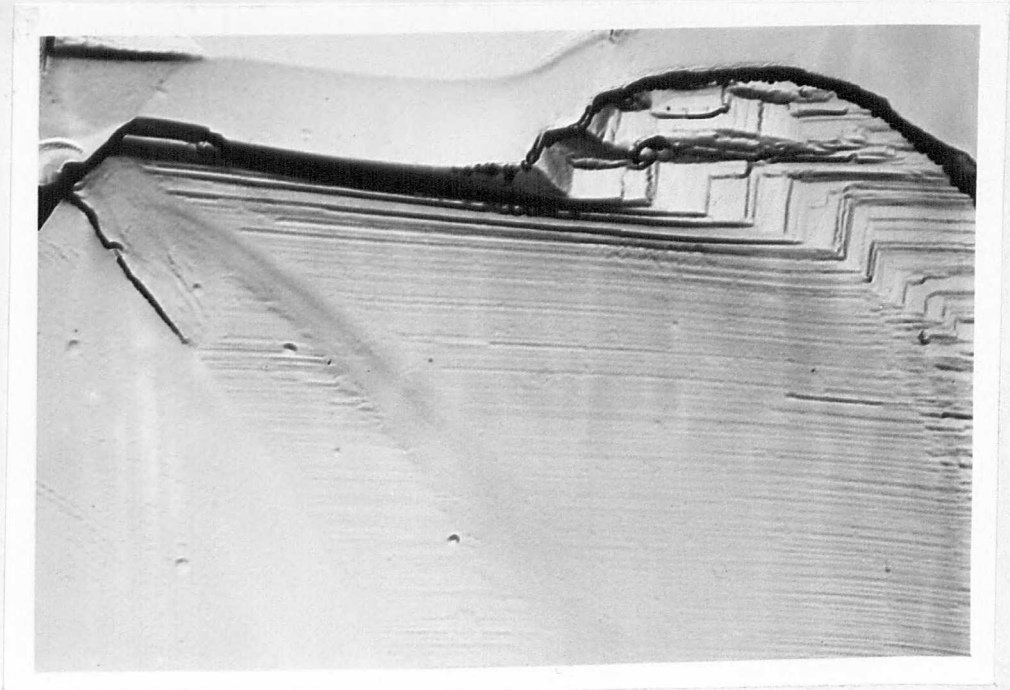

Fig.3.11.1. (c) Fracture surface.4000X.
(d) Transgranular fracture.16000X.

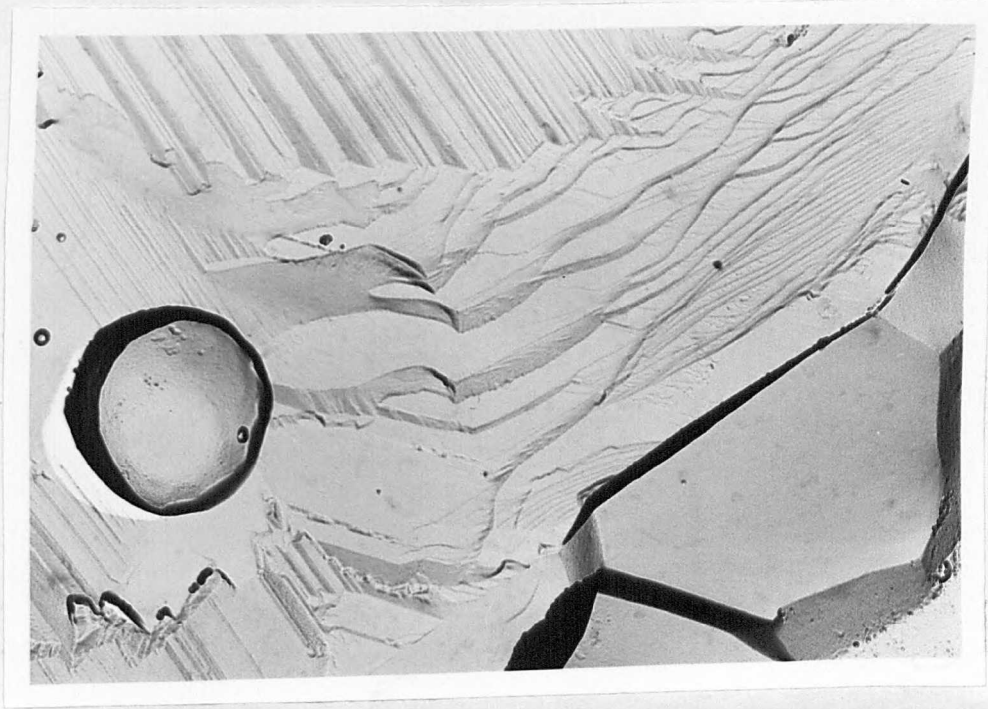

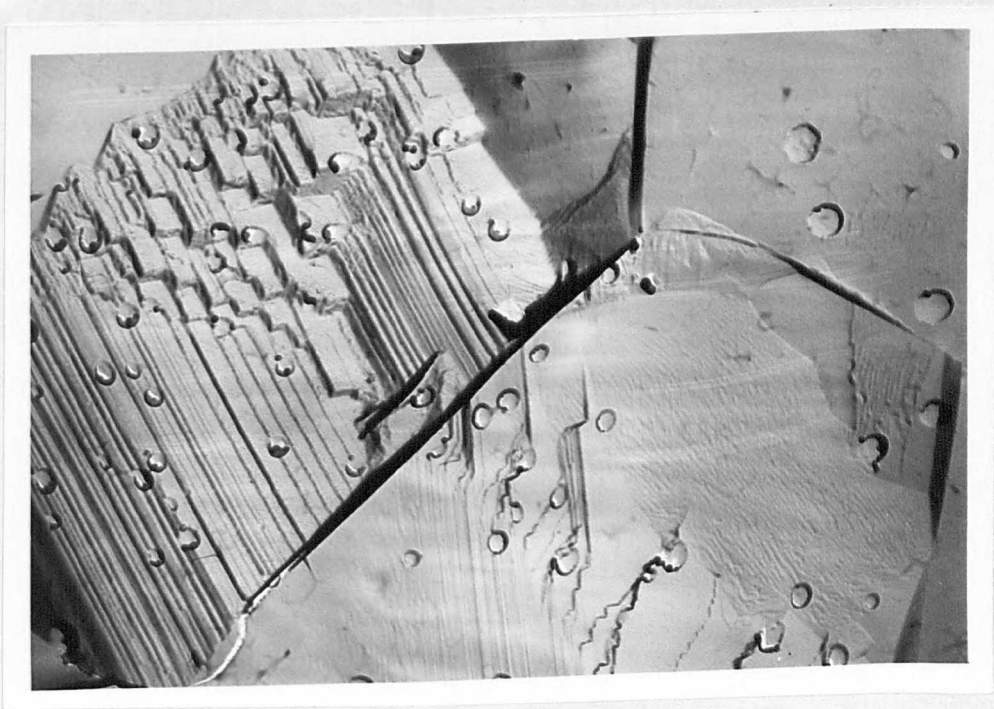

Fig.3.11.1. (e) Isolated alumina sphere inside crystallite.13000X. (f) Fracture surface.10000X.

Fig.3.11.1. (g) Line of pores.20000X.
(h) Fracture surface.2500X.

FIG.4.1.

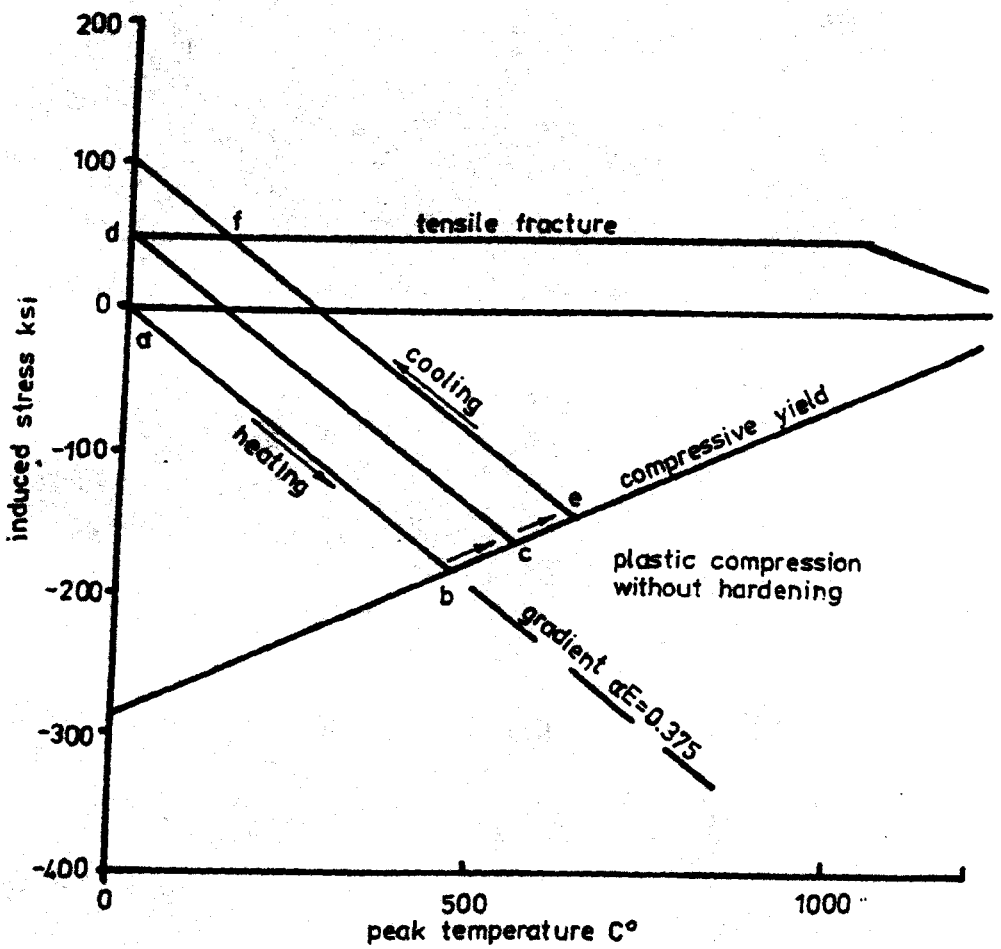

Mechanism of crack formation. On heating to over 500°C path abc is followed, with plastic compression along bc. Cooling along cd sets up a tensile stress. On heating to over 600°C to point e, subsequent cooling gives fracture at f. E = elastic modulus and α = coefficient of thermal expansion.

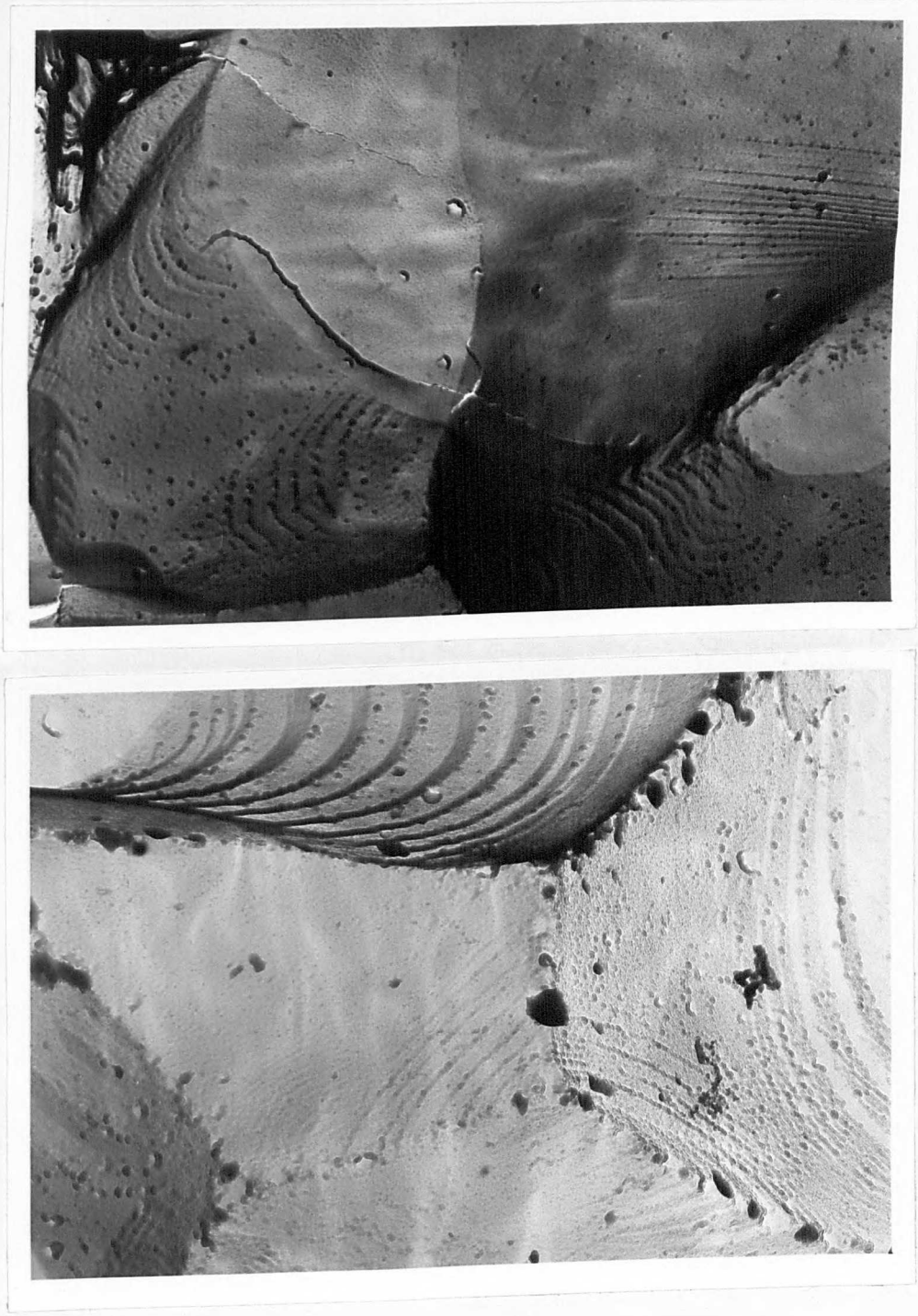

Figs.4.2.(a) and (b). Results of transgranular fracture influenced by pore concentrations. (a) 13000X. (b) 20000X.

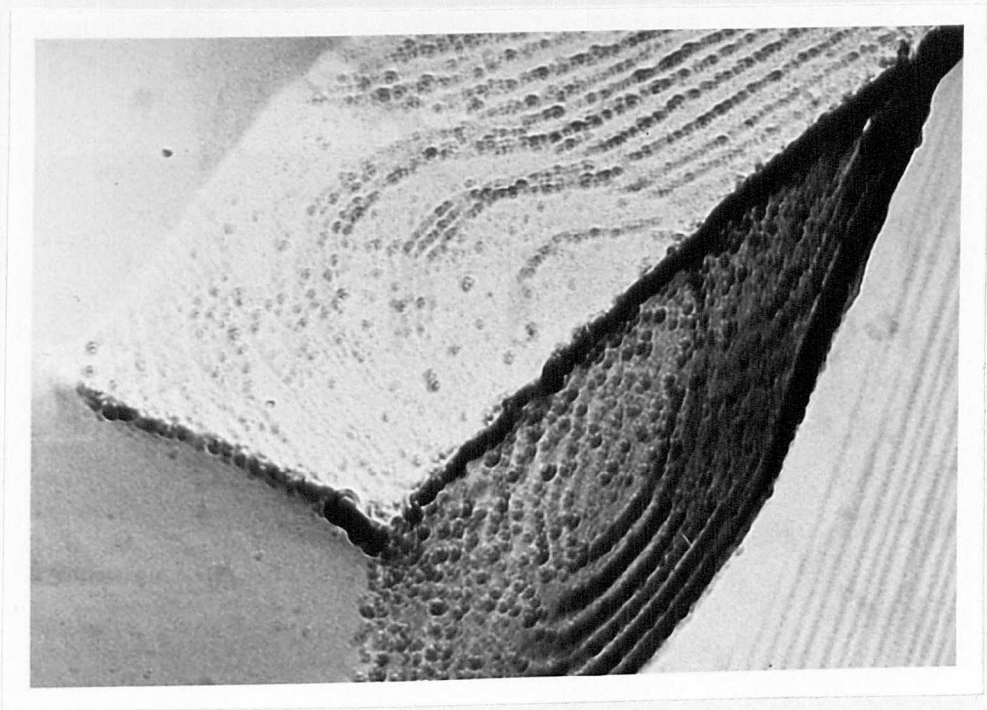

Fig.4.3. Semicontinuous pore concentrations at grain boundaries. 30000X.

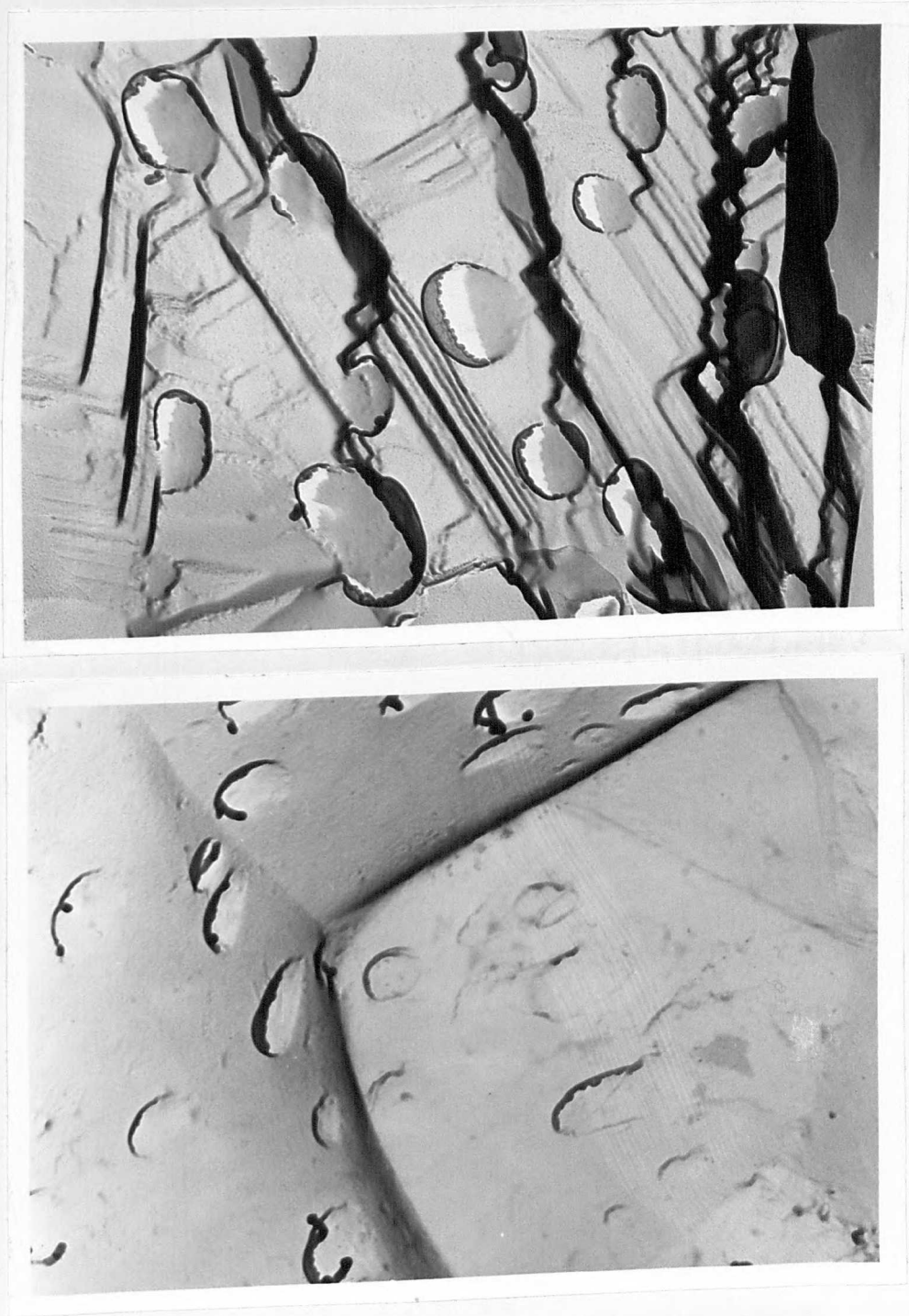

Fig.4.4(a) and (b). Showing random distribution of type 3 pore.
(a) in transgranular fracture surface.13000X.
(b) at grain boundaries. 10000X.

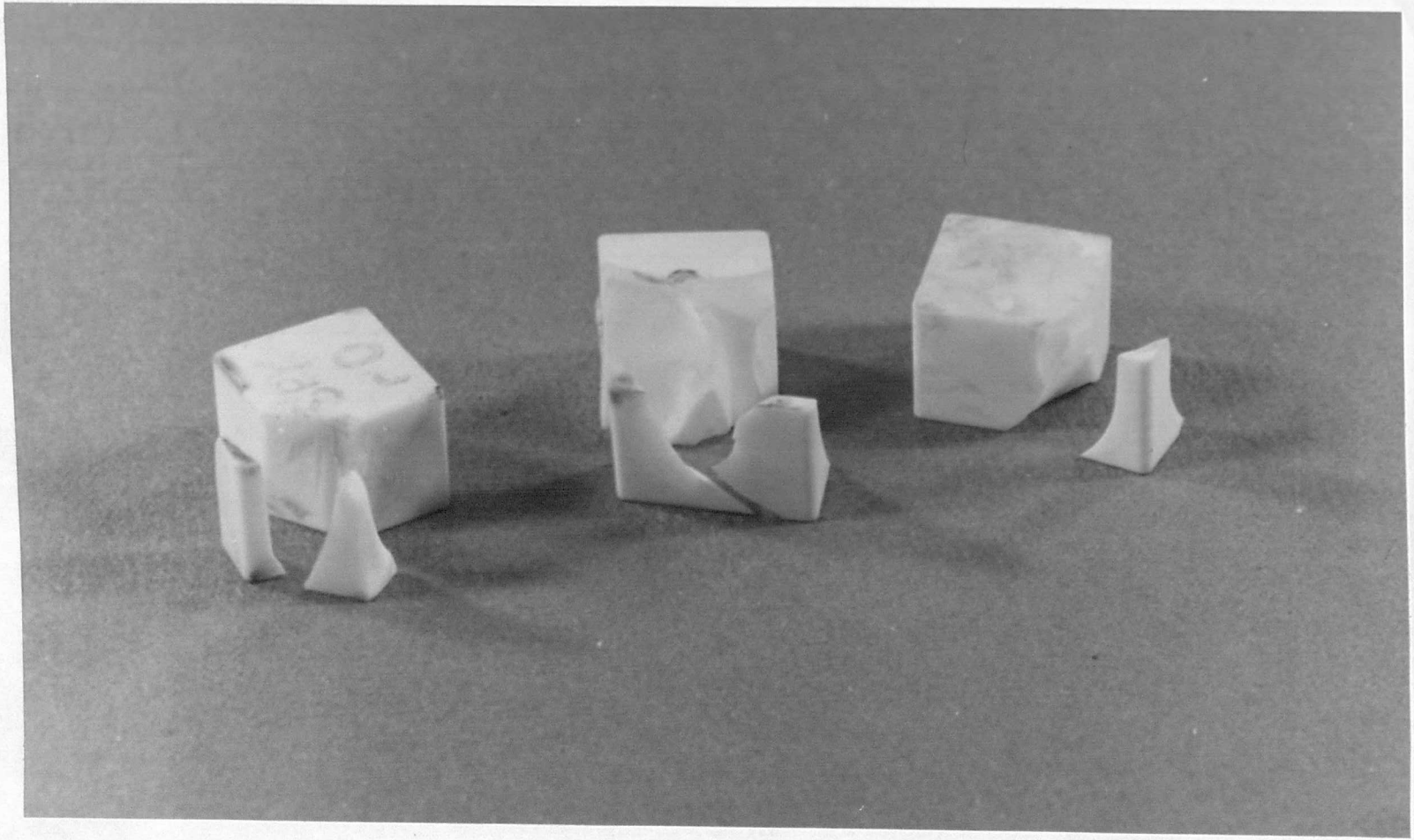

Fig.4.5. Modes of tool tip failure from lathe and test tig.

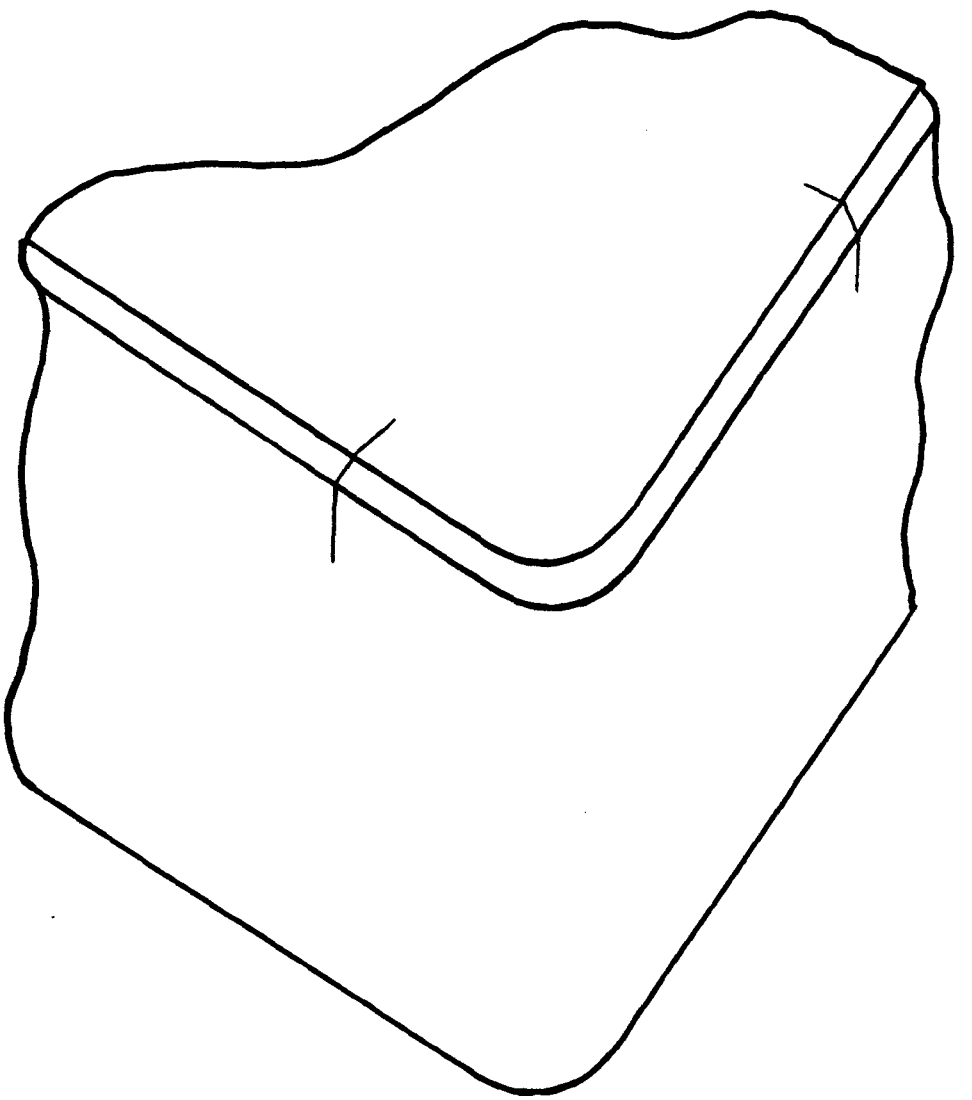

Fig.4.6(a). Cracks at front and side edges at intersections between active and inactive parts of tool tip.

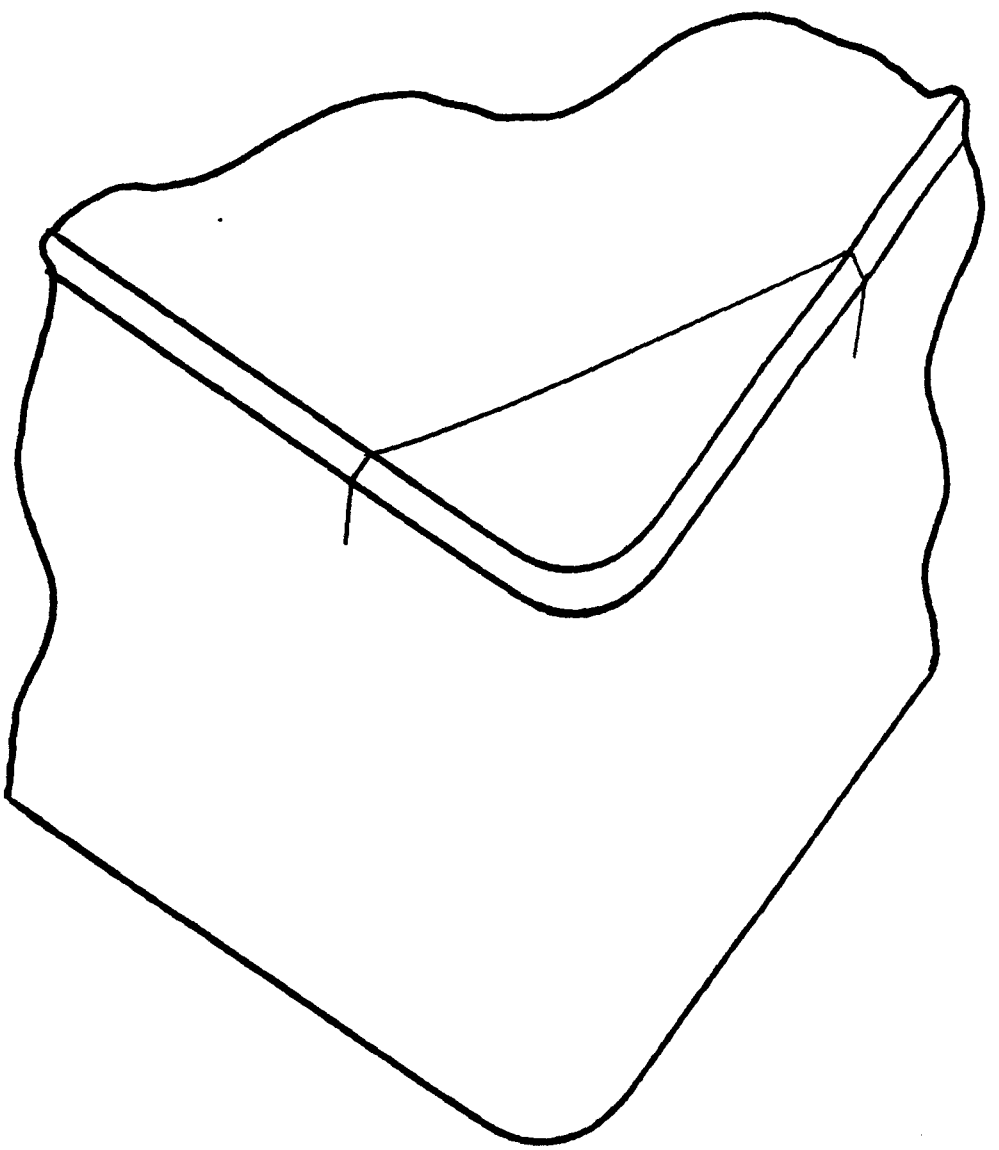

Fig.4.6(b). Edge cracks connected by a crack on the rake face across the tool tip corner.

BIBLIOGRAPHY

(1) King, A.G. and Wheildon, W.M., "Ceramics in Machining Processes". Academic Press, New York and London. (1966).

(2) Feldmühle Aktiengesellschaft, "Werk Südplastik and Keramik". (SPK) Publication. (1972).

(3) Ryshkewitch, E., "Ceramic Cutting Tools". U.S. pat. (1942).

(4) Pavlushkin, N. "Microlite". Znanie-Sila. (1953).

(5) Watertown Arsenal Report No. RPL 23/2., "Minutes of Symposium on Ceramic Cutting Tools". (1955).

(6) Pekelharing, A.J. and Orelio, J.M., "Semi-Roughing of Steel with Ceramic Tools". CIRP, Paris. (1966).

(7) King, A.G., "Ceramic Tool Wear". ASME Paper, 63-Prod-11. (1963).

(8) Sibley, L.B. and Allen, C.M., "Friction and Wear Behaviour of Refractory Materials at High Temperatures and Velocities". Wear 5. (1962).

(9) Thijssen, H. "Het Voordraaien van Staal met Keramisch Snijmateriaal". Metaalberwerking, 33,7. (1967).

(10) Pekelharing, A.J.,"A story about the Cracking of Ceramic Tools when Cutting Steel". CIRP Paper, Prague. (1961).

(11) Miles, J.W., "Disintegration of Alumina Tool-tips". M.Phil.Thesis. Brunel University. (1970).

(12) Griffith, A.A., "The Phenomena of Rupture and Flow in Solids". Phil.Trans.Royal Society. A21. (1921).

(13) Knudsen, F.P., J.Am.Ceram.Soc. 42,376. (1959).

(14) Carniglia, S.C. "Petch Relation in Single-Phase Oxide Ceramics". J.Am.Ceram.Soc. 48,580. (1965).

(15) Carniglia, S.C., Materials Science Research, "The Role of Grain Boundaries and Surfaces in Ceramics". Plenum, New York. (1966).

(16) Stokes, R.J., "Mechanical Behaviour of Polycrystalline Ceramics".
Ed.by Fulrath and Pask. Wiley, New York. (1968).

(17) Coble, R.L., "Effect of Microstructure on the Mechanical Properties of Ceramic Materials". Ceramic Fabrication Processes.
Ed.by Kingery, Technical Press, Wiley, New York. (1958).

(18) Clarke, F.J.P., "Residual Strain and the Fracture Stress-Grain Size Relationship in Brittle Solids".
Acta Metallurgica 12.139. (1964).

(19) King, A.G. in "Materials Science Research", Vol.3. "The Role of Grain Boundaries and Surfaces in Ceramics".
Ed. Kriegel and Palmour. Plenum, New York. (1966).

(20) Kronberg, M.L.
J.Am.Ceram.Soc. 43,458. (1960).

(21) Webster, J.A., "The Machining Characteristics of Disposable Alumina Tool Tips when used for Cutting Various Grades of Steel".
B.Sc.(honours) Project Report. Middlesex Polytechnic. (1976).

(22) El-Zahry, R.M. and Dugdale, D.S., "Resistance of Alumina Tool Tips to Formation of Comb Cracks".
Dept.Mechanical Eng.University of Sheffield.

(23) Kingery, W.D., "Introduction to Ceramics".
John Wiley, New York. (1967).

(24) Davidge, R.W., "Mechanical Behaviour of Ceramics".
Cambridge University Press. (1979).

(25) Coble, R.L. and Burke, J.E., "Progress in Ceramic Science", Vol.3., Pergamon Press. (1963).

(26) Kronenberg, M., "Machining Science and Application".
Pergamon Press. (1966).

(27) Trigger, K.J. and Chao, B.T., "An Analytical Evaluation of Metal-Cutting Temperatures".
Trans. of the ASME Vol.73, Part 1, pp.57 to 68. (1951).

(28) Van Vlack, L.H., "Physical Ceramics for Engineers".
Addison-Wesley Publishing Co.Inc. (1964).

APPENDIX I

HARDNESS TESTS

In view of the unsatisfactory results from earlier hardness tests, more work was undertaken in an effort to improve the technique. A tool tip was highly polished on one face to a good surface quality but this preparation also failed to produce any satisfactory indentations. The polished face was then lightly coated with silver to a few Ångströms thickness, into which several sharp impressions were made at various loads. The silver coating was removed and the indentations inspected between the polishing stages. However, all of the shallow impressions were removed with the silver and the deeper ones revealed the usual collapsed surface structure of the alumina. When viewed under a bench microscope at 600X magnification a well defined cruciform was clearly visible at the bottom of some of the indentations.

Whilst the hardness results were negative, there was at least proof of plastic deformation at room temperature in a normal environment.

APPENDIX II

CUTTING TEMPERATURES

Temperature measurement during machining was attempted, utilising the clearance angle near the corner, on the front face of the tool tip. Fine thermo-couple wires were fused to form a hot-junction and compacted to a thin disc and re-calibrated. The discs were cemented to the tool tip and their locations accurately measured with respect to the top corner. It was anticipated that an estimation of the cutting temperature could be made by extrapolation from a series of values recorded at various positions from the datum. The average temperature rise amounted to 147°C from a spread of readings between 122°C and 164°C with the hot-junction disc at distances between 0.004 in and 0.048 in from the datum. Clearly, direct temperature measurement of the tool in metal cutting processes presents problems of accessibility and heat transfer.

An alternative method was considered using a thermo-couple embedded in the tool tip. Initial trials were to be undertaken to establish a suitable position for the hot-junction by drilling the tool tips from underneath and at an angle from the back face up to the wear crater area of the rake face without unduly weakening the structure. However, problems arose in that the cost of ultrasonically drilling small diameter holes was too high and the idea had to be postponed.

In the past, much work has been devoted to the problem of tool temperature measurement by practical means but, more recently, simulation techniques have emerged which yield comparable values to

those obtained by practical methods. Parallel with these techniques, considerable attention has been devoted to the problem of temperature evaluation by analysis, which has been progressively improved upon by successive researchers in this field.

Kronenberg[26] derived a method of temperature evaluation by the application of dimensional analysis. The interesting points of this approach were the disregard for the tool tip geometry and the thermal conductivity of tool material.

Trigger and Chao[27] developed another analytical method of temperature evaluation for orthogonal cutting based on machining operations in which a type 2 chip is formed, (i.e., continuous chip with built-up edge).

The above cutting tool temperature analyses are two of many examples currently available.

APPENDIX III

MODIFIED TEST RIG

Following the unsuccessful attempts to simulate metal cutting on the modified test rig, consideration was given to the problems of manufacturing a new one. Preliminary design studies were made incorporating the existing lathe tool holder as the best method of maintaining the presentation geometry and location problems of the tool tips. Loads were to be applied hydraulically for ease of monitoring. In the final analysis the project had to be abandoned due to time and the cost involved in producing it. The idea of experimenting with alumina tool tips using a shaping machine originated from the design study of the proposed test rig.

APPENDIX IV

TOOL TIP COMPOSITION SURVEY

The qualitative chemical analysis of the SN37 (1973) tool tips was somewhat surprising in view of the complete absence of magnesia and the presence of calcia as the main sintering auxiliary.

King and Wheildon[1] surveyed thirteen different types of ceramic tool tips manufactured in the following countries:-

America	-	4 types
Germany	-	4 types (including SPK type SN)
Japan	-	2 types
France	-	1 type
Russia	-	1 type
Sweden	-	1 type

Chemical analyses of the above tips revealed the following distribution of the major sintering auxiliaries:-

Minor component	Frequency
MgO	9
TiO	1
TiC	1
Cr_3C_2	1
Cr_2O_3	1
WC	1
Cr	1
Co	1
NiO	1

The absence of calcia in the above analyses is, perhaps, significant.

Magnesium oxide (MgO) is the best known grain growth inhibitor for alumina[1] and this appears to be substantiated from the table above where nine of the thirteen types of tool tips discussed contained MgO as the sintering auxiliary. It is known to be effective in concentrations as low as 0.003% (30 parts per million). Usually, quantities of about 0.3% MgO are added during the manufacture of tool tips and quantities in excess of this limit of solid solubility react with alumina to form the spinel $MgOAl_2O_3$. The formation of $MgOAl_2O_3$ occurs at a temperature well below 1000°C and during sintering it tends to segregate at the grain boundaries where it reduces the boundary mobility and, hence, aids densification. There is no liquid phase formed during sintering between magnesia and alumina.

The use of calcia as the minor constituent results in a liquid phase of the compound $3CaO5Al_2O_3$ during sintering at a temperature of 1700°C. On cooling, this compound retards the grain growth in alumina by reducing the mobility of the grain boundaries in the same way as magnesia additions. The advantage of using grain growth inhibitors such as magnesia or calcia is that they aid densification during sintering by allowing some of the pores near the grain boundaries to collapse by diffusion of the gases from them out of the system through the boundaries. When grain growth in alumina occurs in the absence of inhibitors, the boundaries move at higher rates and sweep past the pores, which prevents the diffusion process taking place. Thus, more pores become isolated within the grains and further densification ceases - a state referred to as "end point" density.

APPENDIX V

ELASTIC MODULUS, PROPERTIES AND PORES

The modulus of elasticity is an index of the strength of the interatomic bonding of a material. Melting temperatures and hardness are also indices of interatomic bond strength and, although the correlation is not precise, it is significant. When considering a two-phase material the elastic modulus is intermediate between the components. Applying this relationship to the sintered alumina tool tips (1973), where the second phase may be regarded as the $CaO\text{-}Al_2O_3$ compound at the grain boundary network, an estimation of the modulus can be obtained from:-

$$E = E_a V_a + E_b V_b$$

where V_a and V_b are the volume fractions of the components. This equation gives a reasonable result if the Poisson ratios and interfacial coherences of the phases are not dissimilar.

According to Van Vlack[28], pores may be considered as a second phase without an elastic modulus. In this case the empirical relationship

$$1 - \frac{E}{E_a} = 1.9P - 0.9P^2$$

can be used for approximations, where P is the volume fraction of pores and $\frac{E}{E_a}$ is the fraction modulus related to the non-porous solid.

APPENDIX VI

SIGNIFICANCE OF FEED RATE AND TOOL FAILURE AT RE-ENGAGEMENT AGAINST METAL REMOVAL RATE

When comparing the metal removal rates for two typical cases, the first in which failure of the tool tips occurred consistently and the second in which failure did not occur, it was evident from re-engagement tests on the lathe that the feed rate was by far the most significant of the three basic machining parameters in relation to catastrophic failure. For example:-

Machining Parameters		Case I	Case II
Cutting velocity	(ft/min)	1000	1500
Depth of cut	(in)	0.05	0.10
Feed rate	(in/rev)	0.03125	0.0225
Workpiece diameter	(in)	3	3
Speed	(rev/min)	1273	1909
Metal removed	(in^3/min)	18.75	40.5

The metal removal rates were at the ratio of slightly more than 1 : 2, but in case (I) catastrophic failure occurred when a second cut was attempted. In case (II) re-engagement was made repeatedly until tool failure was brought about by the normal wear mechanism.